Dissertation

submitted to the

Combined Faculties for the Natural Sciences and for Mathematics

of the Ruperto-Carola University of Heidelberg, Germany

for the degree of

Doctor of Natural Sciences

presented by

Ewa Kamińska, MSc. Biology

born in Katowice, Poland

oral-examination: _____

Post-translational modifications

of RINT1 (RAD50-interacting protein 1)

Referees: Prof. Dr. Ralf Bartenschlager

Dr. Thomas Hofmann

"If you try and take a cat apart to see how it works, the first thing you have on your hands is a non-working cat."

Douglas Adams

Declaration

This thesis is based on the research conducted in the Division of Clinical Cooperation Unit Neuropathology, at the German Cancer Research Center, under supervision of Prof. Dr. Andreas von Deimling and direct supervision of Dr. Pierre-Olivier Frappart in the period from October 2010, to April 2014. The data described here has not yet been presented as a part of a university examination, is original and all the sources have been referenced.

Herewith, I declare that I wrote this thesis independently under supervision and no other sources and aids than those indicated in the manuscript were used.

Heidelberg, 20. IX. 2015

Ewa Kamińska

Table of contents

Abbreviations

AD	Alzheimer's disease
ALS	Amyotrophic Lateral Sclerosis
APC	adenomatous polyposis coli
APC/C	anaphase-promoting complex, cyclosome
APS	ammonium persulphate
ATM	ataxia telangiectasia mutated
ATP	adenosine triphosphate
ATR	ataxia telangiectasia and Rad3-related
bp (kbp)	base pair (kilo base pair)
BRCA	breast cancer
CBL	casitas B-lineage lymphoma
CDKs	cyclin-dependent kinases
cDNA	complementary DNA
CGN	*cis* Golgi network
CHX	cycloheximide
COG1	conserved oligomeric Golgi complex subunit 1
COPI	coat-protein complexes I
COPII	coat-protein complexes II
DDRs	DNA damage responses
DMEM	Dulbecco's Modified Eagle Medium
DMSO	dimethyl sulphoxide
DSBs	double-strand breaks
DTT	dithiothreitol
EDTA	ethylenediaminetetracetic acid
EGTA	ethylene glycol tetraacetic acid
ER	endoplasmic reticulum
ERT2	estrogen receptor

EV	empty vector
FACS	fluorescence-activated cell sorter
FPC	familial adenomatous polyposis of the colon
FSC	forward scatter index
HD	Huntington's disease
HECT	homologous to the E6AP carboxyl terminus
HEK293T	human embryonic kidney 293T cells
HHR	homologous recombination repair
IAPs	inhibitors of apoptosis
kDa	kilo Dalton
LUBAC	linear ubiquitin chain assembly complex
LS	Lynch syndrome
MMR	mismatch repair
Mre11	meiotic recombination 11
MRN	MRE11A-RAD50-NBN
MS	mass spectrometry
MEF	mouse embryonic fibroblast
NBS1	Nijmegen breakage syndrome 1, nibrin, NBN
NEM	N-ethylmaleimide
NHEJ	non-homologous end joining
NSF	N-ethylmaleimide-sensitive factor
PAGE	polyacrylamide gel electrophoresis
PARP1	poly [ADP-ribose] polymerase 1
PBS	phosphate buffered saline
PEI	polyethylenimine
PI	propidium iodide
PMSF	phenyl-methanesulphonylfluoride
PTMs	post-translational modifications
RB	retinoblastoma

RING	really interesting new gene
RINT1	RAD50-interacting protein 1
SCC	side scatter index
SCF	Skp, Cullin, F-box containing complex
SDM	site directed mutagenesis
SDS	sodium dodecyl sulfate
SENPs	sentrin-specific proteases
SMC	structural maintenance of chromosomes
SNARE	soluble NSF attachment protein receptor, SNAP receptor
SUMO	small ubiquitin-like modifier
T-ALL	T-lymphocyte acute lymphoblastic leukemia
TCR	T cell antigen receptor
TBS	Tris-buffered saline
TGN	*trans* Golgi network
Tris	tris-[hydroxymethyl]amino-methane
Ub	ubiquitin
UBD	ubiquitin-binding domain
UIM	ubiquitin-interacting motif
Ulps	ubiquitin-like protein-specific proteases
UVRAG	UV radiation resistance-associated gene protein
Y2H	yeast two-hybrid

Abstract

Initially found to regulate G2/M cell cycle checkpoint upon irradiation-induced DNA damage, RINT1 (RAD50-interacting protein 1) was later shown to be a multifunctional protein. RINT1 participates in telomerase-independent telomere length maintenance, membrane trafficking between Golgi apparatus and endoplasmic reticulum and ER-Golgi homeostasis. Inactivation of Rint1 leads to an early embryonic lethality. RINT1 can act as tumor suppressor, since heterozygous inactivation results in tumor formation in mice, while in humans mutant *RINT1* variants predispose to development of breast- and Lynch syndrome-related cancers. *RINT1* was also proposed to be an oncogene for glioblastoma development. Nevertheless, despite its involvement in a variety of biological pathways, no data regarding post-translational modifications (PTM) of RINT1 or their impact on the protein's function was reported.

The present study shows that RINT1 is subjected to two kinds of post-translational modifications: ubiquitination and, putatively, SUMOylation. It was found that RINT1 is a short-lived protein with a half-life (approx. 40 min) regulated by a proteasomal degradation pathway. RINT1 is ubiquitinated by several ubiquitin linkage types. Since K48-mediated polyubiquitin (polyUb) chains as well as K63- and K29-mediated polyUb chains were detected, functional significance of RINT1 ubiquitination is not limited to proteasomal degradation (K48-mediated polyUb chains) but could also serve to regulate multiple cellular functions of RINT1 (K63- and K29-mediated polyUb chains). Interestingly, RINT1 was also found to interact with lysineless ubiquitin mutant. Thus, monoubiquitination or linear ubiquitination (a less characterized and newly discovered PTM) of RINT1 could also be postulated. Furthermore, analysis of *in silico* predicted ubiquitination sites of RINT1 by co-immunoprecipitation of mutant versions (truncated mutants and site-directed mutagenesis) revealed that RINT1 is ubiquitinated at different sites within the protein. Two E3 ubiquitin ligases, HUWE1 and RNF20/RNF40E3 complex, were identified by mass spectrometry assay as binding partners mediating ubiquitination of RINT1. The specificity of these interactions was subsequently confirmed by co-immunoprecipitation experiments. Importantly, shRNA-induced down-regulation of HUWE1 and RNF20 or RNF40 protein levels resulted in enhanced RINT1 stability, thus indicated their novel role as regulators of proteasomal degradation of RINT1. Moreover,

mass spectrometry analysis and yeast two-hybrid assay identified SUMOylation as another covalent modification of RINT1. First experiments suggested covalent modification of RINT1 by SUMO proteins.

In conclusion, the present study demonstrated that human RINT1 is a protein of a short-half life, heavily ubiquitinated at different sites within the protein and *via* different ubiquitin chain linkage types (K29, K48, K63). It is also modified by a lysineless ubiquitin mutant and potentially SUMOylation. Importantly, RINT1 interacts with HUWE1 and RNF20/40 E3 ubiquitin ligases, which tightly control its cellular levels. This study reveals crucial mechanisms governing homeostatic RINT1 turnover and, in this respect, is the first to address the presence and functionality of RINT1 polyubiquitination.

Zusammenfassung

Nachdem zunächst festgestellt wurde, dass RINT1 (RAD50-interacting-Protein 1) den G2/M-Zellzyklus-Kontrollpunkt nach DNA Schäden durch Bestrahlung reguliert, wurde später herausgefunden, dass RINT1 ein multifunktionelles Protein ist. So beteiligt sich RINT1 an der Telomerase unabhängigen Aufrechterhaltung der Telomerlänge sowie an Membrantransport zwischen Golgi-Apparat und endoplasmatischem Retikulum und deren Homöostase. Inaktivierung von *Rint1* führte zu einer frühen embryonalen Sterblichkeit, während sie im Menschen zu einer Prädisposition für Brustkrebs und dem Lynch-Syndrom beiträgt. Auch wird vermutet, dass RINT1 als Onkogen in der Entstehung von Gliomen mitwirkt. Trotz der Beteiligung an einer Vielzahl biologischer Prozesse gab es bisher keine Daten zu post-translationalen Modifikationen (PTM) von RINT1 und deren Auswirkung auf die Funktionen des Proteins.

Die vorliegende Studie zeigt, dass RINT1 zwei Arten von PTM unterzogen wird: Ubiquitinierung und gegebenenfalls SUMOylierung. Es wurde festgestellt, dass RINT1 ein kurzlebiges Protein mit einer Halbwertszeit von ca. 40 Minuten ist, welche durch proteosomalen Abbau reguliert wird. RINT1 wird auf verschiedene Weisen ubiquitiniert. So konnten sowohl K48-verknüpfte Polyubiquitin (polyUb) Ketten als auch K63- und K29-verknüpfte polyUb Ketten nachgewiesen werden. Dies deutet darauf hin, dass Ubiquitinierung von RINT1 nicht nur dessen proteosomalen Abbau reguliert (vermittelt durch K48-verknüpfte polyUb Ketten) sondern außerdem an der Regulation weiterer biologischer Prozesse beteiligt ist (vermittelt durch K63- und K29-verknüpfte polyUb Ketten). Interessanterweise konnte außerdem eine Interaktion von RINT1 mit Lysine-freien Ubiquitin-Mutanten nachgewiesen werden. Dies lässt sowohl Monoubiquitinierung als auch lineare Ubiquitinierung (eine weniger charakterisiert und neu entdeckte PTM) von RINT1 vermuten.

Des Weiteren bestätigte die Analyse von *in silico* vorhergesagten Ubiquitinierungsstellen mittels Co-Immunpräzipitation mutierter RINT1-Varianten, dass RINT1 an verschiedenen Stellen innerhalb des Proteins ubiquitiniert wird. Zwei E3 Ubiquitin-Ligasen, HUWE1 und RNF20/RNF40E3-Komplex, konnten mittels Massenspektrometrie als Bindungspartner von RINT1 und Vermittler der Ubiquitinierung identifiziert werden. Die Spezifität der Interaktionen wurde anschließend durch Co-Immunpräzipitation bestätigt. Die shRNA-

induzierte Reduktion von HUWE1, RNF20 sowie RNF40 resultierte in einer erhöhten Proteinstabilität von RINT1. Dies bestätigt die bislang unbekannte Rolle dieser Proteine als Regulatoren des proteosomalen Abbaus von RINT1. Des Weiteren konnte in massenspektrometrischen Analysen sowie mittels yeast two-hybrid-assay SUMOylierung von RINT1 als eine weitere kovalente Modifikation identifiziert werden. Diese Ergebnisse wurden mit initialen Versuchen angedeutet.

Zusammenfassend zeigt die hier vorliegende Studie, dass humanes RINT1 ein Protein mit kurzer Halbwertszeit ist, welches an verschiedenen Stellen innerhalb des Proteins und über verschiedene Ubiquitinierungsarten (K29, K48, K63) modifiziert wird. Zusätzlich wird RINT1 auch durch eine Lysine-freie Ubiquitin-Mutante sowie potenziell SUMOylierung modifiziert. RINT1 interagiert mit den E3-Ubiquitin-Ligasen HUWE1 und RNF20/40-Komplex, wodurch die Stabilität des Proteins reguliert wird.

Die vorliegende Studie beschreibt essentielle Mechanismen der homöostatischen Regulation von RINT1 und belegt in diesem Zusammenhang erstmals sowohl Vorhandensein als auch Funktionalität von Polyubiquitinierung von RINT1 als verantwortliche post-translationale Modifikation.

Aim of the study

Post-translational modifications (PTMs) constitute a powerful biochemical tool to modify functions, interactions and localization of a modified protein. PTMs are especially important to diversify cellular roles of a given protein by providing precise regulation and flexibility to perform different functions.

RINT1 (RAD50-interacting protein 1) is a multifunctional protein, which plays an important role in the cell cycle regulation, telomere length maintenance and ER-Golgi trafficking. Recently, it was shown to act as a both proto-oncogene and tumor supressor. Despite its involvement in such diverse processes nothing is known about the PTMs of RINT1, which could regulate and drive the possibility of executing such spatially and temporally distinct cellular functions of the protein.

The objective of the current experimental study was: (1) to investigate and characterize PTMs of RINT1 as well as (2) to reveal novel proteins interacting with RINT1 able to mediate its modifications. The obtained data would help to understand the regulation of RINT1 functions and to further define other putative biological roles of RINT1 protein.

1. Introduction

1.1. General characteristics of RINT1 protein

Human RINT1 (RAD50-interacting protein 1) is a 90 kDa (NCBI Ref. Seq. NP_068749.3) protein, encoded by the *RINT1* gene located on the chromosome 7 in humans (long arm; 7q22.3) and chromosome 5 in mice (5 A3, 5). It was discovered as an interaction partner of RAD50 during late S and G2/M phases of the cell cycle (Xiao, Liu et al. 2001). Although almost 14 years have passed since this initial finding, still surprisingly little is known about biochemical features and exact cellular functions of RINT1 protein. Of note, very recent reports addressing a pivotal role of RINT1 in tumorigenesis, call for more detailed biochemical studies of this protein.

RINT1 is expressed throughout the cell cycle and localized in the cytoplasm, endoplasmic reticulum (ER), Golgi apparatus and centrosome (Xiao, Liu et al. 2001; Hirose, Arasaki et al. 2004; Nakajima, Hirose et al. 2004; Kong, Meloni et al. 2006). Due to its reported association with DNA double-strand brakes repair complex and function in maintenance of telomere length, the nuclear localization of human RINT1 could also be possible (Xiao, Liu et al. 2001; Kong, Meloni et al. 2006). Despite localization of RINT1 protein at the ER and Golgi membranes, RINT1 itself is not considered to be a trans-membrane protein or protein directly associated with the membrane. Experimental results indicate that RINT1 binds to cellular membrane structures *via* protein interaction partners. In that respect, RINT1 interacts with BNIP1, ZW10 and NAG proteins forming a NRZ (NAG-RINT1-ZW10) complex associated with ER SNARE (Hirose, Arasaki et al. 2004; Aoki, Ichimura et al. 2009; Schmitt 2010; Tagaya, Arasaki et al. 2014). This conclusion is supported by *in silico* predictions of hydrophobicity (Kyte & Doolittle) and transmembrane regions of RINT1 (Fig. 1). It Is apparent that no trans-membrane helices of hydrophobic patches reminiscent of transmembrane regions could be identified. Summary of known features of RINT1 protein and comparison between human and mouse RINT1 are presented in Table 1. Interestingly, in human only one isoform of RINT1 have been identified, while in mouse, at least two isoforms of the protein have been described. They are a result of an alternative splicing and differ in 58 amino acids (172 – 229), which are missing in isoform 2 (source: Uniprot).

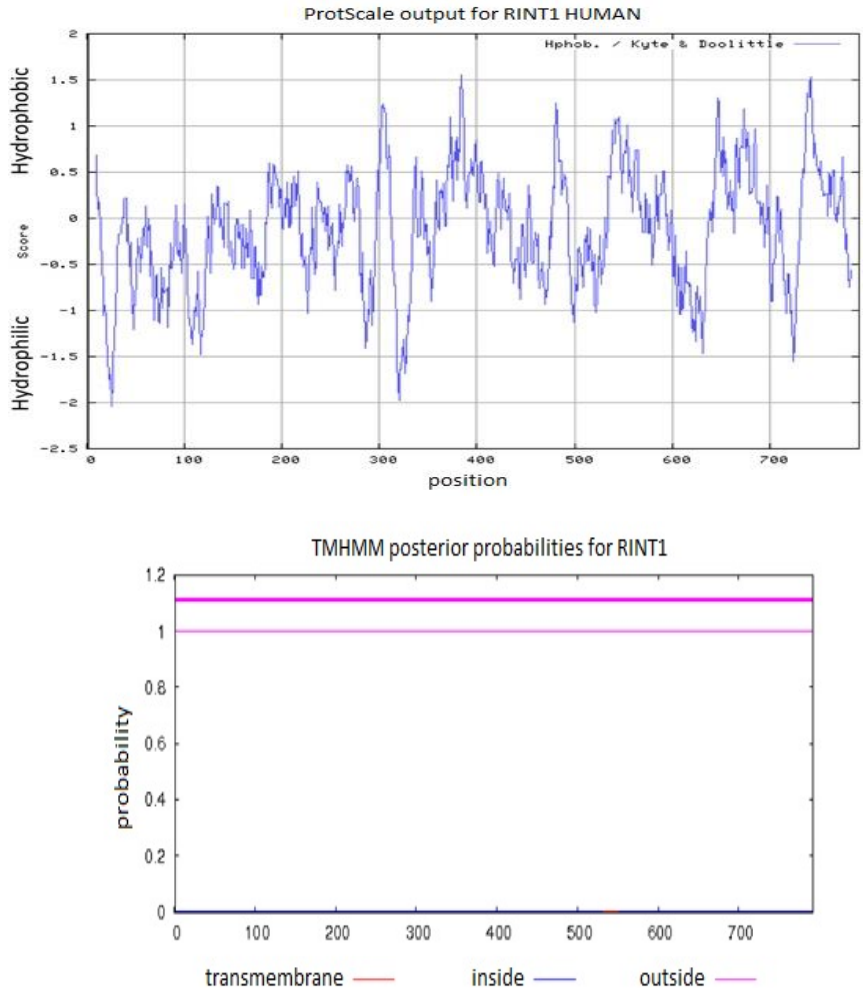

Figure 1. RINT1 is not predicted to be a membrane protein. Hydrophobicity plots and transmembrane region prediction generated with ProtScale (Gasteiger, Gattiker et al. 2003) (upper panel, window size applied = 17) and TMHMM online software (Krogh, Larsson et al. 2001) (lower panel).

Table I. Features of human and mouse RINT1/Rint1.

Feature	*Homo sapiens,* Human	*Mus musculus,* Mouse
Size	792 amino acids, 90 kDa	792 amino acids, 90 kDa
Genomic location	7q22.3	5 A3, 5
Cellular location	ER, cytoplasm, Golgi, centrosome	ER, cytoplasm
Domain	RINT1/TIP20 Position: 304 - 785 aa	RINT1/TIP20 Position: 220 - 792 aa
Coiled coil	Position: 103 – 124 aa	Position: 71 – 123 aa

Source: UniProt database (www.uniprot.org)

1.1.1. Functional RINT1 domains

Several functional and two sequence/structure prediction-based domains have been identified in RINT1. First, a coiled coil (CC) structural motif has been localized between amino acids (aa) 103 and 124 (Table I, UniProt). It is built of alpha-helices forming a supercoil structure potentially suitable for mediating protein-protein or protein-DNA interactions (Burkhard, Stetefeld et al. 2001). A RINT1-characteristic aa stretch from position 220 to 792 was designated as "RINT1/TIP20 domain" on the basis on the high evolutionary conservation of the aa sequence (Fig. A-6, Appendix).

At the functional level, Xiao *et. al.* reported that RINT1 interaction with RAD50 is mediated by protein region at position 257-792 aa ("RAD50 interaction domain") (Xiao, Liu et al. 2001). Similarly, Kong *et. al.* identified the "p130 interaction domain" – position 358-440 aa (Kong, Meloni et al. 2006). Moreover, aa stretch 1-264 identified as the "ZW10 interaction domain" by Arasaki *et. al.* was also reported to be the "COG1 interaction domain" (conserved oligomeric Golgi complex subunit 1) and the "syntaxin 16 interaction domain". (Arasaki, Taniguchi et al. 2006; Arasaki, Takagi et al. 2013). Interestingly, since interactions with ZW10, COG1 and syntaxin 16 are all encompassing CC domain, functional role of the CC structure for mediating protein-protein interaction is highly probable. Figure 2 aligns in graphical way all identified domains of human RINT1 protein.

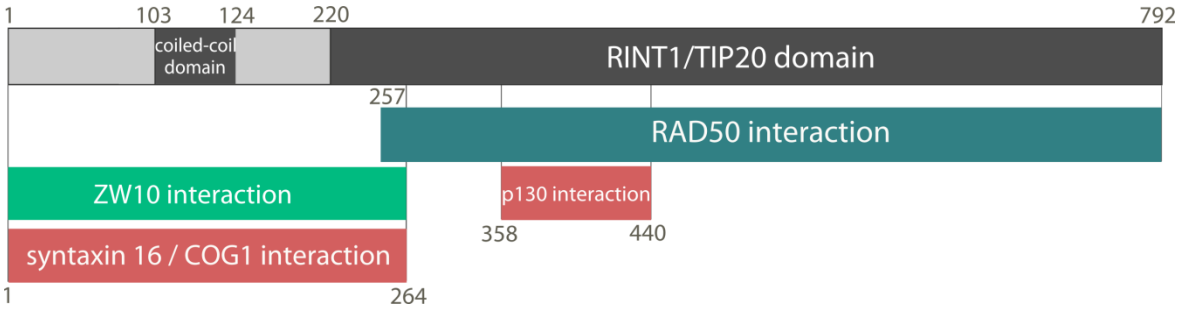

Figure 2. Alignment of functional and "sequence/structure-prediction"-based domains of human RINT1.

1.1.2. RINT1 post-translational modifications

On the basis of published high throughput screens, only few data point towards possibility of post-translational modifications (PTMs) of RINT1. One study reported two putative ubiquitination sites of Rint1, on lysine 69 (Lys69) and on lysine 502 (Lys502), based on proteomic analysis of murine tissue (Wagner, Beli et al. 2011). Subsequent analysis of human multiple myeloma cell line AMO-1, confirmed Lys502 ubiquitination of RINT1 (PhosphoSitePlus database, www.phosphosite.org).

There are few reports regarding phosphorylation of RINT1 protein. Two of them showed modification on serine residue (Ser) at position 10, based on mass spectrometry (MS) analysis of proteins from human male urine sample (Human Proteinpedia, HuPA_00021) and of human cervical cancer HeLA cell line (Sharma, D'Souza et al. 2014). Another piece of data suggesting phosphorylation originated from the in-depth analysis of human liver phosphoproteome and suggested Ser19 to be a phosphorylated residue (Bian, Song et al. 2014). According to MS analysis of human gastric carcinoma samples, threonine (Thr) 94, Ser96 and Ser97 are also subjected to phosphorylation (PhosphoSitePlus database, www.phosphosite.org; NAR, 2012,40:D261-70). Last evidence towards human RINT1 phosphorylation came from the study of Jurkat cell line derived from human T-lymphocyte acute lymphoblastic leukemia (T-ALL). Based on MS data, Ser635 and Thr654 were considered as phosphorylated (PhosphoSitePlus database). Figure 3 summarizes all putative PTMs of Rint1 suggested by the high throughput screen data.

Figure 3. MS-based ubiquitination and phosphorylation sites of RINT1. Scheme represents positions of modified residues: green – ubiquitination (U) on lysine residues, red – phosphorylation (P) on serine residues, blue – phosphorylation (P) on threonine residues.

1.1.3. Phylogenomic analysis of homology and conserved, putative PTMs of RINT1

RINT1 is a prototypic protein of a RINT1 protein family. Its members share sequence similarity with an N-terminal leucine heptad repeat rich coiled, and contain carboxy-terminal "RINT1/TIP20 domain" of ~500-residue length. In general, these proteins play a role in retrograde and anterograde transport between the ER and the Golgi. Besides RINT1, other members are: mouse Rint1 protein *(Mus musculus)*, MAG2 (MAIGO2) and MAG2L protein of *Arabidopsis thaliana*, and RINT1-like protein encoded by the gene CG8605 in *Drosophila melanogaster*. In *Arabidopsis*, MAG2 has a function in transport of storage protein precursors between the ER and Golgi (Li, Shimada et al. 2006). TIP20 (Tip20) is RINT1 orthologue in yeasts *(Saccharomyces cerevisiae)* and it plays a role in the retrograde transport from the Golgi to ER (Sweet and Pelham 1993; Tripathi, Ren et al. 2009).

Phylogenetic tree prediction, based on amino acid sequences of RINT1 homologs, is presented in Figure 4.

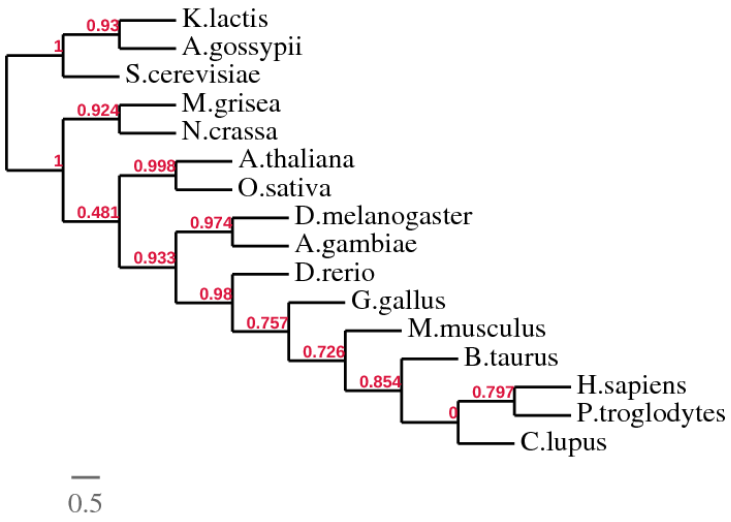

Figure 4. The phylogenetic tree of RINT1 protein. The analysis was performed on the Phylogeny.fr platform (http://phylogeny.lirmm.fr/). The line with the number "0.5" shows the length of branch representing an amount of genetic modification of 0.05 [nucleotide substitution per site]. The phylogenetic tree was reconstructed using the maximum likelihood method implemented in the PhyML program (v3.0). Graphical representation and edition of the phylogenetic tree were performed with the TreeDyn (v198.3) (Castresana 2000; Edgar 2004; Anisimova and Gascuel 2006; Chevenet, Brun et al. 2006; Dereeper, Guignon et al. 2008; Guindon, Dufayard et al. 2010).

Highly evolutionary conserved "RINT1/TIP20 domain" region could be of potential meaning for the identification of residues modified by PTMs. *In silico* prediction of modified residues indicates that RINT1 homologs share evolutionary conserved putative post-translational modification sites. Figure 5 depicts the identified positions and postulated modifications.

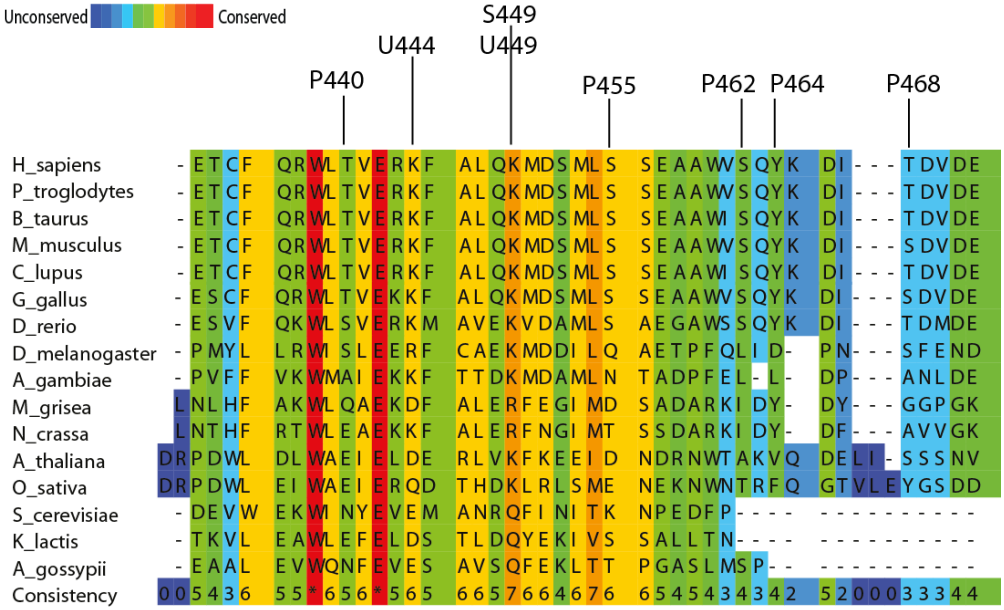

Figure 5. Example of evolutionary conserved RINT1 post-translational modification sites and their localization. The predicted modification sites are indicated: phosphorylation (P), ubiquitination (U) and SUMOylation (S). The number indicates position of the PTM on the human RINT1 amino acid (aa) sequence. The most conserved aa is lysine on the position 449 (K449) and is predicted to be SUMOylated (S449) and ubiquitinated (U449) *(courtesy of Dr. P. Grigaravičius).*

1.1.4. *RINT1* expression pattern in human tissues

High-throughput gene expression profiling allows investigation of transcriptional activity in biological samples of different organisms on a genome scale. Analysis of normal or cancerous tissues, organs or cell lines, gives a tissue-specific pattern of mRNA expression, which can indicate function of the protein encoded by a given gene.

The examination of *RINT1* expression pattern (high-density oligonucleotide arrays; BioGPS database, http://biogps.org) showed that the gene is highly expressed in nervous system,

especially in superior cervical ganglion (a part of the autonomic nervous system), skeletal muscle as well as in immune cells (B-lymphocytes, T-lymphocytes, dendritic cells). The *RINT1* expression higher than average was detected in: tonsil, adrenal cortex, pituitary, fetal thyroid, pancreatic islet, Leydig and interstitial testis cells, smooth muscle, thyroid, liver, heart, uterus corpus, appendix, tongue, retina, in colorectal carcinoma and Burkitts lymphoma.

These results are mostly overlapping with gene expression data stored in another database, Genevestigator (http://Genevestigator.com). According to collected results, *RINT1* is highly expressed in B-lymphocytes, T-lymphocytes, skeletal muscle, heart, brain, eye, salivary gland, colon, rectum, liver, pancreas and macrophages. Figure 6 represents exemplary tissues and cells with medium and high expression of the human *RINT1* gene.

Interestingly, data deposited in Genevestigator concerning *RINT1* expression in cancers, showed its medium to high expression in almost all cancer types, with particularly significant expression potential in colon, liver and pancreas cancers, neoplasms of respiratory system, bone cancers, eye, brain and central nervous system cancers, lymphomas and leukemias.

To judge on their physiological relevance, the gene expression data have to be validated on a protein level. Thus, according to mass spectrometry analyses of the proteome deposited in the MOPED (Multi-Omics Profiling Expression Database) database (www.proteinspire.org), human RINT1 protein is expressed in following tissues: bone, testis, olfactory epithelium, stomach, adrenal gland, liver, rectum, pancreas, colon, salivary, thyroid and adrenal glands, esophagus, frontal lobe, spinal cord, retina, lung, lymph node, B- and helper T-lymphocytes, blood platelet, peripheral blood mononuclear cells, natural killer cell, ovary, placenta, pre-menopause uterus, breast cancer tissue, fetal: ovary, testis, heart, gut and liver.

Therefore, it could be stated that *RINT1* gene expression pattern corresponds well with tissue distribution of RINT1 protein.

A.

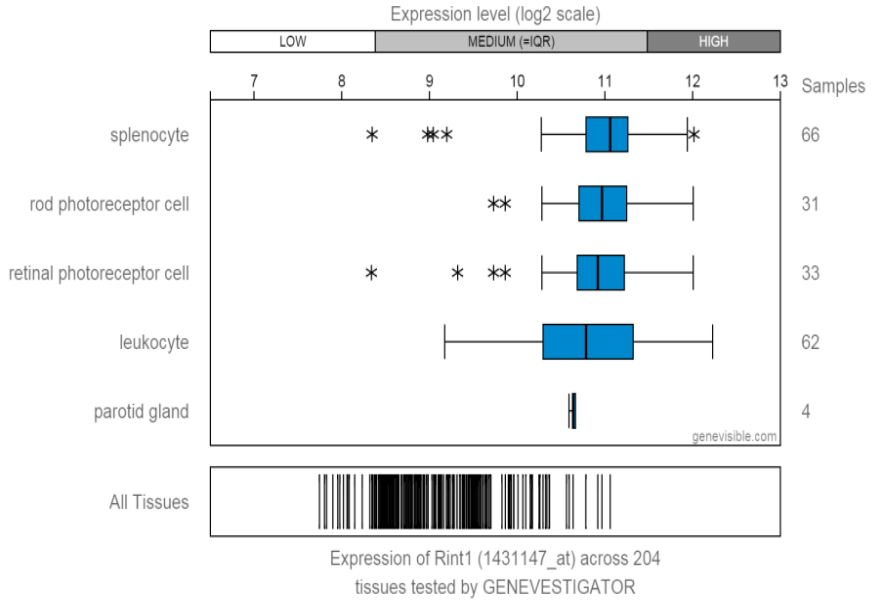

B.

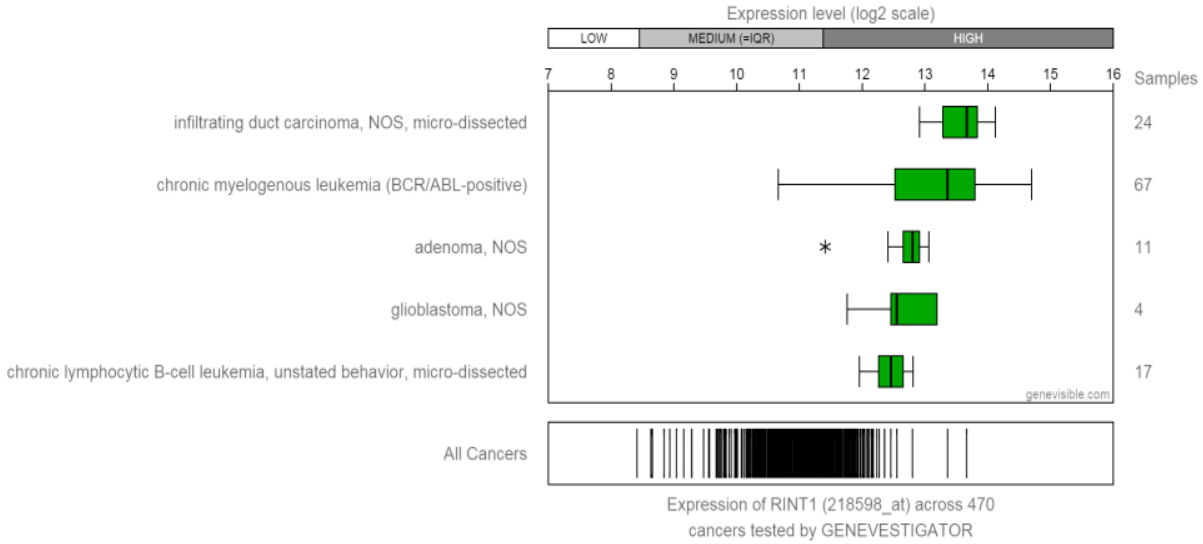

Figure 6. Genevestigator database data showing *RINT1* expression in selected cells and tissues. **A.** *RINT1* expression levels higher than average were found in liver, eye, leukocytes and parotid gland. **B.** Cancer tissues analyzed reveal high expression of *RINT1* in infiltrating duct carcinoma, chronic myelogenous leukemia, adenoma, glioblastoma and chronic lymphocyte B-cell leukemia.

In conclusion, these data indicate that RINT1 is present in tissues of high metabolic rate, *i.e.* heart, liver, brain and skeleton muscle tissue. In addition, presence of RINT1 in cells and tissues, such as nervous system, T-cells and B-cells, support described RINT1 function in cell division (*e.g.* rapid proliferation of T-cells and B-cells upon antigen-induced

activation) and membrane trafficking (*e.g.* antibody production in B-cells and vesicular trafficking at synaptic terminals of neurons).

1.2. Cellular roles of RINT1

Current knowledge about RINT1 functions in, based on miscellaneous research results and places RINT1 amongst multifunctional proteins, participating in very different, spatially and temporarily separate biological pathways. This diversity of RINT1 functions depends on its interactions with various protein-partners, and on the cellular localization. Identified in 2001 as a RAD50-interactor, RINT1 was described for the first time as a protein involved in DNA damage-induced cell cycle checkpoint (Xiao, Liu et al. 2001). Further research studies highlighted its role in other biological processes, such as membrane trafficking (Hirose, Arasaki et al. 2004; Arasaki, Taniguchi et al. 2006; Lin, Liu et al. 2007; Sun, Shestakova et al. 2007; Arasaki, Takagi et al. 2013) and telomere length maintenance (Kong, Meloni et al. 2006). *RINT1* was also reported to be an oncogene and a tumor suppressor gene (Lin, Liu et al. 2007; Quayle, Chheda et al. 2012; Park, Tao et al. 2014).

1.2.1. RINT1 function in DNA repair and double-strand breaks (DSBs)-induced cell cycle checkpoints

In the context of a known role of RINT1 in the maintenance of DNA integrity, particularly interesting cellular processes are: repair of double strand DNA breaks (DSBs), control of G2/M cell cycle checkpoint (Hoeijmakers 2009; Deckbar, Jeggo et al. 2011) and the process of DNA mismatch repair (Park, Tao et al. 2014).

1.2.1.1. DBSs-induced cell cycle checkpoints and DNA mismatch repair (MMR)

As a result of natural metabolic activity of the cells, as well as of the chemical and physical environmental factors, genetic information is exposed to potentially harmful molecular lesions every single day. Once DNA mutation is not properly repaired, it might be

accumulated and lead to premature cell aging or, in case of proliferating cells, be transmitted to the daughter cells during mitosis, thus causing genomic instability. Consequently, at the level of an organism, unrepaired DNA lesions may lead to tumorigenesis, and finally to death. Therefore, permanently active cellular DNA repair processes are necessary to preserve genetic information from destruction, and to restore damaged DNA. Efficient and accurate systems of the DNA damage responses (DDRs), protect genome integrity and guarantee functionality of the cell and accurate cell division (Branzei and Foiani 2008; Ciccia and Elledge 2010). In the course of evolution, cells have developed a number of signaling pathways providing efficient and precise DDRs. Following the detection of DNA damage, molecular complex signaling induces activation of corresponding cell cycle checkpoint (Fig. 7).

The cell cycle checkpoints are specific time-points of the cell cycle, at which it can be stopped if the preceding phase hasn't been properly completed, *e.g.* as a consequence of damaged DNA. There are several cell cycle checkpoints: the G1 checkpoint, named also restriction checkpoint in mammals or start checkpoint in yeast (checking for the DNA damage, cell size, nutrients and growth factors), the G2/M checkpoint (controlling proper DNA replication and cell size), the spindle assembly or metaphase checkpoint (supervising chromosome attachment to spindle), and the intra-S-phase checkpoint (checking for chromosomal DNA structures and replication) – depicted in Fig. 7. Efficient and proper mechanism of the cell cycle control is assured by the family of serine-threonine kinases called cyclin-dependent kinases (CDKs), activated upon their interaction with specific cyclins. For example, the main cyclin-CDK complex driving the G2/M cell cycle checkpoint is Cyclin B-cdc2 (CDK1) complex. When activated, CDKs subsequently activate their substrates characteristic for the specific cell cycle phase and release cascade of downstream processes promoting cell cycle progression.

If the DNA damage occurs and the cell cycle checkpoint is activated, the activity of cyclin-CDKs complexes driving cell cycle transitions is restrained. As a consequence, cell cycle is arrested in G1- (the G1 checkpoint) or G2-phase (the G2/M checkpoint), or the replication in S-phase is slowed down (intra-S checkpoint). This mechanism allows to repair DNA damage and resume the cell cycle, or to completely exit the cell cycle, if the lesions are irreparable (Branzei and Foiani 2008; Shaltiel, Krenning et al. 2015).

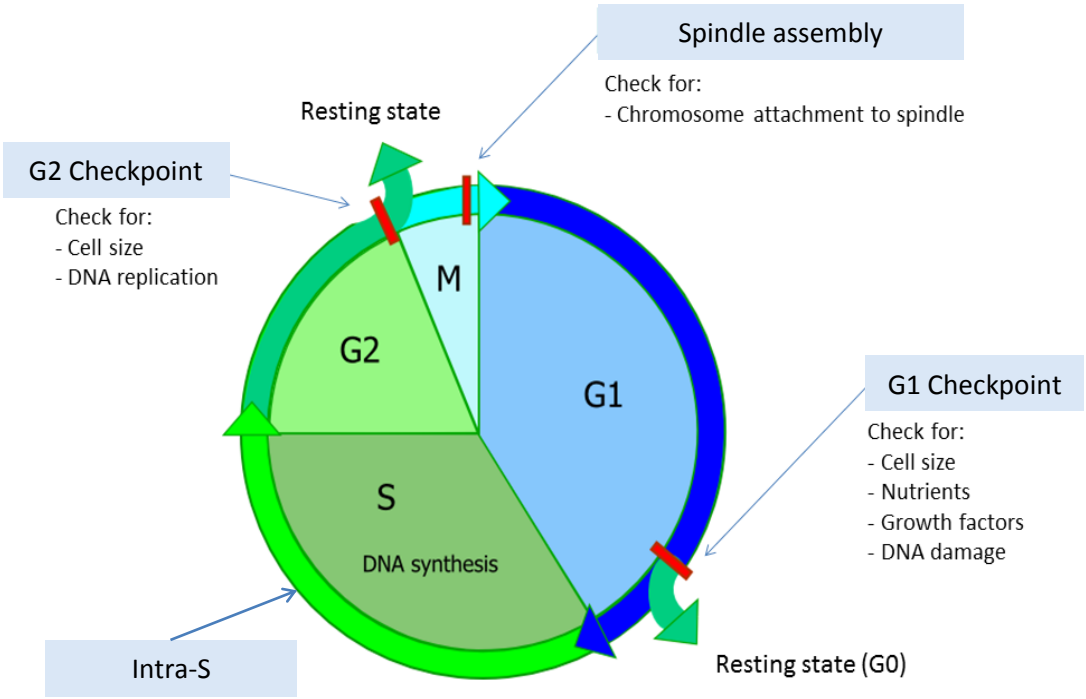

Figure 7. Cell cycle checkpoints. Cell cycle checkpoints assure proper cell cycle progression by monitoring the status of completion of the preceding phase.

Cellular DDR depends both on the stage of the cell cycle, as well as on the character of the DNA damage. There are few common types of DNA damages, which are: base modification, mispairs, cross-linked nucleotides or double-strand DNA breaks (DSBs).

DSBs are especially harmful type of lesions, as they can contribute to structural rearrangements and chromosome missegregation (Hoeijmakers 2009). Response to DSBs in G2-phase induces reversible cell cycle arrest , preventing cell from entering mitosis (M-phase), thereby blocking proliferation of the cell with damaged genomic DNA. DNA repair machinery fixes the damage, mainly by homologous recombination repair (HRR) or non-homologous end joining (NHEJ). The cell can also exit the cell cycle to undergo apoptosis, if the damage is irreparable (Liang, Deng et al. 2005; Klein, Hoffmann et al. 2015).

Activation of the cellular response to DSBs in G2 phase occurs through the recognition of the DNA damage by the MRN complex (proteins: MRE11, RAD50 and NBN), followed by the recruitment and activation of the checkpoint kinase ATM (ataxia telangiectasia

mutated), which phosphorylates and activates its downstream targets (Fig. 8). This particular molecular pathway involves following steps: amplification of the signal by mediator proteins (MDC1, 53BP1, MRN complex, BRCA1), phosphorylation of checkpoint kinases CHK1 and CHK2, and phosphorylation of M-phase inducer phosphatase 3, CDC25C. Under normal conditions, non-phosphorylated CDC25 removes inhibitory phosphate residues from the Cyclin B-CDK1 complex. Dephosphorylation activates the complex thereby triggers entry into the next phase of the cell cycle, the mitosis (Fig. 8). Phosphorylation of active CDC25C by CHK1 inhibits its activity and, as a consequence, Cyclin B-CDK1 remains phosphorylated by protein kinase WEE1, thus inactive. The transition from G2 to M phase is inhibited. The block of CDK1 function is the most essential stage of this pathway (Lobrich and Jeggo 2007; Matsuoka, Ballif et al. 2007; Ciccia and Elledge 2010; Langerak and Russell 2011).

One of the key-regulators of DNA repair and stress-induced cell cycle arrest is the p53 protein, which levels are regulated by Mdm2 E3 ubiquitin ligase. The role of p53 in the regulation of the cell entry into mitosis is well established. DNA damaging factors, such as UV or ionizing radiation, activate the DDR; ATM/ATR kinases phosphorylate p53 protein directly, or activate CHK2 kinase also phosphorylating p53. Modification of p53 activates the protein and leads to its stabilization and induction of its DNA binding activity and transcriptional regulatory response. Moreover, upon activation p53 indirectly inhibits cdc2, required for entering the mitosis, by regulating three targets: (i) 14-3-3, which binds to phosphorylated Cyclin B-cdc2 complex and exports it from the nucleus, (ii) GADD45, binding and dissociating Cyclin B-cdc2 complex, and (iii) p21 Cip1, inhibiting several CDKs, and among them cdc2 (Taylor and Stark 2001; Hein, Ouellette et al. 2014).

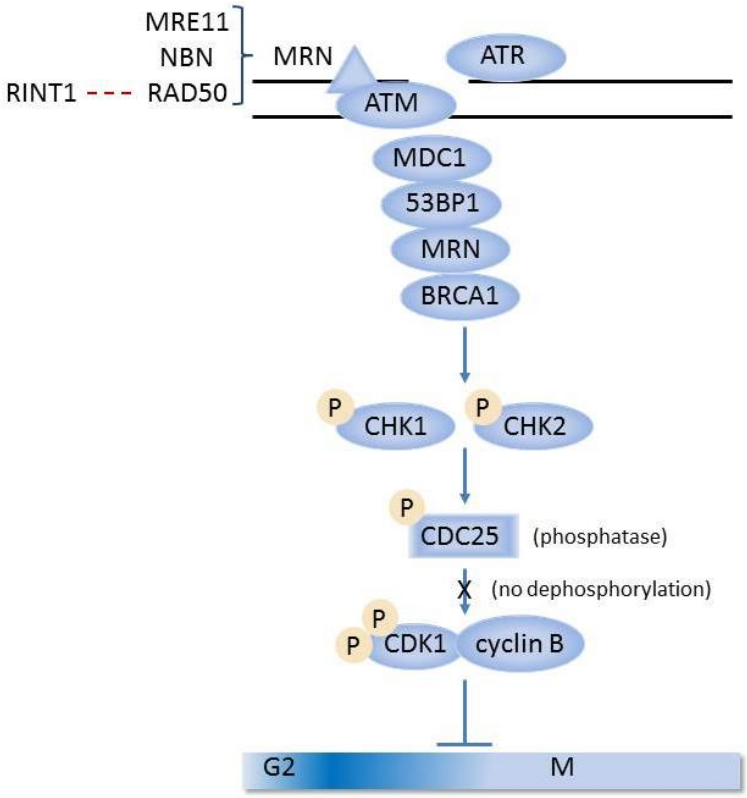

Figure 8. Molecular pathway of double-strand breaks (DSBs) repair and G2/M checkpoint activation (adapted from Löbrich *et al.* (Lobrich and Jeggo 2007)). ATR protein responds to single stranded DNA.

DNA damages that occur during DNA replication and recombination, such as small insertions, small deletions or base-base mismatches (G/T or A/C pairing), are repaired *via* the DNA mismatch repair (MMR) pathway. This allows for genomic stability maintenance by control of the cell cycle arrest and cell death. The mechanism of DNA mismatch repair was investigated and described in great details based on the studies in *E. coli*. Nevertheless, as a highly conserved process, MMR exhibits substantial similarities between *E. coli* and human, *i.e.* in substrate specificity and bi-directionality. Briefly, the process of MMR in humans begins with the detection of damaged DNA fragment by the MMR machinery. Heterodimer MSH (MutS homologs, hMutSα (MSH2-MSH6), hMutSß (MSH2-MSH3)) recognizes small insertions. In turn, deletions and mismatched bases and the template and non-template DNA strands are determined. Heterodimeric hMutLα (MLH1-PMS2), which endonucleolytic activity depends on the PCNA and RFC proteins, interacts with MSH to increase the detection of mismatched DNA. MutLα is responsible

for the incision 5' to the mismatch. The excision of damaged DNA is catalyzed by the EXO1 exonuclease (5'→3' excision), while the DNA polymerase Pol δ drives DNA re-synthesis. The incorrect nucleotide and adjacent base pairs are eliminated and replaced by matching bases. During this step, single-strand DNA-binding protein RPA plays an important role in the termination of DNA excision and stimulation the process of DNA re-synthesis. DNA ligase I is responsible for the nick ligation (Li 1999; Stojic, Brun et al. 2004; Kunkel and Erie 2005; Iyer, Pluciennik et al. 2006; Hsieh and Yamane 2008; Li 2008). Failures in appropriate completion of the MMR process caused by gene mutations result in predisposition to diseases and serious dysfunctions, *i.e.* cancers related to the Lynch syndrome (mutations in genes: MLH1, MSH2, PMS2), sporadic cancers, resistance to chemotherapeutics or sterility in mammals (Modrich and Lahue 1996; Kunkel and Erie 2005).

1.2.1.2. Role of RINT1 in DNA repair and DNA damage-induced cell cycle checkpoints

RINT1 protein was discovered in the context of irradiation-induced G2/M checkpoint control (Xiao, Liu et al. 2001). It was identified by yeast two-hybrid (Y2H) screen of a human B-cell cDNA library using a C-terminal fragment of human RAD50 protein as a bait. RAD50 is one of the SMC (structural maintenance of chromosomes) protein family members, and as component of the MRN complex, participates in DSBs repair (Fig. 8). The interaction between RINT1 and RAD50 was detected specifically during late S and G2/M phases of the cell cycle. Expression of an N-terminally truncated, dominant negative mutant of RINT1, which binds to RAD50, led to delay of G2/M cell cycle checkpoint following γ-irradiation. These observations suggested a role of RINT1 in G2/M cell cycle checkpoint regulation after DSBs repair (Xiao, Liu et al. 2001).

1.2.1.3. RINT1 and DNA mismatch repair (MMR)

Recently, RINT1 function has been putatively linked to the Lynch syndrome (LS), a disease caused by the mutations in genes encoding proteins of the MMR pathway (Park, Tao et al. 2014). The exome-sequencing study of multiple case breast cancer family members,

detected three rare *RINT1* mutant variants (*RINT1* c.343C>T (p.Q115X), c.1132_1134del (p.M378del), c.1207G>T (p.D403Y)), predisposing their carriers not only to breast cancer, but also to the LS, a disease often called hereditary nonpolyposis colorectal cancer (HNPCC). LS is hereditary autosomal dominant genetic disease resulting in predisposition for colon cancers, but also other cancer types such as stomach and liver cancers, cancer of the small intestine, upper urinary tract cancer, cancer of skin, brain and hepatobiliary tract. In women, the LS increases probability of ovary and endometrium cancer (Kohlmann and Gruber 1993; Park, Tao et al. 2014). LS-affected individuals have a lifetime risk for colon cancer of 80%. The prevalence of the LS was estimated to be 1-3% (de la Chapelle 2005). At molecular level, the LS is caused by a defective MMR pathway and germline defects in mismatch repair genes: *MLH1, MSH2, MSH6, PMS2* or *EPCAM* (Jang and Chung ; Peltomaki 2005; Tiwari, Roy et al. 2015). Thus, it is a matter of question, what is the role of *RINT1* in the MMR pathway and how this gene function could be linked to the occurrence of the Lynch syndrome.

1.2.2. RINT1 and ER-Golgi trafficking

1.2.2.1. Membrane trafficking

Membrane trafficking, named also vesicle trafficking, refers to the cellular activity by which proteins as well as other macromolecules are administered and distributed throughout the cell and released to, or incorporated from the extracellular milieu. It is thus a core mechanism in cellular biosynthesis, secretion and endocytosis, underpinning cell homeostasis. Membrane trafficking processes are inseparably connected with the cytoskeleton, cell metabolism, signaling, movement and proliferation (Bonifacino and Glick 2004).

Fundamental structures in membrane trafficking network are endoplasmic reticulum (ER) and Golgi apparatus. These are two organelles constitute the major route of vesicular transport. Briefly, ER functions as an organelle where the synthesis of proteins and membrane lipids takes place. The Golgi is responsible for packaging proteins received from the ER into membrane-bound vesicles before their shuttle to the final place of destination. Golgi itself consists of compartments forming two networks: the *cis* Golgi

network (CGN), originating from fused cargo-bearing vesicles coming from the ER, and the *trans* Golgi network (TGN), a terminal structure of Golgi, where cargo is bundled up into vesicles and transported to the target compartment (Fig. 9). Vesicle transport from the ER to Golgi complex is called anterograde transport, while in the opposite direction is named retrograde transport (Bonifacino and Glick 2004; Guo, Sirkis et al. 2014; Spang 2015).

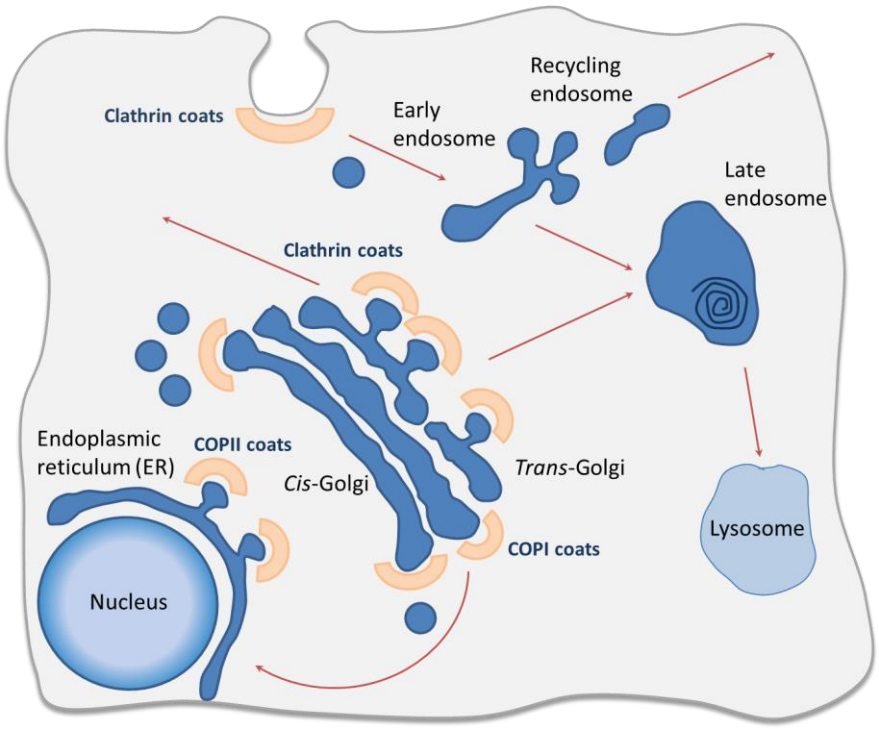

Figure 9. Membrane vesicular trafficking in the cell (adapted from Kirchhausen *(Kirchhausen 2000)*).

Highly organized and dynamic network of membrane-bounded vesicles mediates the intracellular shuttle processes. Transported proteins are associated with vesicle membranes or enclosed within them. The transport occurs in a step-wise manner, and each step is precisely regulated by the complex molecular machinery controlling sorting and burdening of cargo, as well as vesicle movement and unloading of transported molecules. Characterization of the proteins required for cargo selection, loading and carrier budding, allowed to identify three different types of transporting vesicles: (i) COPI- (coat-protein complexes I) coated, (ii) COPII- (coat-protein complexes II) coated and (iii) clathrin-coated vesicles (CCVs) (Fig. 9). The COPI- and COPII-coated vesicles participate in the secretory pathway (retrograde and anterograde transport) and CCVs are a part of the

transport within the endosomal membrane system and mediate endocytosis at the plasma membrane. COP-vesicles are made of large protein complexes consisting of seven (in case of COPI) or four (in case of COPII) coat-protein subunits and associated small GTPases (hydrolase) enzymes, participating in the cargo loading. Clathrin-coated vesicles are critical for the process of endocytosis, thus ensure the import of proteins and lipids from the extracellular milieu. Clathrin made of polypeptide chains building three-legged structures named triskelions aggregates with the help of adaptin protein complex to form coated cavities on the surface of a membrane (the vesicular coat) while GTPase separates the mature CCV from the membrane (Schekman and Orci 1996; Nickel, Brugger et al. 2002; Bonifacino and Glick 2004; Saito and Katada 2015).

Other group of proteins needed for accurate membrane trafficking are NSF (N-ethylmaleimide-sensitive factor) and SNARE (soluble NSF attachment protein receptor, SNAP receptor) proteins, which mediate docking and fusion of transport vesicles with their target membrane compartments. The SNAREs could be divided into two classes: vesicle or v-SNAREs, incorporated into the membranes of transport vesicles during budding process, and target or t-SNAREs, located in the membranes of destination compartments (Bonifacino and Glick 2004; Jung, Inamdar et al. 2012; Stow 2013; Meng and Wang 2015).

1.2.2.2. RINT1 function in membrane vesicle trafficking and dynamic integrity of the Golgi apparatus and centrosome

Valuable information about putative role of RINT1 in membrane vesicle trafficking and correct cell cycle progression were provided by the RNA interference (RNAi) experiments performed in HeLa cells (Lin, Liu et al. 2007). The experiments demonstrated that depletion of *RINT1* led to dispersal of Golgi apparatus and loss of its pericentrioliar location, with simultaneous centrosome amplification in interphase. Further studies on synchronized cells shown that *RINT1*-depleted cells exhibited various abnormalities upon the mitotic entry: missegregation of chromosomes, multiple spindle poles formation and abnormal Golgi dynamics during early mitosis as well as incorrect reassembly of Golgi in the telophase. As a consequence of faulty mitosis and multiple cellular defects, cells

underwent cell death. Concluding, based on the research of Lin and colleagues, RINT1 was found to be a protein essential for dynamic integrity maintenance of both centrosome and Golgi apparatus.

Other studies confirmed significance of RINT1 for vesicle trafficking (Fig. 10). Extensive binding assays shown that RINT1 interacts with ER-localized t-SNARE, syntaxin 18 (Table II), thus it is involved in the regulation of the membrane trafficking between ER and Golgi. Together with ZW10, p31 and NAG proteins, RINT1 forms subcomplex which is a peripheral membrane component of SNARE, essential for both retrograde and anterograde membrane flow (Hirose, Arasaki et al. 2004; Aoki, Ichimura et al. 2009; Schmitt 2010). Immunoprecipitation studies demonstrated direct interaction of RINT1 with the conserved oligomeric Golgi complex (COG) subunit 1 (COG complex subunit 1), which is required for appropriate Golgi morphology and function. Thus, in coordination with the COG complex, RINT1 regulates SNARE complex assembly at TGN. Interestingly, N-terminal ZW10-interaction domain of RINT1 overlaps with COG1 interaction domain of RINT1 (Fig. 2), suggesting existence of some kind of “shifting” mechanism.

Another study on RINT1 and vesicular trafficking uncovered important role of ZW10/RINT1 complex in appropriate Rab6-dependent membrane trafficking and homeostasis. Rab6 belongs to the family of Rab GTPases, which promotes Golgi-to-ER retrograde trafficking (Sun, Shestakova et al. 2007). Participation of RINT1 in endosome-to-TGN vesicle trafficking was discovered *via* its interaction with the SNARE domain of syntaxin 16 (Sun, Shestakova et al. 2007; Arasaki, Takagi et al. 2013). Not surprisingly, *RINT1* knock-down in HeLa cells blocked endosome-to-TGN membrane flow and led to redistribution of protein markers of TGN (Arasaki, Takagi et al. 2013). Figure 10 summarizes known interactions of RINT1 with components of the ER and TGN SNAREs, while in Table II lists all known RINT1 interactors together with functional significance of the given interaction.

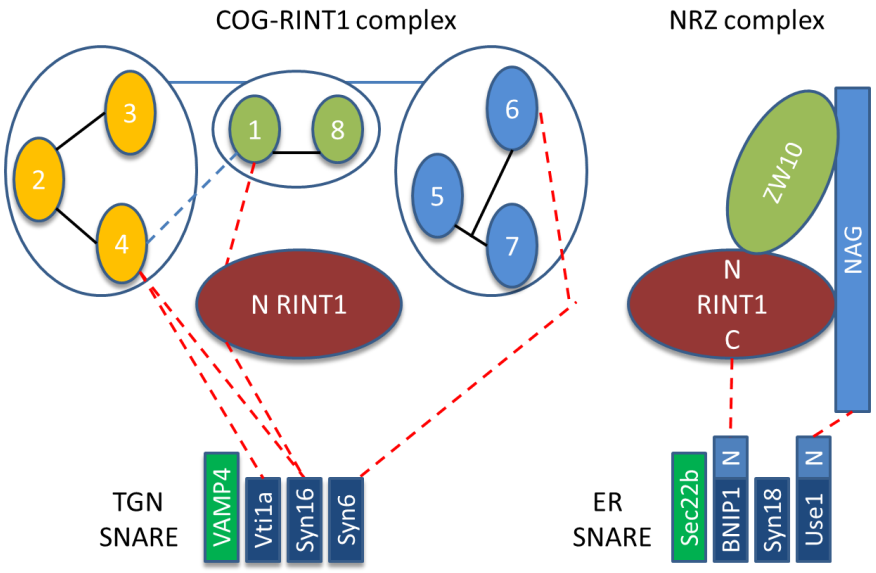

Figure 10. The interactions of RINT1 with tethers and SNAREs in the TGN and ER (adapted from Tagaya *et. al.* (Tagaya, Arasaki et al. 2014)). SNARE binds the COG complex through RINT1 (left panel). RINT1 and NAG bind to N-terminal regions of BNIP1 and Use1/p31, respectively (right panel). N and C represent N- and C-terminal regions of the protein. Numbers 1-8 indicate subunits of COG (Cog1 – Cog8) organized in three heterodimeric subcomplexes. Dashed lines indicate connections between proteins/SNAREs.

Table II. RINT1 interaction partners and functions of the interactions.

Name of RINT1 partner	Function of the interaction
BNIP/SEC20L	ER-Golgi trafficking (Nakajima, Hirose et al. 2004)
COG complex subunit 1	vesicle trafficking (Arasaki, Takagi et al. 2013)
UVRAG	positive regulator of the ER-tether in Golgi-ER retrograde transport, *cis*-Golgi maintenance (He, Ni et al. 2013)
p130 (RBL2, retinoblastoma-like 2)	telomerase-independent telomere length maintenance (Kong, Meloni et al. 2006)
RAD50	irradiation-induced G2/M cell cycle checkpoint regulation (Xiao, Liu et al. 2001)
syntaxin 16 (STX16)	endosome-to-TGN trafficking (Arasaki, Takagi et al. 2013)
syntaxin 18 (STX18)	ER-Golgi trafficking (Hirose, Arasaki et al. 2004; Aoki, Ichimura et al. 2009; Civril, Wehenkel et al. 2010)
ZW10	ER-Golgi trafficking (Hirose, Arasaki et al. 2004; Arasaki, Taniguchi et al. 2006)

1.2.3. Oncogenic and tumor suppressor functions

1.2.3.1. Oncogenes and tumor suppressor genes

Oncogenes and tumor supressor genes are the key players in cancer development. Both classes of genes encode proteins involved in cell growth control and proliferation.
The oncogenes are derived from proto-oncogenes, which code for proteins enhancing cell growth and division, controlling cell cycle progression or proteins inhibiting cell death. Thus, products of oncogenes are aberrant versions of proteins normally involved in molecular signal transduction cascades mediating growth, proliferation or pro-survival signals, such as membrane receptors, proteins transporting the signal across the cytoplasm, and finally, transcription factors in the nucleus activating *e.g.* genes responsible for cellular division. Importantly, oncogenic versions of proteins, being dominant, tend to activate signaling pathways unceasingly, resulting in excessive production of cell growth stimulators, thus contributing to development of cancer.

Alteration from an oncogene to the proto-oncogene might be a result of mutation. It could also be a consequence of chromosomal rearrangement changing genomic location of the proto-oncogene (*e.g.* a novel location results in strong transcription of proto-oncogene due to hyper-activated gene promoter of novel gene locus or in fusion with other highly expressed protein, *e.g.* BCR-Abl). A shift from proto-oncogene to oncogene could also be caused by an increase in number of gene copies (*e.g.* duplication). In addition, conversion from proto-oncogene to an oncogene could be an effect of infection and resulting insertions of viral DNA disrupting correct genomic architecture of proto-oncogene.

All of these processes result in gain-of-function mutations. Moreover, since most of the oncogenes carry dominant mutations, only single copy of mutated proto-oncogene may result in cancerous transformation. If such mutation occurs in germ line cells, offspring will acquire predisposition to tumor formation.

Exemplary proto-oncogene is c-Myc gene, which encodes a transcription factor and controls expression of plethora of genes involved in cellular growth, proliferation and differentiation. Mutations in this gene transforms it to an oncogene associated with most

forms of cancers. Another example of proto-oncogene is Ras, which, if mutated, causes unrestrained cell growth. Products of Ras gene are involved in kinase signaling pathways controlling gene transcription and regulating cell growth and differentiation. Another oncogene is Src, the first oncogene described. It encodes a tyrosine kinase, regulating cellular growth, differentiation and motility.

Moreover, viruses may carry their own oncogenes, which are transduced to infected cells. These include: Tax protein deregulating cell cycle and encoded by human T-lymphotropic virus (HTVL), E6 and E7 proteins inactivating tumor supressor proteins p53 and pRb, respectively, carried by human papilloma viruses (HPV16 or HPV18), or v-FLIP protein inhibiting pro-apoptotic proteins caspase 8 and 10 and encoded by human herpesvirus 8 (HHV-8).

Tumor suppressor gene, or anti-oncogene, usually encodes protein inhibiting cell proliferation or leading to cellular death, and therefore naturally preventing tumor growth. When mutated and lacking their original function, tumor suppressor genes lead to deregulation of cell growth and proliferation processes. Mutations are usually recessive, meaning that both copies of a gene are mutated, and lead to a loss-of-function.

An example of the disease caused by mutated tumor suppressor gene, is retinoblastoma, a tumor developing in early childhood due to dysfunction of Rb gene (Giacinti and Giordano 2006). Other example is familial adenomatous polyposis of the colon (FAP), generated by mutations of APC gene, which product controls the availability of transcription factor ß-catenin (Ficari, Cama et al. 2000). Hereditary breast cancer results from mutations of BRCA2 tumor suppressor gene, and hereditary breast and ovarian cancer is related to mutations in BRCA1 gene (Lee and Muller 2010). Another important tumor suppressor gene is TP53, encoding transcription factor p53 regulating cell division and cell death. Its mutation is related with cancers of colon, breast and lung. Moreover, modified p53 protein is involved in leukemias, lymphomas, sarcomas, and neurogenic tumors (Royds and Iacopetta 2006; Olivier, Hollstein et al. 2010).

1.2.3.2. Oncogenic and tumor suppressor function of RINT1

In line with extensive function of RINT1 in controlling the ER-Golgi homeostasis, RINT1-depleted cells exhibited abnormalities in Golgi dynamics and integrity as well as improper functioning of centrosome during cell division (Arasaki, Taniguchi et al. 2006; Lin, Liu et al. 2007; Arasaki, Takagi et al. 2013). Such observations suggest tumor suppressor function of RINT1. The tumor suppressor role was confirmed by the study demonstrating that *Rint1* is involved in the tumor development in mice. Inactivation and heterozygous loss of *Rint1* led to tumor formation in about 81% of knock-out mice. Interestingly, homozygous deletion of *Rint1* caused early embryonic lethality and the failure of blastocyst outgrowth *ex vivo* (Lin, Liu et al. 2007). Another, recently published data revealed, that *RINT1* could be a gene predisposing to breast cancer. Multiple-case, breast cancer family whole exome sequencing analysis, showed that rare *RINT1* sequence variants may lead to the development of breast cancer and to Lynch syndrome-spectrum cancers (Park, Tao et al. 2014). Since another known function of RINT1 is telomerase-independent telomere length maintenance realized by RINT1 interaction with Rb-related, p130 protein (Kong, Meloni et al. 2006), a RINT1 mutation could potentially lead to decreased chromosomal stability, and thus contribute to tumorigenesis.

However, there are also studies showing that *RINT1* is a cancer-promoting gene. The gain- and loss-of-function screens identified *RINT1* as a novel oncogene in glioblastoma (Quayle, Chheda et al. 2012). Other research results demonstrated that high expression of RINT1 in low-grade glioma patients was associated with higher risk of epileptic seizure occurrence (Fan, Wang et al. 2014).

Figure 11 summarizes cellular processes involving RINT1 and regulatory interactions described until now.

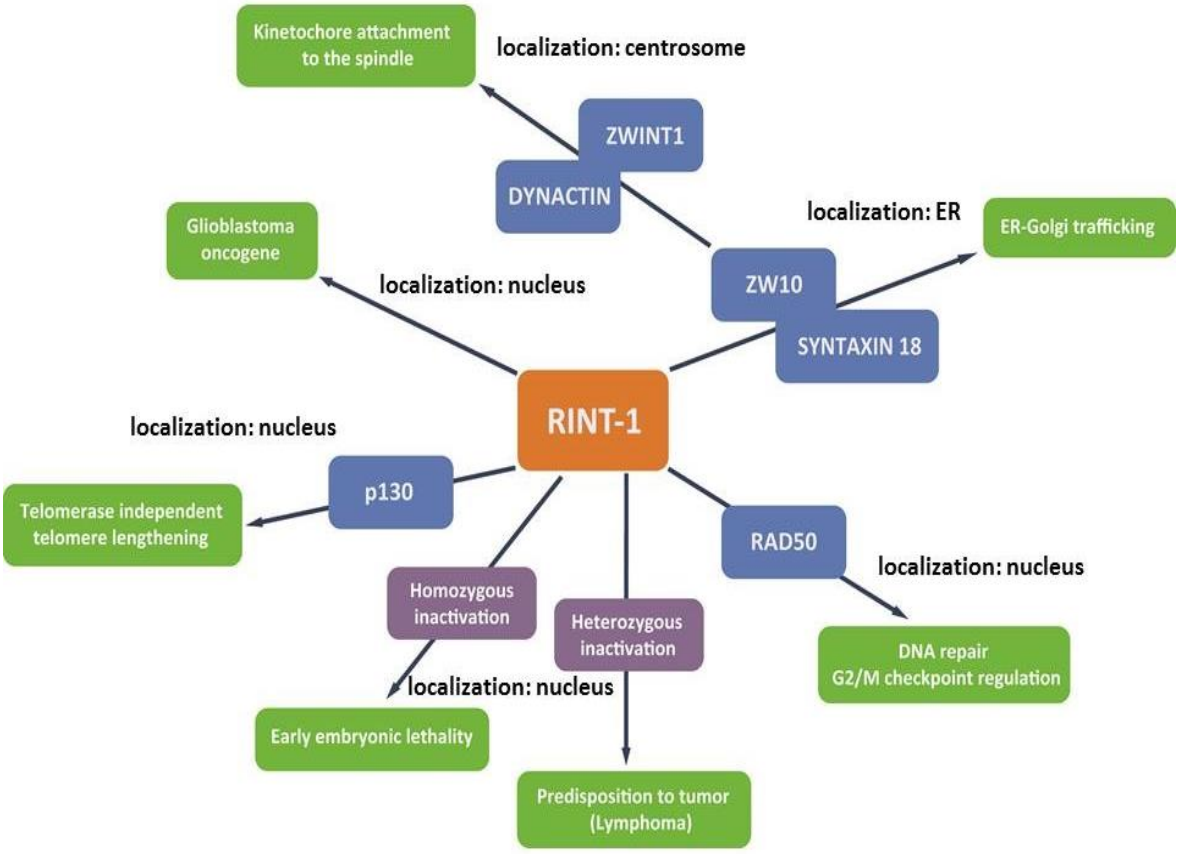

Figure. 11. Cellular processes involving RINT1 and their cellular localization together with respective interaction partners.

1.3. General mechanisms regulating protein functions

In order to provide and control accurate functioning of the cell, proteins need to be precisely regulated. The protein regulatory mechanisms could be divided into several groups: transcriptional and translational control, processes modifying spatial localization of the proteins, covalent or non-covalent interactions with effector molecules, control of the quantity and lifetime of active proteins and control of protein activity due to changes of intracellular pH and redox environment. A single protein may be subjected to various regulatory operations (Perutz 1989; Goodsell 1991; Jensen and Shapiro 2000; Kornitzer and Ciechanover 2000).

Significant category of mechanisms influencing protein function are post-translational protein modifications (PTMs). They are fundamental and powerful biochemical tool influencing whole proteome, thereby having an impact on various aspects of cell biology,

(*i.e.* modification of tubulin leads to diversity in microtubules, which differ depending on the cellular developmental stage, cell compartment, or the cell cycle stage (Song and Brady 2015)). By modulating protein activity, localization, fate, and interaction with other molecules, PTMs increase functional diversity of proteins. Sometimes reversible and very often enzyme-mediated (*e.g.* ligases, phosphatases, kinases), PTMs are executed by: (i) the covalent addition of functional groups or specific molecules to the proteins, (ii) by the cleavage of different regulatory subunits or (iii) by the degradation of the proteins. Ubiquitination, phosphorylation, methylation, acetylation, SUMOylation and glycosylation, are among the most ubiquitous and important PTMs (Hunter 2007; McDowell and Philpott 2013).

Importantly, precise mechanisms controlling cellular functions of RINT1 are not yet known or described. Foremost, there was no functional data available regarding RINT1 PTMs until now.

1.3.1. Regulation of protein lifetime

One of the ways to regulate protein function is to control its lifetime. Half-life of a protein may vary from few minutes to many days, depending on the stability of protein structure and on the cellular mechanisms and rates of the degradation. Proteins of the shortest half-life are generally significant for crucial cellular processes, therefore, usually involved in the regulation of cell growth and proliferation or catalyzing important steps in metabolic signaling. Fast adjustment of the concentration of a gene product, allows for rapid response to environmental changes and provides cellular homeostasis (Hochstrasser 1995; Toyama and Hetzer 2013). Moreover, selective protein degradation regulates the relative timing of molecular events in the cell (Liu, Urbe et al. 2012) and is indispensable for removing proteins that are no longer needed, even if still functional. Another important function of protein lifetime regulation is to eliminate damaged and potentially harmful proteins. Once misfolded or subjected to abnormal PTM, protein may become toxic and unwanted component of the cell and cause, so called “protein deposition diseases”, such as Alzheimer’s disease, Huntington’s disease (HD), Parkinson’s disease, Amyotrophic Lateral Sclerosis (ALS) or spongiform encephalopathies (Kaytor and

Warren 1999; Bucciantini, Giannoni et al. 2002; Goldberg 2003; Haynes, Titus et al. 2004; Ciechanover and Kwon 2015).

One of the characteristics of the intracellular protein degradation, is its dependence on the cellular energetic status (ATP pool). Another important feature is its processiveness; meaning, that if a protein is selected for the degradation, it is completely degraded to small peptides and no intermediate larger fragments are produced (Ciechanover 2005).

In eukaryotic cells proteasomal degradation pathway and lysosomal degradation pathway constitute major mechanisms leading to protein degradation.

1.3.1.1. Proteasomal degradation of proteins

Proteasomal degradation or the ubiquitin-proteasome system, is the major pathway of protein degradation. It is thought to occur in both the nucleus and the cytoplasm (Floyd, Trausch-Azar et al. 2001; von Mikecz, Chen et al. 2008). Nevertheless, recent studies question the possibility of nuclear proteasomal degradation (Chen and Madura 2014). In order to be subjected to proteasomal degradation, protein has to be covalently modified by a chain of ubiquitin polypeptide at first (Fig. 14). Then, tagged for the degradation by polyubiquitination, a target protein binds to the 26S proteasome, situated in the cytoplasm (Fig. 12). 26S proteasome is a highly specialized and very large (~2.5 MDa) ubiquitin-dependent protease, that consists of at least 32 different polypeptides, forming a complex (Fig. 14).

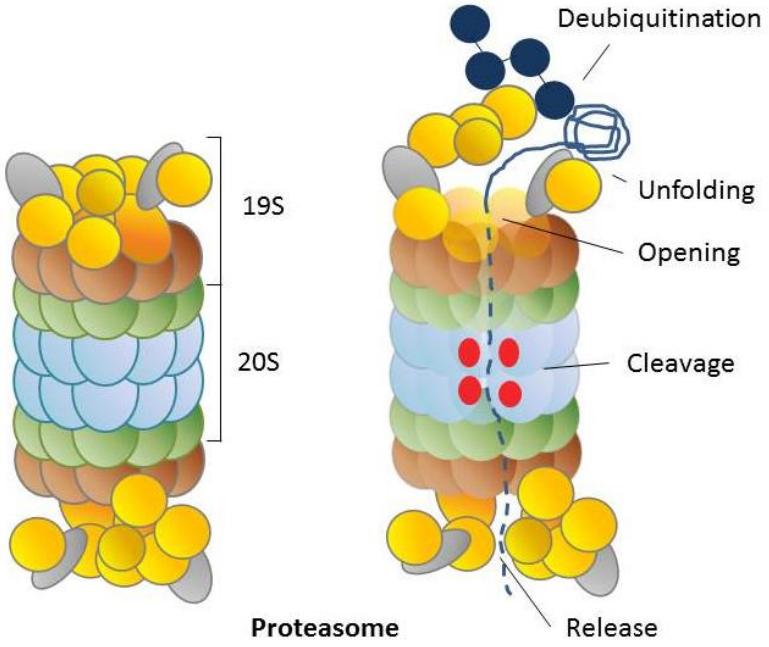

Fig. 12. Schematic subunit composition of the 26S proteasome and proteasomal protein degradation. 20S catalytic core complex and two 19S regulatory complexes constitute the 26S proteasome (left panel). The proteasome recognizes Ub-tagged protein and initiates degradation at a relaxed region of the substrate. The protein is translocated through the degradation channel, cleaved into peptides and finally released (right panel).

Prior to proteolysis within the 26S proteasome, polyubiquitin chain tag has to be removed from the substrate by deubiquitinating enzymes, located in the 19S regulatory subcomplexes (or caps) of the proteasome (Fig. 14). Moreover, these parts of the protease contain ATPase subunits that use the energy of ATP hydrolysis to perform unfolding of the protein. Such processed protein is subsequently translocated to the core of 26S proteasome, a central 20S subcomplex forming a hydrolytic chamber, where processive proteolysis takes place. As a consequence, small peptides of ~8 to 12 amino acids are generated and released from the proteasome.

1.3.1.2. Non-proteasomal degradation of proteins

1.3.1.2.1. Lysosomal proteolysis

Protein degradation may also occur in lysosomes, which are membrane-enclosed organelles, containing a variety of hydrolytic proteases. Proteins that are to be degraded by this mechanism are shifted to lysosomes and subjected to the intra-lysosomal proteolysis. In particular, selective proteolysis of the cytosolic substrates is fulfilled by the recognition of the dedicated peptide sequence (related to the sequence Lys-Phe-Glu-Arg-Gln) on a given protein, which results in subsequent sorting towards lysosome. Another particular feature of the lysosomal degradation is conferred by the regulatory function of intra-lysosomal pH, *i.e.* lysosomal proteases of cathepsin family are active only under highly acidic pH conditions of the lysosome (pH 4.8) (Ciechanover 2005; Schulze, Kolter et al. 2009; Appelqvist, Waster et al. 2013).

1.3.1.2.2. Autophagy

Generally, autophagy is a cellular mechanism to degrade random cytoplasmic proteins under stressful conditions, *e.g.* during starvation. In such unselective mode autophagy can also play a role in programmed cell death. However, in its selective mode autophagy contributes to repair of damaged organelles (*e.g.* mitophagy - selective digestion of damaged mitochondria) or could be strictly linked with the lysosomal pathway of protein degradation. Selective autophagy is a complex process, based on cargo-specific autophagy receptors and tightly regulated on a molecular level.

Autophagy involves enclosing organelles and cytosol within double-membrane structures, which are subsequently degraded by the lysosome. The whole process starts with the formation of a transient pre-autophagosome (PAS). Next, two-lipid bilayers-surrounded organelle, the autophagosome (Fig. 13) is formed, which insulates the cytoplasmic structures that are to be degraded. Subsequently, outer membrane of autophagosome is fused with lysosome, creating a membranous vesicle within lysosome. This structure, called an autophagic body, is decomposed and its interior digested by lysosomal enzymes (Noda, Suzuki et al. 2002; Klionsky 2007; Levine, Mizushima et al. 2011).

Over 30 genes and their products have been identified as autophagy-related (Atg) and classified into one of the following groups: (i) ULK1 kinase complex, responsible for the autophagy induction, (ii) Atg9, involved in the recycling of the membrane, (iii) PI3K complex I (including beclin 1), which drives autophagosome formation (isolation of membrane nucleation, elongation and completion) (iv) PI(3)P-binding ATG2-ATG18 complex, (v) ubiquitin-like protein conjugation system ATG5-ATG12/ATG16L1, essential for the pre-autophagosome creation, and (vi) ubiquitin-like protein conjugation system LC3-PE (LC3-phosphatidylethanolamine), playing a role in membrane expansion. The ULK1 complex is negatively regulated by a mammalian Target of rapamycin complex 1 (mTORC1) kinase (Pyo, Nah et al. 2012; Boya, Reggiori et al. 2013).

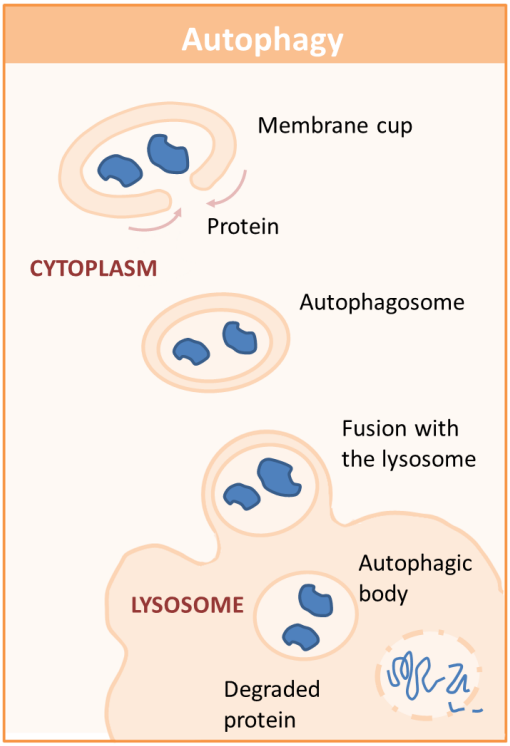

Figure. 13. Schematic representation of autophagy process. First, the cellular component subjected to autophagy is being isolated by a double-membrane autophagosome. Next, the whole structure fuses with lysosome and forms an autophagic body. Finally, the content of a vesicle is degraded.

1.3.2. Ubiquitination and its biological significance

Ubiquitination, also known as ubiquitylation, is a versatile enzymatic reaction, in which ubiquitin (Ub) molecules are covalently attached to lysine residue on substrate proteins or itself, at one or multiple sites. This post-translational modification directs eukaryotic proteins to miscellaneous fates, and is considered to be spatial-, temporal- and substrate-specific. Ubiquitin is a small, 8-kDa polypeptide that consists of 76 amino acids and is highly evolutionary conserved. In humans, Ub is a product of four genes: *UBB, UBC, UBA52* and *RPS27A*. *UBB* and *UBC* genes code for a linear ubiquitin chain precursor consisting of at least four Ub molecules. Two other genes, UBA52 and RPS27A, encode a single copy of Ub fused to the ribosomal proteins L40 and S27a, respectively. In order to ensure functionality, the *UBB*- or *UBC*-encoded Ub precursor is processed by deubiquitinating enzymes (ubiquitin proteases) and cleaved to monomers.

As it is shown in Figure 14, ubiquitin has seven internal lysines (Lys, K) used during polyubiquitin chain formation, and C-terminal diglycine motif (GG) serving for attachment to ubiquitinated substrate (Peng, Schwartz et al. 2003; Kimura and Tanaka 2010; Komander and Rape 2012).

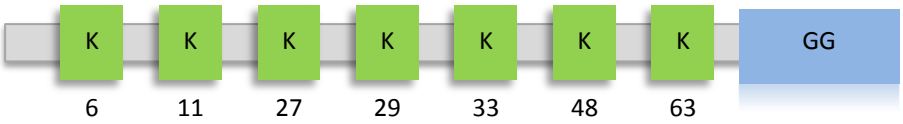

Figure 14 Schematic representation of ubiquitin molecule and positions of internal ubiquitin lysines. K = lysine, GG = diglycine.

1.3.2.1. Process of ubiquitination

The process of attaching ubiquitin to the substrate is mediated by the sequential action of three classes of enzymes: ubiquitin-activating enzymes (E1s), ubiquitin-conjugating enzymes (E2s, also known as UBCs or ubiquitin carrier proteins) and ubiquitin-protein ligases (E3s) (Pickart 2001; Ye and Rape 2009). At first, C-terminal carboxyl group of Ub forms a thioester linkage with the active site of the cysteine of E1, and therefore activates

Ub. This step is energy-dependent and requires Adenosine-5'-triphosphate (ATP). Then, Ub is transferred (trans-thiolated) from the E1 to the catalytic cysteine of one of around 40 E2s. This conjugate associates with the third enzyme of the cascade, E3 ubiquitin ligase, to finally transfer Ub from E2 to the Ɛ-amino group of target protein lysine (Fig. 15).

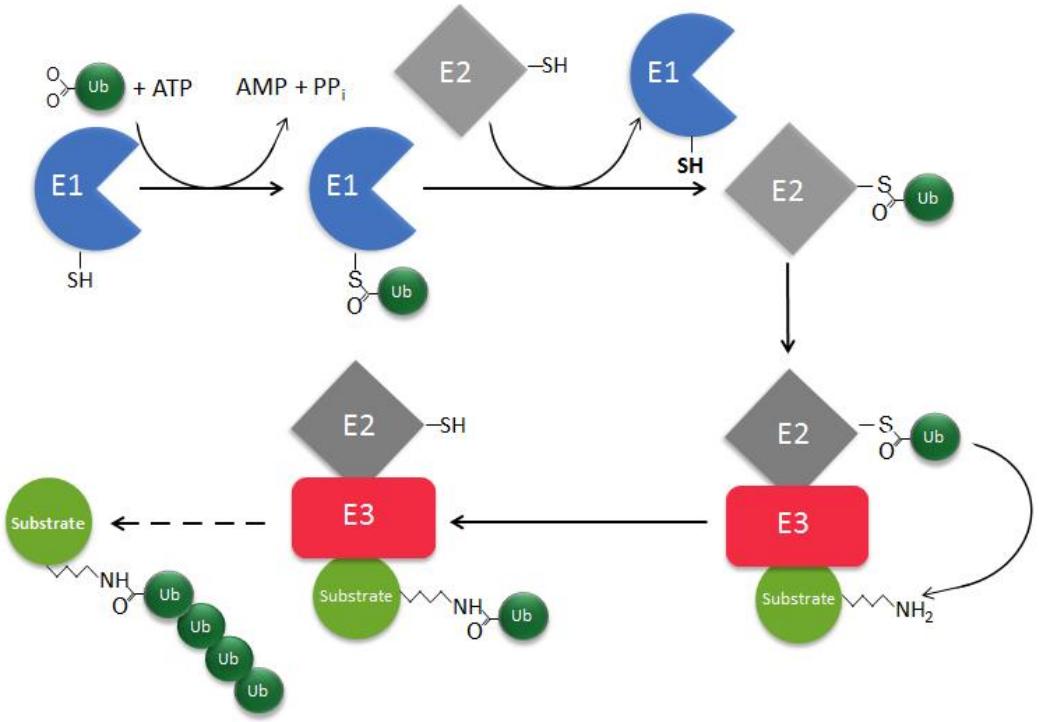

Figure 15. Schematic representation of ubiquitination process. Attachment of ubiquitin to the substrate lysine is executed by the cascade activity of three enzymes: ubiquitin-activating enzyme (E1), ubiquitin-conjugating enzyme (E2) and ubiquitin ligase (E3). The protein recognition by E3 ligase assures the specificity of reaction.

Initial attachment of a single Ub molecule to its target, called monoubiquitination, is usually, but not always, followed by the attachment of another Ub molecule(s). In this case, lysine of the Ub already conjugated with the substrate serves as an acceptor for the next Ub(s). Ubiquitin conjugation is a reversible process through the activities of proteases, called deubiquitinases or deubiquitinating enzymes (DUBs), which are able to cleave off the single Ub molecule or Ub polychain. DUBs have several functions in the ubiquitination pathway. They remove single molecule or polyUb chain from the target, thus serve as antagonists for the ubiquitination process. They also activate polyUb precursor by the proteolysis and recycle the pool of monoUb in the cell by the cleavage of free polyUb chains. Some DUBs are able to cleave ubiquitin-like proteins such as SUMO.

1.3.2.2. E3 and E4 ubiquitin ligases

E3 ubiquitin ligases are enzymes that enable binding of Ub to the substrate. They also confer the specificity of ubiquitination by recognizing a specific protein target. For example, they are the factors which provide the specificity to proteasomal degradation by recognizing and ubiquitinating the proteins subsequently degraded. Currently, there is more than 600 E3s described, that belong to the one of two major families of E3 ubiquitin ligases, which are: the Really Interesting New Gene (RING) family, and the Homologous to E6-AP Carboxyl Terminus (HECT) family (Tab. 3.). These two groups of ligases catalyze ubiquitination reaction in a different manner. RING domain E3 ligases bind both the E2~Ub conjugate and the substrate protein and lead to the direct transfer of C-terminal diglycine of Ub to a substrate lysine, and therefore allow formation of an isopeptide bond, and as a consequence, ubiquitination.

Table III. Comparison between RING domain and HECT domain family of E3 ubiquitin ligases.

	RING family	**HECT family**
number of members	~600	~30
characteristics	RING finger is Zn^{2+}-coordinating domain; consists of a series of cysteine and histidine residues; does not form a catalytic intermediate with Ub; function as monomers, dimers or multi-subunit complexes	HECT domain consists of ~350 aa, is located at the C-terminus; N-terminal domain serve for targeting a substrate
main functions	cell cycle progression, apoptosis, proteasomal degradation of the proteins, angiogenesis (Metzger, Hristova et al. 2012)	protein trafficking, immune response, signaling pathways regulating cellular growth and proliferation (Rotin and Kumar 2009)
examples	MDM2 (regulates p53), IAPs, APC/C family, SCF family, CBL family	UBE3A (E6AP), NEDD4 family

The RING finger domain serves as a scaffold bringing E2 and the target protein together. Members of the HECT E3 Ub ligases first bind Ub from the E2~Ub complex onto catalytic cysteine and form thioester intermediate with the catalytic cysteine, and then transfer it to the target protein (Deshaies and Joazeiro 2009; Metzger, Hristova et al. 2012; Sadowski, Suryadinata et al. 2012; Berndsen and Wolberger 2014).

LUBAC (Linear Ubiquitin Chain Assembly Complex) is a special E3 ubiquitin ligase, which catalyzes formation of linear ubiquitin-chains. In humans, it is known to consist of HOIL-1 (RBCK1), HOIP (RNF31) and SHARPIN and has a MW of approximately 600 kDa, probably due to the hetero-multimeric assembly of a complex. Although, as a separate protein, HOIL-1 was previously described as an ubiquitin ligase, in the case of LUBAC complex the HOIP protein is responsible for the E3 ligase activity of LUBAC. As for now, LUBAC is one of the two E3 ligases known to participate in the head-to-tail ubiquitin chain formation (Haas, Emmerich et al. 2009; Emmerich, Schmukle et al. 2011; Ikeda, Deribe et al. 2011; Tokunaga and Iwai 2012; Rieser, Cordier et al. 2013). Another E3 ubiquitin ligase recently suggested to mediate linear connection of the ubiquitin molecules is Parkin (Muller-Rischart, Pilsl et al. 2013). Table IV briefly describes E3 ubiquitin ligases found as RINT1 modulators in the course of the experimental part of presented work.

Table IV. E3 ubiquitin ligases found as interacting partners of RINT1.

E3 ubiquitin ligase	Alternative names	Biological processes involving ligase activity
HUWE1	MULE, LASU1, UREB1, ARF-BP1, HSPC272, HECTH9, URE-B1	base-excision repair (Parsons, Tait et al. 2009), histone ubiquitination (Liu, Oughtred et al. 2005), protein mono- (Parsons, Tait et al. 2009) and polyubiquitination (Zhong, Gao et al. 2005)
RNF20	BRE1, BRE1A	histone H2B ubiquitination (Zhu, Zheng et al. 2005), histone monoubiquitination (Kim, Hake et al. 2005), regulation of cell migration (Shema, Tirosh et al. 2008), regulation of transcription (Pavri, Zhu et al. 2006; Shema, Tirosh et al. 2008), protein polyubiquitination (Liu, Oh et al. 2009), regulation of mRNA polyadenylation (Pirngruber, Shchebet et al. 2009)
RNF40	BRE1B, RBP95, STARING	

It should be noted, that ubiquitination may also occur in E3 ligase-independent manner. Such modification is possible through direct and non-covalent interaction between Ub molecule and ubiquitin-binding domain of a substrate (UBD) (Hoeller, Hecker et al. 2007). Currently, there are more than twenty UBDs described, which exhibit preference for the specific Ub chains, *i.e.* depending on the length of Ub chains or inter-ubiquitin linkage type. The interplay between Ub and UBD plays an important role in such processes as proteolysis (*e.g.* α-helix UIM domain of proteasome subunit S5a), endocytosis (*e.g.* SH3 domain of CIN85 protein) or in DNA repair (*e.g.* zinc finger UBZ domain of polymerase-h) (Bienko, Green et al. 2005; Wang, Young et al. 2005; Stamenova, French et al. 2007; Dikic, Wakatsuki et al. 2009).

The nomenclature of enzymes involved in the ubiquitination process includes additional group of ligases, named E4 ubiquitin ligases or ubiquitin chain assembly factors. They serve as the enhancers of E3 ligase-mediated transfer of Ub to a protein target, thus are involved in multiubiquitin chain assembly and facilitate polyubiquitination. Examples of E4 enzymes are UFD2 in yeast and its human homolog UBE4B (Wu and Leng 2011; Micel, Tentler et al. 2013).

1.3.2.3. Types of ubiquitination

There are two major types of ubiquitination depending on nomenclature: (i) number of target lysines (K), which are ubiquitinated, (ii) number of molecules of Ub attached to the substrate. If a protein is subjected to ubiquitination on a single lysine, this process is called monoubiquitination; if several lysines of the substrate are involved, it is multiubiquitinated. Nevertheless, monoubiquitination occurs also when Ub is attached to the target protein as a monomer. Conversely, successive addition of another Ub(s) results in polyubiquitination. Alternative mode of inter-ubiquitin linkage that does not involve Ub lysine, results in linear, so-called “head-to-tale” ubiquitin chain formation *(see also 1.2.1.4.)*. Some examples of different ubiquitination types are shown in Figure 16.

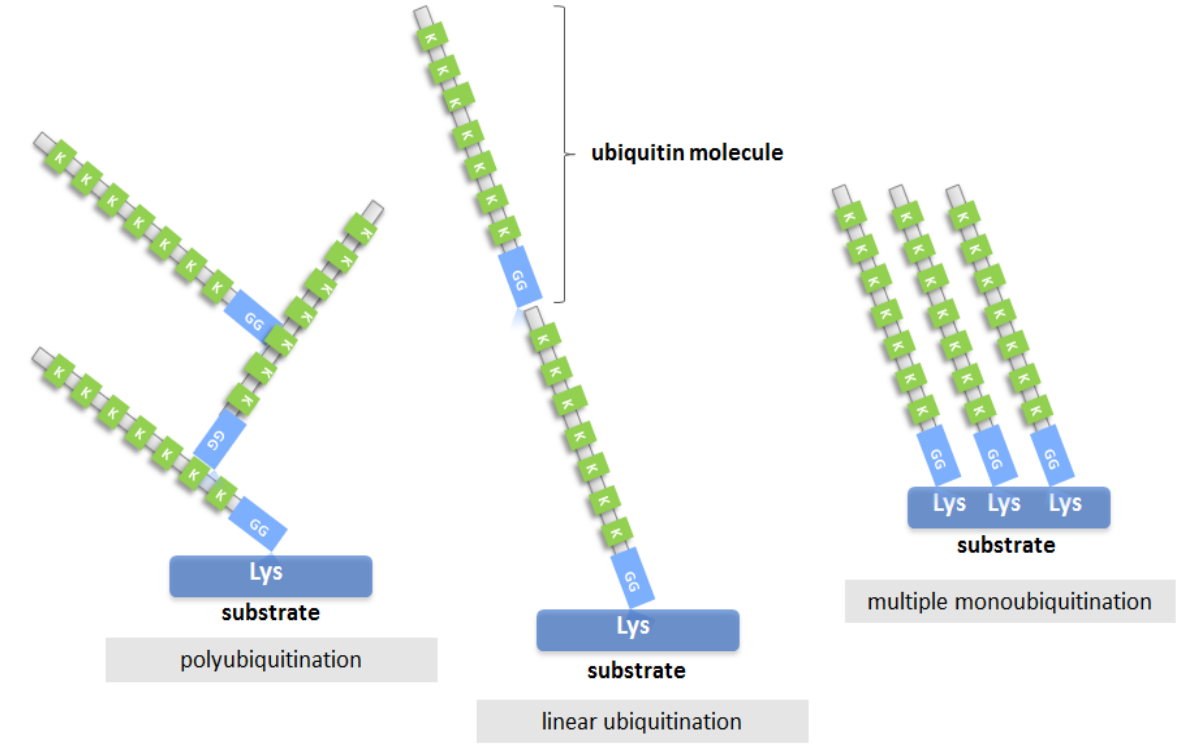

Figure 16. Nomenclature of ubiquitination depending on the ubiquitin chain typology and number of targeted lysine residues.

In the canonical ubiquitination process, substrate protein is modified by a covalent linkage of Ub to the amine group of lysine residue of the target protein. Recently, some new modes of ubiquitin chain attachment have been described. It was reported, that Ub may covalently modify its substrate and bind to non-lysine site of the protein, such as N-terminal amine group, the hydroxyl group of serine and threonine residues (Wang, Herr et al. 2007), or the thiol groups of cysteine residues (Cadwell and Coscoy 2005; Williams, van den Berg et al. 2007).

1.3.2.4. Ubiquitin chain typologies

Ubiquitin chains vary in structure, which translates to the function of ubiquitination. Since there are seven lysine residues in the Ub molecule, each of them might be potentially used to form the polyubiquitin chain (Hochstrasser 2006). Based on homo-/heterogeneity of the Ub lysines serving as an inter-Ub linkage, one can distinguish homotypic or mixed chains, respectively (Fig. 17). The last ones are branched structures, generated by specific RING E3 Ub ligases. Moreover, the α-amino group of the N-terminal methionine (M)

residue of Ub can generate the eighth linkage type, which is linear and called “head-to-tail” or “M1” linkage (Fig. 16) (Kirisako, Kamei et al. 2006; Emmerich, Schmukle et al. 2011; Walczak, Iwai et al. 2012). In addition, heterologous chains might be formed, if post-translational protein modification involves not only Ub, but also *e.g.* SUMO2 molecule.

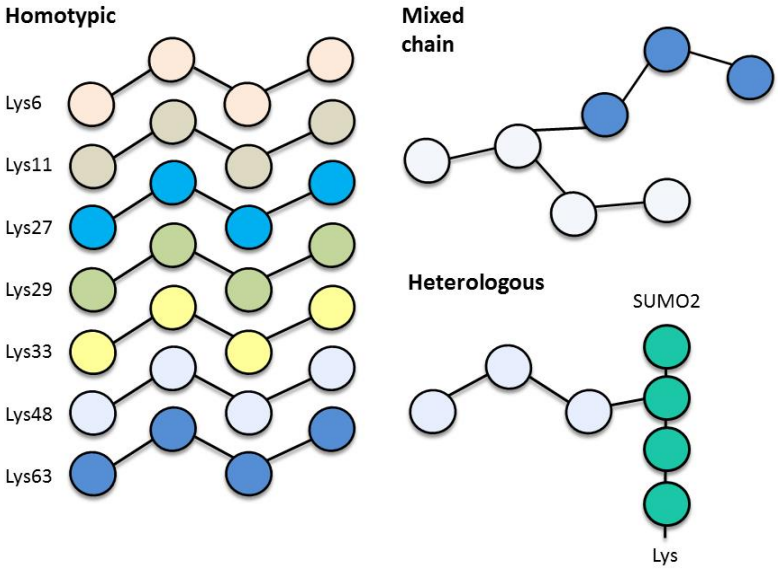

Figure 17. Ubiquitin-chains typology. Adapted from (Ikeda and Dikic 2008).

1.3.2.5. Functions of ubiquitination

Although ubiquitination was originally described and is best known as a mechanism targeting proteins for degradation by the 26S proteasome (Chau, Tobias et al. 1989; Hershko and Ciechanover 1998), it is currently known, that it is also crucial for a variety of other cellular processes, *e.g.* autophagic and lysosomal protein degradation, modulation of protein-protein interactions, DNA repair, gene transcription, alteration of subcellular localization and distribution, cell cycle regulation or cellular signaling (Passmore and Barford 2004; Pickart and Eddins 2004; Hunter 2007; Clague and Urbe 2010; Mocciaro and Rape 2012). Such wide range of ubiquitination functions is specified by the inter-ubiquitin chain typologies, *i.e.* the role of ubiquitination and fate of the protein substrate largely depend on which lysine residue of Ub serves as an inter-ubiquitin chain linker. Of course, other factors influencing ubiquitination are Ub receptors and deubiquitinating enzymes (DUBs) (*see 1.3.2.1. and 1.3.2.2.*). The most characterized mode of

ubiquitination, is K48-mediated polyubiquitination (Ub K48), where at least four Ub molecules are linked one to another *via* lysine residue on position 48. Its main role is to regulate cellular protein levels by targeting them for the proteasomal degradation (Hershko and Ciechanover 1998). Other, relatively well-described type of ubiquitination, is K63-mediated polyubiquitination (Ub K63). These poly-Ub chains are mostly associated with non-degradative functions, such as lysosomal protein sorting, signal transduction, DNA damage or endocytosis (Passmore and Barford 2004; Mukhopadhyay and Riezman 2007; Chiu, Zhao et al. 2009; Lauwers, Jacob et al. 2009; Yang, Zhang et al. 2010), but recent studies show that they might also serve as a tag for degradation. Different types of ubiquitination linked to known functions are presented in Table V. Currently, the exact functions of the different types of ubiquitination remain a subject of intensive research.

Table V. Ubiquitination types and their functions.

Type of ubiquitination	Examples of ubiquitination function
polyubiquitination: K6 linkage	regulation of microtubule stability and mitotic spindle orientation by α-tubulin ubiquitination mediated by MGRN1 ligase
polyubiquitination: K11 linkage	proteasomal degradation*, e.g.* the anaphase-promoting complex (APC/C) triggers degradation of its mitotic substrate Cyclin B1 by assembling K11-linked Ub chains
polyubiquitination: K27 linkage	monoubiquitination of histone H2A, important in mitochondrial and T cells biology*, e.g.* E3 ligase Parkin catalyzes K27-linked Ub chains on voltage-dependent anion-selective channel protein 1 (VDAC1), which leads to mitophagy
polyubiquitination: K29 linkage	protein degradation, *e.g.* lysosomal degradation of Deltex (DTX) protein mediated by ITCH/AIP4
polyubiquitination: K33 linkage	important in T cell antigen receptor (TCR) signaling, *i.e.* K33-linked polyubiquitination of ζ-chain of TCR catalyzed by ITCH leads to the reduction of TCR phosphorylation and, as a consequence, lessens TCR signaling
polyubiquitination: K48 linkage (at least 4 Ubs)	generaly proteasomal degradation, *e.g.* of protein MDC1, a key component of DDR followed by DSB repair; lysosomal degradation, *e.g.* of LDL receptor
polyubiquitination: K63 linkage	kinase activation and localization (*e.g.* K63-linked ubiquitination of transforming growth factor-ß activating kinase 1 (TAK1) triggered by TRAF6 and indispensable for TAK1 auto-

	phosphorylation), DNA damage tolerance, signal transduction, endocytosis (*e.g.* Epsin1-mediated endocytosis of MHCI; TNFα-mediated NF-κB activation), lysosomal degradation (*e.g.* of LDL receptor)
monoubiquitination	transcriptional silencing and X-inactivation, *i.e.* as a consequence of monoubiquitination of histone H2A; viral budding, gene expression, DNA repair, *e.g.* monoubiquitination of FANCD2 in response to DNA damage, triggering the recruitment of repair proteins to the damaged site
multiubiquitination or monoubiquitination on multiple sites	receptor endocytosis, *e.g.* multiple monoubiquitination of receptor tyrosine kinases (RTKs) leads for their endocytosis and degradation
linear (M1) ubiquitination	NF*κ*B signaling, *i.e.* linear ubiquitination of NEMO is necessary for NF*κ*B activation; protein degradation, *i.e. in vitro* degradation of Ub-GFP

The table was based on following publications: (Thrower, Hoffman et al. 2000; Hicke 2001; Sarcevic, Mawson et al. 2002; Haglund, Di Fiore et al. 2003; Haglund, Sigismund et al. 2003; Passmore and Barford 2004; Ben-Saadon, Zaaroor et al. 2006; Chastagner, Israel et al. 2006; Kirisako, Kamei et al. 2006; Jin, Williamson et al. 2008; Shi, Ma et al. 2008; Bergink and Jentsch 2009; Tokunaga, Sakata et al. 2009; Yang, Zhang et al. 2010; Kulathu and Komander 2012; Zhang, Xu et al. 2013; Longerich, Kwon et al. 2014; Srivastava and Chakrabarti 2014; Luo, Zhou et al. 2015)

1.3.3. SUMOylation and SUMO protein

SUMOylation is a post-translational modification of the proteins mediated by members of the Small Ubiquitin-related Modifier (SUMO) protein family and resulting in a covalent attachment of a SUMO family member to a target protein. In vertebrates, four SUMO isoforms encoded by distinct genes have been identified: SUMO1, SUMO2, SUMO3 and SUMO4. Moreover, SUMO2 and SUMO3 proteins share 97% of similarity, thereby are specified as SUMO2/3 (Hay 2005; Henley, Craig et al. 2014). Theoretical weight of SUMO family members is 10-11 kDa, however, it should be noted that on SDS-PAGE gel SUMO is detectable as a 15-17 kDa protein (Park-Sarge and Sarge 2009). As it is the case with ubiquitination, SUMOylation as a process is reversible through proteases, such as ubiquitin-like protein-specific proteases (Ulps) and sentrin-specific proteases (SENPs) that

remove SUMO molecule(s) from SUMO-modified proteins (Johnson 2004). Mature SUMO, processed from the precursor form by proteases, is generated when at least four C-terminal amino acids have been cut off. Such SUMO possesses a carboxy-terminal diglycine motif, necessary to form an isopeptide bond with an acceptor lysine residue on the substrate.

SUMOylation regulates and alters a variety of cellular processes, such as transcription (*e.g.* modification of DEC1 protein modifies its transcriptional activity), protein-protein interactions and localization (*e.g.* SUMOylation of the von Hippel-Lindau (VHL) tumor suppressor protein leads to its nuclear redistribution), ER stress response and activation of unfolded protein response (UPR) (*e.g.* regulation of PML function), cell cycle progression (*e.g.* modification of Forkhead box transcription factor M1 (FoxM1) modulates its transcriptional activity), DNA damage response (*e.g.* SUMOylation of PCNA) and chromosome segregation (Mahajan, Delphin et al. 1997; Kretz-Remy and Tanguay 1999; Huang, Wuerzberger-Davis et al. 2003; Girdwood, Tatham et al. 2004; Li, Evdokimov et al. 2004; Liang, Melchior et al. 2004; Besnault-Mascard, Leprince et al. 2005; Cai and Robertson 2010; Hong, Xing et al. 2011; Schimmel, Eifler et al. 2014; Enserink 2015).

1.3.3.1. SUMOylation process

SUMO conjugation occurs in analogous manner to ubiquitination. Covalent attachment of SUMO protein to the acceptor lysine of substrate involves a cascade of enzymes acting in particular sequence; first, activating enzymes (E1s), then conjugating enzymes (E2), and protein ligases (E3) at the end. At the beginning of the SUMO conjugation cycle, SUMO protein undergoes processing by proteases to its mature form. Following maturation, E1 activating enzyme adenylates C-terminal diglycine of SUMO that subsequently forms an E1~SUMO thioester with E1 conserved cysteine residue. Next, SUMO is transferred to the active site of conjugating enzyme E2, generating an E2~SUMO thioester. In the last step of the process, SUMO E3 ligase might catalyze reaction in two distinct manners. It either recruits both E2~SUMO thioester and the substrate into a complex, to allow an optimal conformation and to facilitate conjugation, or binds to the E2~SUMO thioester to orientate it and to facilitate E2-dependent substrate interaction and binding SUMO to the target protein. Second mechanism does not require direct interaction between E3 ligase

and the substrate. In both cases, as a result an isopeptide bond between the C-terminal carboxyl group of SUMO and the Ɛ-amino group of a lysine residue of the substrate is formed. E3 ligase function in SUMO conjugation pathway might be also omitted. In some cases, E2 conjugating enzyme interacts directly with SUMO substrate in an E3 ligase-independent manner, to transfer the cargo directly to acceptor lysines (Gareau and Lima 2010). Unlike ubiquitination-involved enzymes, only few have been identified in the SUMO pathway (Tab. VI), and among them, merely single E2 enzyme in human, which is SUMO-conjugating enzyme 9 (UBC9, UBCE9, UBE2I) (Geiss-Friedlander and Melchior 2007; Zhao 2007; Wilson and Heaton 2008; Yang and Chiang 2013).

Table VI. Examples of E1 and E3 enzymes involved in the SUMOylation.

E1 activating enzyme	**Function**
SAE1 (UBLE1A)	E1 ligase for SUMO1, SUMO2, SUMO3, and probably SUMO4
SAE2 (UBA2, UBLE1B)	E1 ligase for SUMO1, SUMO2, SUMO3, and probably SUMO4
UBA5	Activates SUMO2
E3 ligase	**Examples of proteins modified by the enzyme**
CBX4	HNRNPK, ZNF131
EGR2 (KROX20)	NAB1, NAB2
MUL1	DNM1L
NSE2 (NSMCE2)	SMC6L1, TRAX, TERF1, TERF2, TINF2, TERF2IP
PIAS1	PML, CEBPB
PIAS2	PML, PARK7 (isoform PIAS2-alpha), NCOA2, MDM2 (isoform PIAS2-beta)
PIAS3	CCAR2, MTA1
PIAS4	CEBPA, PARK7, HERC2, MYB, TCF4, RNF168
RANBP2	PML, facilitates SUMO1 and SUMO2 conjugation
RNF212	MSH4, MSH5
TRIM28	IRF7, TRIM28

Source: UniProt database (www.uniprot.org)

2. Materials and methods

2.1. Materials

2.1.1. Chemical reagents used for the cell treatment

Name	Producer, catalogue number
Ammonium chloride (NH_4Cl)	Sigma-Aldrich, #254134
Chloroquine	InvivoGen, #tlrl-chq
Cycloheximide (CHX)	Sigma-Aldrich, #C4859
DAPI (4'6-diamidino-2-phenylindole)	Invitrogen, #D1306
Etoposide	Sigma-Aldrich, #E1383
FuGENE® HD Transfection reagent	Promega, #E2311
Leupeptin	GERBU Biotechnik GmbH, #1335
MG132	Calbiochem, #474790
N-ethylmaleimide (NEM)	Sigma-Aldrich, #E3876-5G
Polyethylenimine (PEI)	Sigma-Aldrich, #408727
Propidium iodide (PI)	Sigma-Aldrich, #P4170
Rapamycin	Sigma-Aldrich, #R8781

2.1.2. Buffers and solutions

Buffer	Reagents	Concentration
Protein lysis buffer	Tris-HCl (pH=7.4)	20 mM
	$MgCl_2$	1 mM
	NaCl	0.5 M
	Glycerol	20% (v/v)
	NP40	0.5% (v/v)
	EDTA	1 mM
	EGTA	1 mM
	DTT	1 mM
	PMSF	1 mM
	NaF	2.5 mM
	Na_3VO_4	200 mM
	ß-glycerolphosphate	1 mM
	Protease inhibitor cocktail	1 tablet / 50 ml

Protein lysis buffer for IP	Tris-HCl (pH=7.4)	50 mM
	NaCl	150 mM
	EDTA	1 mM
	Triton X-100	1% (v/v)
PBS (10x)	NaCl	137 mM
	KCl	27 mM
	$Na_2HPO_4 \cdot 2H_2O$	10 mM
	KH_2PO_4	2 mM
TBS (10x)	Tris-HCl (pH=7.4)	500 mM
	NaCl	1500 mM
Reducing sample buffer (5x)	Tris-HCl (pH=6.8)	0.27 M
	Glycerol	50% (v/v)
	SDS	8.3% (w/v)
	Bromophenolblue sodium salt	0.12% (w/v)
	DTT	0.5 M
Running buffer (SDS-PAGE)	Tris base	25 mM
	Glycine	192 mM
	SDS	0.1% (w/v)
Transfer buffer (Western blot)	Tris base	25 mM
	Glycine	192 mM
	Methanol	20% (v/v)
Blocking buffer	non-fat dry milk in TBST	4% (w/v)
$TE_{10/1}$	Tris-HCl (pH=8.0)	10 mM
	EDTA (pH=8.0)	1 mM
PCR buffer (10x)	KCl	0.5 M
	Tris-HCl (pH=8.3)	0.1 M
	$MgCl_2$	15 mM
TAE (50x)	Tris acetate	2 M
	EDTA (pH=8.2)	0.05 M
Nicoletti lysis buffer	Sodium citrate (pH=7.4)	0.1% (w/v)
	Triton X-100	0.1% (w/v)
	Propidium iodide	50 µg/ml
S1 Resuspension buffer	Tris-HCl (pH=8.0)	50 mM
	EDTA	10 mM
	RNase A	50 µg/ml
S2 Lysis buffer	NaOH	200 mM
	SDS	1% (v/v)
S3 Neutralization buffer	KAc (pH=5.1)	3 M

2.1.3. Eukaryotic cell lines and bacterial strains

Cell line	Characteristics
COS-7	African green monkey (*Cercopithecus aethiops, Chlorocebus aethiops*) kidney fibroblast-like cell line, derived from the CV-1 cell line, transformed with an origin defective mutant of SV40, which encodes for wild type T antigen.
HEK293T	Human (*Homo* sapiens) embryonic kidney 293 cells constitutively expressing the simian virus 40 (SV40) large T antigen; derivative of the 293 cell line.
POF35-5 CER	Mice embryonic fibroblast (MEF) cell line, generated by Dr. Pierre-Olivier Frappart, carrying CreER(T2) construct, tamoxifen-inducible *Rint1* conditional knock-out
POF35-5 EV	MEF cell line, generated by Dr. Pierre-Olivier Frappart, carrying Cre recombinase construct, EV control cell line
POF39-4 CER	MEF cell line, generated by Dr. Pierre-Olivier Frappart, carrying CreER(T2) construct, tamoxifen-inducible *Rint1* conditional knock-out
POF39-4 EV	MEF cell line, generated by Dr. Pierre-Olivier Frappart, carrying Cre recombinase construct, EV control cell line

Bacterial strain	Resistance	Experimental purpose
E. coli DH5α	Nalidixic acid	Propagating DNA/shRNA plasmids
E. coli TOP10	Streptomycin	Propagating DNA/shRNA plasmids
E. coli DB3.1	Streptomycin	Propagating DNA plasmids containing the ccdB operon

2.1.4. Culture media

2.1.4.1. Bacterial culture media

Medium type	Content	Manufacturer
LB-Broth	10 g/l tryptone 5 g/l yeast extract 5 g/l NaCl pH=7.0	Carl Roth GmbH, #X968.2

LB-Broth agar plates	LB-Broth 2% Agar-agar	Carl Roth GmbH, #X968.2 GERBU Biotechnik GmbH, #1340

For the preparation of LB-medium agar plates, 6 g of agar was added to 300 ml of LB-Broth medium, autoclaved and cooled down to 55°C. At this temperature, antibiotic was added: 50 µg/ml of ampicillin or 100 µg/ml kanamycin. Petri dishes were filled with the solution. Plates were stored at 4°C.

2.1.4.2. Eukaryotic cell lines culture medium

Medium	**Cell type**	**Composition**	
D-MEM (Dulbecco's Modified Eagle Medium)	COS-7, HEK293T, MEF	Liquid with L-glutamine, 4500 mg/l D-glucose, 25 mM HEPES	
This medium was supplemented with:		FCS	10% (v/v)
		sodium pyruvate	1 mM
		penicillin/streptomycin	100U/100µg
		ß-mercaptoethanol	0.1 mM
		L-glutamine	2 mM
Freezing medium	COS-7, HEK293T, MEF	D-MEM	80% (v/v)
		FCS	10% (v/v)
		DMSO	10% (v/v)

D-MEM and all the reagents were purchased from Gibco, Karlsruhe, with an exception of FCS, purchased from Perbio Sciences.

2.1.5. Antibodies

2.1.5.1. Primary antibodies

Name (clone)	**Antigen**	**Isotype**	**Producer, catalogue number**
anti-FLAG® (M2)	FLAG Tag	mouse monoclonal IgG_1	Sigma-Aldrich, #F3165
anti-FLAG® (M2) Affinity Gel	FLAG Tag	mouse monoclonal IgG_1	Sigma-Aldrich, #A2220
anti-GFP (B-2)	GFP Tag	mouse monoclonal IgG_{2A}	Santa Cruz Biotechnology, sc-9996

anti-HA (3F10)	HA Tag	rat monoclonal IgG_1	Roche, #11867423001
anti-HA Affinity Matrix (3F10)	HA Tag	rat monoclonal IgG_1	Roche, #11815016001
Calreticulin	Calreticulin	rabbit polyclonal IgG	Affinity Bioreagents, #PA3-900
Caspase-3/CPP32 (Clone 46)	Caspase-3	mouse monoclonal IgG_1	BD Biosciences, #611048
GADD 153 (F-168)	GADD 153 (CHOP10)	rabbit polyclonal IgG	Santa Cruz Biotechnology, sc-575
GFP-Trap®_A	GFP		ChromoTek, #gta-20
Lasu1/Ureb1	HUWE1 (LASU1, UREB1)	rabbit polyclonal IgG	Bethyl Laboratories, #A300-486A
PARP (C2-10)	PARP1	mouse monoclonal IgG_1	Trevigen, #4338-MC-50
RINT1	RINT1	rabbit polyclonal IgG	Proteintech Europe, #14567-1-AP
RNF20 (D6E10)	RNF20	rabbit monoclonal IgG	Cell Signaling, #11974
RNF40 (KA7-27)	RNF40	mouse monoclonal IgG_1	Sigma-Aldrich, #R9029-25UL
SUMO1	SUMO1	mouse monoclonal IgG	generous gift from Dr. F. Melchior
SUMO2	SUMO2	mouse monoclonal IgG	generous gift from Dr. F. Melchior
Ubiquitin (P4D1)	Ubiquitin	mouse monoclonal IgG_1	Santa Cruz Biotechnology, sc-8017

2.1.5.2. Secondary antibodies

Name (catalogue number)	**Antigen**	**Producer, catalogue number**
Secondary HRP-conjugated	goat polyclonal IgG anti-mouse IgG	Dianova, #115-035-003
Secondary HRP-conjugated	goat polyclonal IgG anti-rabbit IgG	Dako, #00033131
Secondary HRP-conjugated	goat polyclonal IgG anti-rat IgG	Santa Cruz Biotechnology, sc-2065

2.1.6. Plasmids

Name, Producer	Producer
MISSION® shRNA HUWE1, pLKO.1	Sigma-Aldrich, #SHCLNG NM_031407
MISSION® shRNA RNF20, pLKO.1	Sigma-Aldrich, #SHCLNG NM_019592
MISSION® shRNA RNF40, pLKO.1	Sigma-Aldrich, #SHCLNG NM_014771
pcDNA3.1-HA	Invitrogen
pcDNA3.1-HA-Ubiquitin	generous gift from Dr. T. Hofmann
pFLAG-CMV2	Sigma-Aldrich
pEGFP-C1	Clontech
pFLAG-CMV2-RINT1	generous gift from Dr. M. Tagaya
pFLAG-CMV2-RINT1-N	generous gift from Dr. M. Tagaya
pFLAG-CMV2-RINT1-M	generous gift from Dr. M. Tagaya
pFLAG-CMV2-RINT-C	generous gift from Dr. M. Tagaya
pRK5-HA-Ubiquitin-K29	Addgene #22903
pRK5-HA-Ubiquitin-K48	Addgene #17605
pRK5-HA-Ubiquitin-K63	Addgene #17606
pRK5-HA-Ubiquitin-KO	Addgene #17603

2.1.7. Primers

Name	Primer sequence
Quantitative PCR	
Oligo-dT	$(dT)_{15}$
human Huwe1	sense 5’-TGTAATGATGAGCAACTCCTCTT-3‘ anti-sense 5’-GGTCCAACAGATCCACCCA3-‘
human ß-actin	sense 5’-ACCCACACTGTGCCCATCTACGA-3’ anti-sense 5’-CAGCGGAACCGCTCATTGCCAATGG-3’
Quantitative PCR primers were designated using “Roche Universal ProbeLibrary for Human” (www.lifescience.roche.com)	
Generation of truncated human RINT1 mutants	
Rint1-Δ1	sense: 5'-AAGCGGCCGCAGAAGTTGGAAATGACCTTAAATC-3' anti-sense: 5'-AAGGATCCTTATTTTCCAGTATTAGGCCAATTTG-3'
Rint1-Δ2	sense: 5'-AAGCGGCCGCACAATTTCTTAATCAGTTTCTGGAGC-3' anti-sense 5'-AGGATCCTTATTTTCCAGTATTAGGCCAATTTGTCC-3'

Rint1-Δ3	sense: 5'-AAGCGGCCGCATACTCTCTTCCTGCCTCCCC-3' anti-sense: 5'-AAGGATCCTTATTTTCCAGTATTAGGCCAATTTGTCC-3'
Site directed mutagenesis – Rint1 putative ubiquitination site	
Rint1-A71G	sense: 5'-GTGACGAAAGGAGGAACCTCGAGGAG-3' anti-sense: 5'-CTCCTCGAGGTTCCTCCTTTCGTCAC-3'

2.1.8. shRNA

Name	**shRNA sequence**
shRNA HUWE1	CGGGCTCCCACTATAACCTCACTTCTCGAGAAGTGAGGTTATAGTGGGAGCTTTTTG
shRNA RNF20	CCGGCGGAGGAACTAGACATTAGAACTCGAGTTCTAATGTCTAGTTCCTCCGTTTTTG
shRNA RNF40	CCGGGCAGAAGTTTGAGATGCTGAACTCGAGTTCAGCATCTCAAACTTCTGCTTTTT

2.1.9. Commercial kits and materials

Commercial kit/material	**Manufacturer, catalogue number**
ApopTag Plus® Fluorescein *In Situ* Apoptosis Detection Kit	Chemicon International, #S7111
Gateway® BP Clonase® II Enzyme Mix	Life Technologies, #11789-020
Gateway® LR Clonase® II Enzyme Mix	Life Technologies, #11791-020
GeneAmp RNA PCR	Applied Biosystems, #4312765
KOD Hot Start DNA Polymerase	Novagene, #71086-3
LigaFast™ Rapid DNA Ligation System	Promega, #M8221
Power SYBR Green PCR Master Mix	Applied Biosystems, #4368708
ProLong® Gold Antifade Mountant	ThermoFisher Scientific, #P36930
QIAGEN Plasmid *Plus* Maxi Kit	Qiagen, #12965
QIAquick Gel Extraction Kit	Qiagen, #28706
QIAquick PCR purification Kit	Qiagen, #28106
Reverse Transcriptase	Applied Biosystems, #4311235
RNeasy Mini Kit	Qiagen, #74106
Western Lightning® Plus-ECL	PerkinElmer, USA, #NEL103001EA

2.1.10. Instruments

Instrument	Manufacturer
Agarose gel electrophoresis chamber	Bio-Rad
Bacterial culture incubator/shaker	Eppendorf
Basic pH Meter PB-11	Sartorius
Blotting system, Mini Trans-Blot® Cell	Bio-Rad
Centrifuges:	
• 5415R	Eppendorf
• 5418	Eppendorf
• 5804R	Eppendorf
Chemiluminescence visualization system	Bio-Rad
CO_2-cell culture incubator	Sanyo
DNA Engine Thermal Cycler PTC-200	Bio-Rad
Electrophoresis power supply, PowerPac Basic	Bio-Rad
Electroporation system, Gene Pulser Xcell™	Bio-Rad
Gel documentation system:	
• UV Transilluminator, UST-20M-8K	Biostep
• Digital camera, EOS 500D	Canon
• EF 28mm f/1.8 USM	Canon
Heat block	Eppendorf
Light microscope	Leica Microsystems
MicroPulser electroporation cuvettes	Bio-Rad
Magnetic stirrer, MR Hei-Standard	Heidolph Instruments
Microwave oven	Samsung
Platform shaker, Unimax 1010 orbital	Heidolph Instruments
Quartz cuvettes	Sigma-Aldrich
Rotary shaker	Stuart
Sonicator	Qsonica
Spectrophotometer	Bio-Rad
Spectrophotometer NanoDrop 1000	PEQLAB
Thermomixer compact	Eppendorf
Vortex Genie 2	Scientific Industries

2.1.11. Software

Software	Company/Link
BDM-PUB	www.bdmpub.biocuckoo.org
GENtle, version 1.9.4	Magnus Manske, University of Cologne
GPS-SUMO	sumosp.biocuckoo.org/online.php
ImageJ, version 1.46r	Public domain, Wayne Rasband, NIH
Multi-Omics Profiling Expression Database	www.proteinspire.org
PHOSIDA	www.phosida.com
PhosphoSitePlus	www.phosphosite.org
Phylogeny.fr	http://phylogeny.lirmm.fr
PRALINE	www.ibi.vu.nl/programs/pralinewww
Roche Universal ProbeLibrary for Human	www.lifescience.roche.com
Scaffold, version 4.0.7.	Proteome Software
Sequence Detection Software	Applied Biosystems
UbPred	www.ubpred.org

2.2. Methods

2.2.1. Molecular biological methods

2.2.1.1. Transformation of plasmid DNA in competent bacteria

Competent *E. coli* bacteria (50 µl) were thawed on ice and a plasmid (25 ng) was transferred to the bacterial solution. Bacterial solution was subsequently gently mixed and incubated on ice for 30 min After this time, a heat shock at 42°C for 50 sec in water bath was performed. Then, the reaction mix was incubated on ice for 3-4 min, and 250 µl of LB-medium was added. Eppendorf tube containing the solution was transferred to a shaker and incubated for 1h at 37°C, 300 rpm. Afterwards, 100 µl of the mixture was transferred to LB-agar selective plate containing the appropriate antibiotic (ampicillin or kanamycin). The plate was incubated o/n at 37°C.

2.2.1.2. Preparation of plasmid DNA

2.2.1.2.1. Large-scale purification of plasmid DNA

Large-scale plasmid purification was performed using commercially available QIAGEN Plasmid *Plus* Maxi Kit, according to the manufacturer's protocol. Bacteria containing the transformed plasmid were cultured o/n in 300 ml of LB-medium, containing appropriate antibiotic for selection pressure in an incubator at 37°C, 300 rpm. The next day, bacteria was harvested by centrifugation at 6000 x g, for 15 min at 4°C. The supernatant was carefully discarded and the bacterial pellet was resuspended in 10 ml of the supplied buffer P1. In order to lyse the cells, 10 ml of buffer P2 was added, the content of the tube was mixed thoroughly by inverting it 4-6 times, and the mixture was incubated at RT for 5 min To stop the lysis, 10 ml of chilled buffer P3 was added. Solution was mixed, incubated on ice for 20 min and subsequently centrifuged at 20000 x g for 30 min at 4°C. The supernatant containing plasmid DNA was applied to equilibrated with 10 ml of QBT buffer QIAGEN-tip 500 column. The column was washed two times with 30 ml of buffer QC. In order to elute the plasmid DNA, 15 ml of buffer QF was applied to the column and the eluate was collected into fresh tube by free-flow. Precipitation of the DNA was performed by adding 10.5 ml (0.7x volume) of RT isopropanol to the eluate and by immediate centrifugation of mixed solution at 15000 x g for 30 min at 4°C. The DNA pellet was washed with 5 ml of RT 70% ethanol and centrifuged again at 15000 x g for 10 min at 4°C. The ethanol was discarded, the DNA pellet was air-dried for 10-15 min and resuspended in 100 µl of TE buffer. The quantity and the quality of purified plasmid DNA were verified by agarose gel electrophoresis and using NanoDrop 1000 spectrophotometer.

2.2.1.2.2. Preparation of plasmid DNA using home-made buffers

Purification of DNA plasmids up to 25 µg was performed using home-made S1, S2 and S3 buffers. 1.5 ml of o/n bacterial culture containing the plasmid was centrifuged at 14000 x g for 1 min. and the supernatant was carefully removed. Bacterial pellet was resuspended in 250 µl of buffer S1 and 250 µl of S2 lysis buffer was added. The tube was inverted 5-6 times and incubated on ice for 5 min Next, 350 µl of S3 neutralization buffer was added, the tube was again inverted 5-6 times and incubated on ice for additional 5 min

Subsequently, the tube was centrifuged for 10 min at 14000 x g and the supernatant (750 µl) was transferred to a fresh 1.5 ml tube. Single volume (750 µl) of ice-cold 100% ethanol was added, the tube was vortexed and centrifuged again for 10 min at 14000 x g. The pellet of plasmid DNA was washed with 1 ml of ice cold 70% ethanol and the tube was centrifuged as before. The supernatant was carefully discarded, the pellet was air-dried for 10-15 min at RT and resuspended in 30-50 µl of $TE_{10/1}$ buffer. The quantity and the quality of purified plasmid DNA was verified by agarose gel electrophoresis and using NanoDrop 1000 spectrophotometer. Briefly, the spectrophotometer was equilibrated with 1 µl of H_2O pipetted onto the lower measurement pedestal. Then, 1 µl of DNA sample was placed onto measurement pedestal and the reading was initiated using the operating software on the PC. The absorbance was recorded at 260 nm and 280 nm.

2.2.1.3. Restriction enzyme digestion and ligation of DNA fragments

Restriction enzyme-mediated digestion of DNA was performed as one of the steps for cloning of the DNA fragments into another plasmid, or in order to verify the sequence of cloned construct according to a restriction map. Plasmid DNA and DNA fragments were digested with appropriate restriction enzymes (and their concentrations), typically for 4 h at 37°C. Following reaction mixture were prepared (volumes are given for one reaction vial):

Restriction digest of DNA fragments obtained by PCR-mediated synthesis:

Reagent:	Volume:
DNA fragment	5 µl (final concentration: 1 µg)
restriction enzyme	1 µl (10 U)
respective restriction buffer 10x	3 µl
H_2O	to a final volume of 30 µl

Restriction digest of plasmid DNA:

Reagent:	Volume:
plasmid	1 µg
restriction enzyme	1 µl (10 U)
respective restriction buffer 10x	3 µl
H_2O	to a final volume of 30 µl

DNA fragments were subsequently separated on an agarose gel, and purified using QIAquick Gel Extraction Kit (Qiagen), according to the manufacturer's protocol. For the ligation, following reaction was performed:

Reagent:	Volume:
vector DNA	100 ng
insert DNA	33 ng
2X Rapid Ligation Buffer	5 µl
T4 DNA Ligase (Weiss units)	3 U

Reaction mix was incubated o/n at 4°C.

2.2.1.4. Gateway® Recombination Cloning Technology

Gateway® Recombination Cloning Technology was used to quickly and efficiently clone genes into multiple destination vectors, without a need to use restriction enzymes, ligase and subcloning steps. Gateway cloning was performed in two steps and following manufacturer's protocol. First, a BP recombination reaction between an *att*B-flanked DNA fragment and an *att*P-containing donor vector was performed, to create an entry clone. During a second step a LR recombination reaction between an *att*L-containing entry clone and an *att*R-containing destination vector was performed to generate an expression clone. Reactions were prepared as follows:

BP recombination reaction:

Reagent:	Volume:
*att*B-PCR product	1-7 µl (10 ng/µl, final amount ~15-150 ng)
pDONR™ vector	1 µl (150 ng/µl)
5X BP Clonase™ reaction buffer	2 µl
$TE_{10/1}$	to final volume of 8 µl

Reaction was incubated at RT for 1 h. Then, 2 µl of 2 µg/µl proteinase K solution was added and the mix was incubated at 37°C for 10 min Competent *E. coli* were transformed with the reaction mix and selected for appropriate antibiotic-resistant entry clones.

LR recombination reaction:

Reagent:	Volume:
entry clone	1-7 µl (50-150 ng)
destination vector	1 µl (150 ng/µl)
5X LR Clonase™ reaction buffer	2 µl
$TE_{10/1}$	to final volume of 8 µl

Reaction was incubated at RT for 1 h. Then, 2 µl of 2 µg/µl proteinase K solution was added and the mix was incubated at 37°C for 10 min. Competent *E. coli* were transformed with the reaction mix and selected for the appropriate antibiotic-resistant expression clones.

2.2.1.5. Total cellular RNA extraction

Total RNA was extracted using RNeasy Mini Kit (Qiagen). Briefly, cells were first lysed and homogenized by adding 600 µl of buffer RLT. Single volume of ethanol 70% (in RNase-free water) was added to the lysate to provide ideal binding conditions, and mixed by pipetting. 700 µl of the sample was loaded onto the RNeasy mini spin column placed in a 2 ml collection tube. Tube was centrifuged for 15 s at 8000 x *g*. Contaminants were washed away with sequential washing with buffer RW1 (700 µl) and RPE (500 µl, twice), and spinning for 15 s at 8000 x *g*. RNA was eluted in 30 µl H_2O by centrifugation for 1 min at 8000 x *g*. RNA concentration was measured as described for DNA (section 2.2.1.2.2.). The RNA samples were stored at -80°C.

2.2.1.6. Reverse-transcription reaction for cDNA generation (RT)

Total RNA extracted using RNeasy Mini Kit was subjected to mRNA-specific RT-PCR reaction to synthesize cDNA. Buffers and reagents were from the RNA PCR Core Kit (Applied Biosystems). The reaction mixture was prepared as follows (volumes are given for one reaction vial):

Reagent:	Volume:
10x PCR buffer (without $MgCl_2$)	5 µl (final concentration: 1x)
25 mM $MgCl_2$	10 µl (final concentration: 5 mM)
10 mM dNTPs mix	5 µl (final concentration: 1 mM)
20 U/µl MuLV Reverse Transcriptase	2.5 µl (final concentration: 2.5 U/µl)
Oligo dT primer (50 µM in 10 mM Tris)	2.5 µl (final concentration: 2.5 µM)
RNA	2.5 µg
RNase-free H_2O	to final volume of 50 µl

The mixture was incubated in a thermocycler using following conditions:

Step:	Time and temperature:
annealing	15 min at 25°C
elongation	1h at 42°C
inactivation of reverse transcriptase	5 min at 95°C

Synthesized cDNA was stored at -20°C.

2.2.1.7. Polymerase chain reaction (PCR)

Classical polymerase chain reaction (PCR) mix was prepared as following (volumes are given for one reaction vial):

Reagent:	Volume:
10x PCR buffer	2.5 µl
25 mM $MgCl_2$	2.5 µl
5 U/µl *Taq* DNA Polymerase	0.4 µl
10 mM dNTPs mix	0.5 µl
100 pmol primer forward	0.75 µl
100 pmol primer reverse	0.75 µl
DNA template	1 µl
H_2O	to volume of 25 µl

Steps of the PCR reaction used for gene cloning were as following:

Step:	**Time and temperature**:	
initialization	5 min at 95°C	
denaturation	1 min at 95°C	
annealing	1 min at 58°C	30-35 cycles
elongation	2 min at 72°C	
termination	10 min at 72°C	
final hold	4°C	

The PCR conditions (annealing temperature, elongation time) were optimized for specific genes and primers. The PCR products were electrophoretically separated on an agarose gel containing ethidium bromide.

2.2.1.8. Site directed mutagenesis (SDM)

In order to introduce point mutation to the DNA sequence, site directed mutagenesis (SDM) using linear amplification PCR technique was performed. As a first step, primers introducing the desired mutation into the amplified sequence were designed. The criteria for primer design were as follows: melting temperature (T_m) of the primers was higher than 65°C, and the mutation site was located in the middle of the primer sequence. Total volume of PCR reaction mix was of 50 µl. In order to minimalize the chances of introducing unwanted mutations, high fidelity KOD Hot Start DNA Polymerase (Novagene) was used. Maximum 20 cycles were executed. Following PCR, in order to digest methylated template plasmid, reaction mix was subjected to the restriction reaction with DpnI enzyme, for 1h. Finally, PCR mutated product was transformed into competent *E. coli* bacteria. Clones were analyzed using restriction digest mapping and subsequently sequenced, to confirm the occurrence of a desired mutation.

2.2.1.9. Purification of PCR products and other DNA fragments

Purification of PCR products/DNA fragments was performed prior to restriction enzyme digestion and/or sequencing using QIAquick PCR purification kit (Qiagen) and according to the manufacturer's protocol. Briefly, 5 volumes of buffer PB were added to 1 volume of the PCR product and mixed (until a color of the mixture turned yellow, indicating pH value equal or lower than 7.5, suitable for DNA/column binding). Sample was applied on the column and centrifuged for 1 min at 17 000 x *g*. All the following centrifugation steps were carried out under the same conditions. Next, the column was washed with 0.75 ml of buffer PE and centrifuged. Additional spinning was performed, to remove residual wash buffer from the column. QIAquick column was then placed in a fresh collecting tube and the purified DNA was eluted with 30-50 µl of buffer EB.

2.2.1.10. Quantitative real-time PCR (qRT-PCR)

The cDNA was pipetted into a 96-well plate. Each reaction was performed as triplicate of total volume of 25 µl. qPCR was performed using Power SYBR Green PCR Master Mix (Applied Biosystems). Quantitative RT-PCR reaction mixture consisted of:

- 1 µl of reverse-transcribed cDNA (product of a reaction described at p. 2.2.1.6)
- 1 µl forward/reverse primer respectively;
  primer stock solutions were: for HUWE1 – 10 µM (400 pM end concentration)
  for ß-actin – 5 µM (200 pM end concentration)
- 9.5 µl of H_2O
- 12.5 µl of the Power SYBR Green PCR Master Mix

Gene expression was analyzed using the 7500 Real-Time PCR Systems and Sequence Detection Software v.2.0.2. (Applied Biosystems). Huwe1 gene expression level was calculated relatively to ß-actin mRNA as an endogenous reference using the following formula: $X = 2^{-\Delta Ct}$, where Ct stands for cycle threshold and $\Delta Ct = Ct_{\text{gene of interest}} - Ct_{\text{reference gene}}$, *i.e.* $2^{-(\Delta Ct \text{ of Huwe1} - \Delta Ct \text{ of ß-actin})}$. The resulting relative increase in reporter fluorescent dye emission was monitored for 42 cycles. The mean expression values +/- SD were calculated from triplicated samples.

2.2.1.11. Agarose gel electrophoresis

Agarose gel electrophoresis was applied to separate DNA fragments according to their size. The percentage of the gel was dependent on the predicted size of DNA fragments to be detected and separated. The agarose suspension in TAE buffer, usually between 0.7% (w/v) and 2% (w/v), was boiled in a microwave oven until completely dissolved, and cooled down to the temperature ~50°C. Next, ethidium bromide was added to the final concentration of 0.003% and the agarose gel was poured to the cast and cooled down until set. The DNA samples, mixed with 1/5 volume of 5x loading buffer, were loaded on the gel. The gel was run for 30 min to 1 h, at 100 V. DNA fragments were visualized with the UV transilluminator.

2.2.1.12. Purification of PCR products and DNA fragments from agarose gel

PCR products and DNA fragments subjected to cloning, were purified from agarose gel using QIAquick Gel Extraction kit according to manufacturer's protocol. First, slice of the agarose gel containing desired DNA fragment was excised with a scalpel, transferred to an Eppendorf tube and weighed. Next, to 1 volume of the gel, 3 volumes of QG buffer were added. Tube was incubated at 50°C for 10 min or until the gel slice completely dissolved. To increase the yield of DNA fragments, 1 gel volume of isopropanol was added to the sample, and mixed. Afterwards, sample was applied to the QIAquick column and centrifuged for 1 min at 10000 x *g.* The DNA was washed with 0.75 ml of PE buffer, and centrifuged using the same conditions. To remove any residues of PE buffer, centrifugation step was repeated after discarding the flow-through. The DNA was eluted into the fresh tube using 30 µl of EB buffer. The concentration and the quality of the DNA was measured by NanoDrop 1000 and agarose gel electrophoresis. Samples were stored at -20°C for further use.

2.2.1.13. Transient transfection and shRNA-mediated knock-down

2.2.1.13.1. Electroporation of mammalian cells

COS7 cells were transiently transfected with different expression plasmids using electroporation system – Gene Pulser Xcell™ (Bio-Rad). For one electroporation, two T175 flasks of COS7 cells growing in confluence were used. Briefly, cells were washed with 20 ml of PBS and trypsinized with 5 ml of trypsin-EDTA (0.25%) solution for 5 min at 37°C. In order to stop the trypsinization process, 10 ml of MEF medium was added and the cells were collected to 50 ml Falcon tubes. Next, cells were centrifuged for 5 min at 1000 rpm and, after discarding the medium, washed with 10 ml of PBS. Centrifugation step was repeated. 40 µg of plasmid DNA intended for electroporation was placed in 0.4 cm gap electroporation cuvette. COS7 cells were resuspended in 0.8 ml of ice-cold PBS and transferred to the cuvette containing plasmid. Cells were electroporated with 400 V, 960 µF capacitance and the resistance +∞. Electroporated cells were immediately transferred to 20 ml of MEF medium and centrifuged for 5 min at 1000 rpm. The cell pellet was resuspended in 50 ml of fresh MEF medium and the cells were plated in 5 x T75 flasks.

2.2.1.13.2. Polyethylenimine (PEI)-mediated transient transfection

HEK293T cells were transiently transfected with mammalian expression plasmids using branched polyethylenimine (PEI) transfection reagent. PEI solution used for transfection was prepared as follows: 100 µl of PEI stock solution (10 mg/ml PEI in H_2O, density=1.030 g/ml) was diluted in 10 ml of ddH_2O or 1x PBS. Solution was kept at 4°C. One day before the procedure, cells were seeded the way they reach 70% confluency on the day of transfection. For 150 mm dish, 6.5 x 10^3 of HEK293T cells was seeded and incubated overnight at 37°C. Shortly before the transfection, DNA plasmid and PEI stock solution were diluted in DMEM as follows: 13 µg of plasmid in 3.125 ml of DMEM and 2.5 µg of PEI per 1 µg of plasmid DNA in 3.125 of DMEM. Diluted PEI solution was combined with the DNA solution, immediately vortexed and incubated at RT for 10 min. MEF medium was aspirated from 150 mm dish and replaced with 30 ml of DMEM. DNA-PEI mix was added drop-wise to the cells evenly over the entire surface of the dish. After 6 h of incubation at

37°C, PEI-containing DMEM was replaced by MEF medium. Next, cells were incubated for 24-48 h at 37°C in CO_2 atmosphere, and harvested for the experiment.

2.2.1.13.3. shRNA-mediated gene knock-down

The expression of target genes (Huwe1, Rnf20, Rnf40) was knocked-down by selective inactivation of corresponding mRNA induced by the short hairpin RNA (shRNA). The experiments were performed simultaneously with transient transfection of RINT1 expression construct in order to analyze the effect of knock-down on RINT1 protein stability. Briefly, plasmid encoding shRNA and plasmid encoding *RINT1*, were transiently introduced to the cells using FuGENE® HD transfection reagent, according to manufacturer's instructions. The ratio of FuGENE® HD : DNA used was 2:1, and the ratio of shRNA plasmid to DNA plasmid was 5:1. Cells were harvested 48h post-transfection, lysed and analyzed by Western blot.

2.2.2. Cellular biological methods

2.2.2.1. Cell culture

All the cell lines were propagated at 37° in an incubator with a humidified 5% CO_2 atmosphere. Cells were grown as adherent culture, maintained by replacement of fresh MEF medium every 2-3 days and passaged when reached the confluency of 80%. All cell culture work was performed under sterile conditions.

2.2.2.2. Maintenance of eukaryotic cell lines

For a long-term use, cell lines were stored in liquid nitrogen, and for a short-term use, at -80°C.

Freezing of the cells

Adherent cells from one confluent T175 culture flask were harvested by washing them with 15 ml of PBS 1x, trypsinizing with 5 ml of trypsine-EDTA (0.25%) for 5 min at 37°C, and centrifuging in 15 ml of MEF medium for 5 min at 1000 rpm. Next, the cell pellet was resuspended in 10 ml of freezing medium (see Materials section) and evenly distributed

in 10 x 1ml Nunc™ cryogenic tubes (Thermo Scientific). Tubes with cells were kept on ice for 2 min and placed at -80°C or in the liquid nitrogen, according to the purpose of their use.

Thawing of the cells

Thawing procedure is characterized by a rapid increase in temperature and fast exchange of culture medium in order to avoid toxic effects of the high content of DMSO in the freezing medium. To thaw the cell line, cryo tubes with frozen cells were placed directly in the water bath at 37°C. As soon as frozen medium started to thaw, cells were immediately transferred into Falcon tube with 10 ml of pre-warmed MEF medium and resuspended. Cell suspension was centrifuged for 5 min at 1500 rpm. Cell pellet was washed with 10 ml of PBS, centrifuged again for 5 min at 1500 rpm, and resuspended in 5 ml of MEF medium. Finally, medium with cells was pipetted to the T25 culture flask and placed at 37°C in the cell incubator.

2.2.2.3. Flow cytometric analysis of cell death

2.2.2.3.1. Plasma membrane permeabilization

Cell death analysis was performed using flow cytometry. Dying cells shrink and become more granular resulting in a lower forward scatter index (FSC) and increased side scatter index (SCC), respectively. Death-associated loss of membrane impermeability can be monitored by using propidium iodide (PI) staining (SCC/strength of PI emission signal). In living cells, PI does not penetrate. However, PI stains nuclei of dead cells fluorescent red. Briefly, cells were centrifuged for 5 min at 1000 rpm, washed with PBS, suspended in PBS and stained by mixing with 1:1 volume of PI solution (5 µg/ml in PBS). Next, cells were immediately subjected to FACS analysis (PI excitation wavelength is 535 nm and emission wavelength is 617 nm).

The results are presented as percentage of “specific cell death”, calculated according to the following formula (Ehret, Westendorp et al. 1996):

$$\text{“Specific cell death” [\%]} = \left(\frac{\text{dead cells [\%]} - \text{dead cells [\%]}_{\text{(untreated control)}}}{100 - \text{dead cells [\%]}_{\text{(untreated control)}}} \right) \times 100$$

2.2.2.3.2. Analysis of apoptotic nuclear fragmentation

Fragmentation of cell nuclei was analyzed essentially according to the method of Nicoletti *et al.* (Nicoletti, Migliorati et al. 1991). Cell nuclei were isolated by cell lysis and staining with PI using following buffer: 0.1 % Na-citrate, 0.1% (v/v) Triton X-100 and 50 μg/ml PI. Measurement of fluorescence signal enables an assessment of the amount of subG1 nuclear fraction, which is characteristic for apoptotic nuclear fragmentation. Cells were centrifuged at 2000 rpm for 5 min, washed with PBS, and carefully suspended in 100 μl of Nicoletti lysis buffer. After overnight lysis at 4^{o}C in dark, isolated nuclei were analyzed by flow cytometry (PI fluorescence readout).

2.2.2.4. Flow cytometric analysis of cell cycle

Cells were harvested and suspended in a 1 ml of wash buffer (PBS + 0.1% FBS), then fixed by drop-wise addition of 3 ml of absolute ethanol while vortexing. Next, cells were incubated o/n at 4^{o}C, washed with PBS and suspended in 1 ml of the PI staining solution (3.8 mM Na-citrate, 40 μg/ml PI) supplemented with 50 μl of RNAase A stock solution (10 μg/ml RNase A, Qiagen). Subsequently, samples were analyzed by FACS.

2.2.2.5. DAPI and TUNEL staining

In order to investigate morphological changes of nuclei characteristic for apoptotic fragmentation, labeling of nuclear DNA in *Rint1* inducible knock-out MEF cell lines was performed. Cells were stained using 4'6-diamidino-2-phenylindole (DAPI) blue-fluorescent dye (Invitrogen, #D1306) according to the manufacturer's protocol. Briefly, cells growing on the microscope slides were fixed and permeabilized (4% paraformaldehyde in PBS and 0.1% Triton X-100 in PBS, respectively), followed by equilibration with PBS. Diluted DAPI stock solution (end concentration 300 nM in PBS) was applied on the cells and incubated for 5 min. Samples were rinsed 2-3 times in PBS, drained and mounted with a ProLong Gold antifade reagent (ThermoFisher Scientific, #P36930).

Further verification of putative apoptosis was performed using ApopTag Plus® Fluorescein *In Situ* Apoptosis Detection Kit (Chemicon International, #S7111) following manufacturer's manual. This technique uses principles of the TUNEL (terminal deoxynucleotidyl

transferase dUTP nick end labeling) assay and allows for detection of single- and double-stranded DNA breaks .

2.2.2.6. 4-hydroxytamoxifen (OHT)-induced knock-out

Mouse embryonic fibroblast (MEF) cell lines were generated by Dr. Pierre-Olivier Frappart. Cells were isolated from embryonic day E13.5 *Rint1* Flox/Flox embryos and immortalized following the "3T3 protocol" (Todaro and Green 1963). After immortalization, MEFs were transduced with retroviruses carrying pMSCVpuro construct (to generate EV control) or pMSCVpuro-Cre-ER(T2) (construct encoding Cre recombinase under control of estrogen receptor-driven promoter); for cell line specification see Materials and Methods p. 2.1.3.. To delete *Rint1,* cells were treated with 1 µM 4-hydroxytamoxifen (4-OHT) (Sigma-Aldrich, #H7904) for 48 h or 96 h. The knock-out efficiency was monitored by genomic DNA PCR, with following primers: for WT allele: RINT7512F (5'-TTCCTACTGACTTGCTGTGAT-3') and RINT8345R (5'-ACTTCTGGATGACTGAGGAC-3'), for Δ allele: RINT6542F (5'-TAACCCCTGACCCATCTCTC-3') and RINT8345R.

2.2.3. Biochemical methods

2.2.3.1. Yeast two-hybrid assay

The yeast two-hybrid assay was performed by Dr. Stefan Push, University of Heidelberg, Heidelberg, Germany as previously described (Weiler, Blaes et al. 2014).

2.2.3.2. SDS-PAGE and Western blotting

Cell pellet was resuspended in ice-cold lysis buffer with protease inhibitor mixture and incubated for 30 min at 4°C on a rotary shaker. Next, cell lysates were sonicated for 4-5 sec, 30% of amplification, and centrifuged at 14000 x *g* for 15 min at 4°C. The supernatant was transferred to a fresh tube and the protein concentration was determined using the spectrophotometric analysis. Aliquots of cell lysates (*e.g.* 40 µg) were separated using SDS-facilitated polyacrylamide gel electrophoresis (SDS-PAGE). Separation conditions

were: polyacrylamide gels of single percentage (8%, 10% or 12%, depending on the protein size), or a gradient gel (4-15%), used in case of HUWE1-specific IP experiments (MW 482 kDa) and 100 V with 25 mA. The gel was blotted to nitrocellulose membrane (Hybond ECL, GE Healthcare Life Sciences) o/n using wet transfer system (Bio-Rad) at 4°C (with ice coat and constant mixing). Transfer conditions were 30 V (const.) and 90 mA. After blotting, membranes were blocked by 1 h washing in blocking solution (4% powdered milk in TBST 0.05%), washed 10 min with TBST 0.05% and incubated for 1h or o/n with primary antibody (suspended in 4% powdered milk, TBST 0.05%), at RT or 4°C, respectively. Then, membranes were washed 3 x 10 min with TBST 0.1% solution and stained with horseradish peroxidase-conjugated secondary antibody for 1 h at RT. Next, membranes were 3 x washed, each washing step of 10 min, with TBST 0.1%, TBST 0.05% and TBS, consecutively. The protein-specific signal was detected by enhanced chemiluminescence using Western Lightning Chemiluminescence Reagent (PerkinElmer), according to the manufacturer's protocol. Signal intensity was analyzed by densitometry using ImageJ software.

2.2.3.3. Protein immunoprecipitation

Cells were lysed using lysing buffer for immunoprecipitation experiments (see Materials section). Immunoprecipitation of tag-fused proteins was performed using anti-FLAG® M2 Affinity Gel (Sigma-Aldrich), anti-HA Affinity Matrix (Roche) or GFP-Trap®_A (ChromoTek), depending on the protein's tag and according to manufacturer's protocol. Briefly, cell lysates were incubated with specific antibody conjugated with matrix (*e.g.* agarose beads), for 30 min to o/n, at 4°C. Next, matrix was washed 6 x with ice-cold TBS buffer. Tag-fused protein was eluted using SDS-PAGE sample buffer and by boiling the samples for 5 min at 95°C. Samples were subjected to Western blot analysis immediately after being eluted.

2.2.3.4. Mass-spectrometry analysis

Mass spectrometry analysis of immunoprecipitated GFP-tagged RINT1 protein and GFP-tagged empty vector control, was performed by the Genomics and Proteomics Core Facility, DKFZ, Heidelberg, Germany, and by the Core Facility for mass spectrometry,

ZMBH, Heidelberg, Germany. Analysis of obtained results was performed using Scaffold4 software.

3. Results

3.1. RINT1 degradation

3.1.1. RINT1 has a short half-life

Despite the ubiquitous expression of *RINT1* in a large number of mammalian tissues (*e.g.* according to BioGPS database, biogps.org, and others, see Introduction section), endogenous RINT1 levels are hardly detectable using commercially available antibodies. Although low specificity of the antibodies definitely contributes to this observation, it also indicates putative fast turnover and/or low stability of the protein. Indeed, the initial study showed that the level of overexpressed RINT1 decreased fast and spontaneously during 24-48 h upon the expression (Fig. 18A), suggesting a short half-life of RINT1. Consistently with this assumption, an inhibition of protein translation by cycloheximide (CHX) in COS-7 cells expressing N-terminally FLAG-tagged RINT1, resulted in almost complete depletion of RINT1 levels already within 8 h of the treatment (Fig. 18B). A significant decrease of the protein level was observed after 1 h of the CHX administration (Fig. 10B).

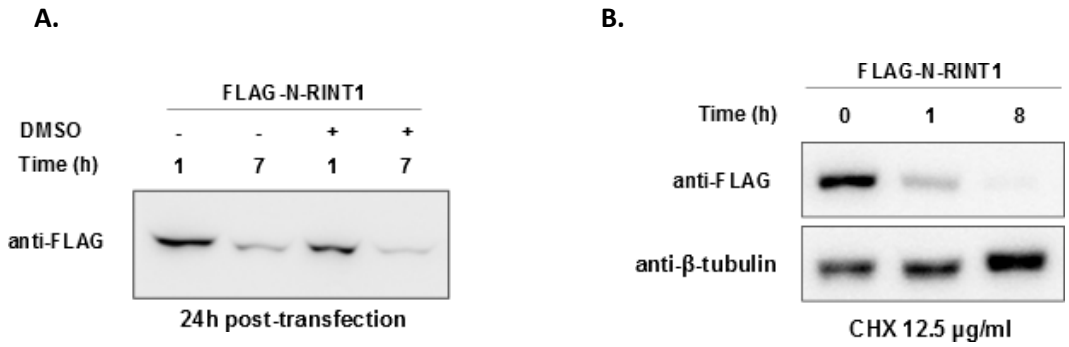

Figure 18. RINT1 is an unstable protein. (A) Overexpressed RINT1 levels in COS-7 cells decrease fast and spontaneously during 24 h post-transfection. (B) FLAG-RINT1 levels in COS-7 cells significantly decrease upon cycloheximide treatment.

To verify whether the N-terminal position of the FLAG-tag influences fast decay of RINT1 upon the CHX treatment, an experiment with C-terminally tagged protein version was performed. The results were similar to the ones previously described: FLAG-C-RINT1 levels significantly decreased after 1h of protein biosynthesis inhibitor treatment, and 8 h of drug activity was enough to deplete protein from the cells completely (Fig. 19). This

experiment showed, that low stability of overexpressed RINT1 is not tag-position-dependent.

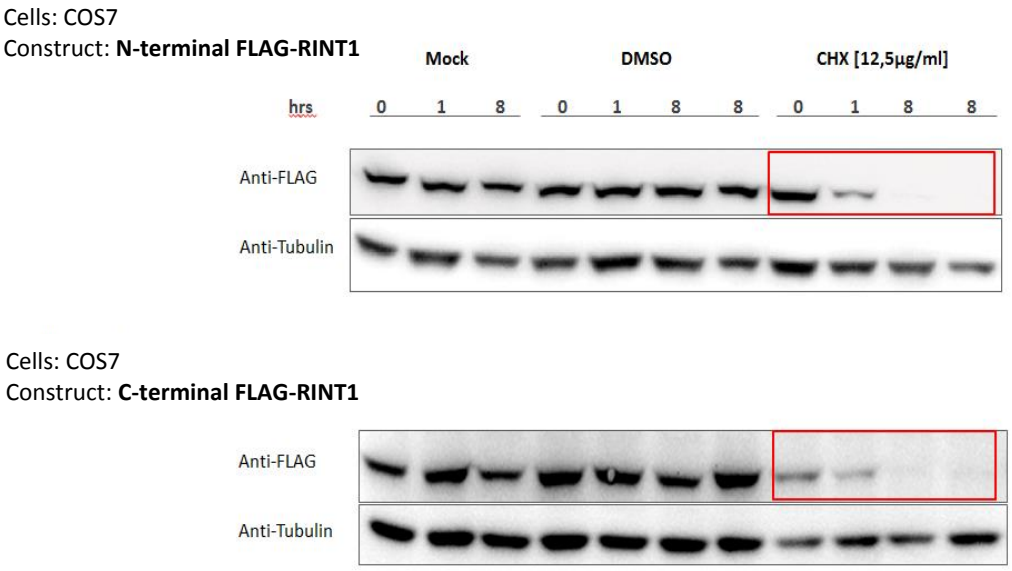

Figure 19. Fast cellular turnover of overexpressed RINT1 is not tag-position-dependent. COS-7 cells were electroporated with indicated plasmids. At 24 h post-transfection, the cells were incubated with 12.5 µg/ml CHX for 0 h, 1 h and 8 h and were collected for WB. ß-tubulin was used as a control.

In order to quantify RINT1 degradation and to determine the exact half-life of the protein, a CHX-chase study was performed. To do this, HEK293T cells were transfected with FLAG-N-RINT1 or FLAG-C-RINT1 plasmids, and the CHX was added. Cellular levels of FLAG-RINT1 were detected by Western blot (WB) at indicated time points, and quantified using ImageJ software. As expected, RINT1 decay was fast and resulted in total depletion after 6 h of the CHX treatment (Fig. 20). The half-life of the N-terminally FLAG-tagged protein was calculated to be 38.5 min, and 40.46 min for the C-terminally tagged protein version.

A.

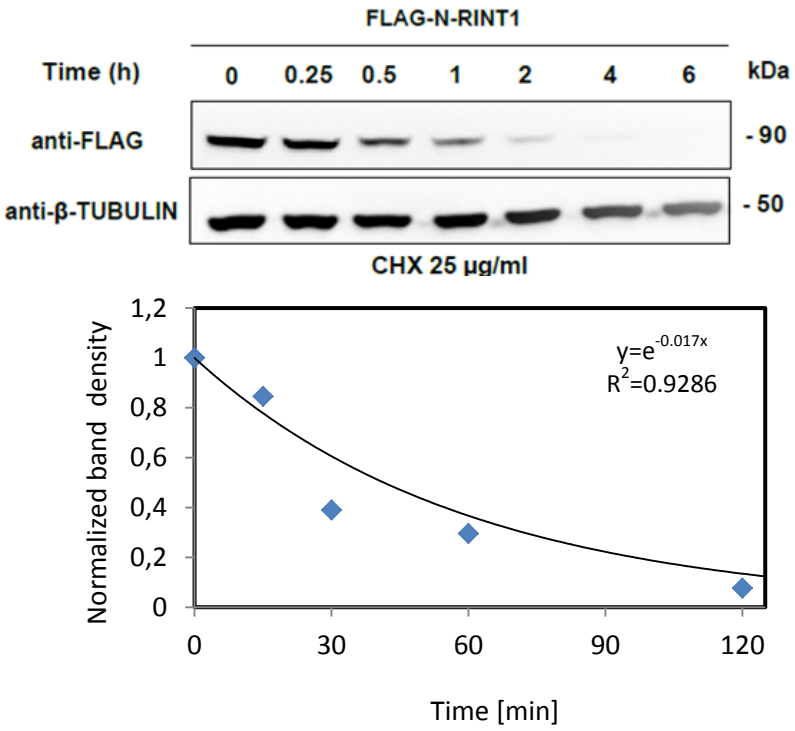

B.

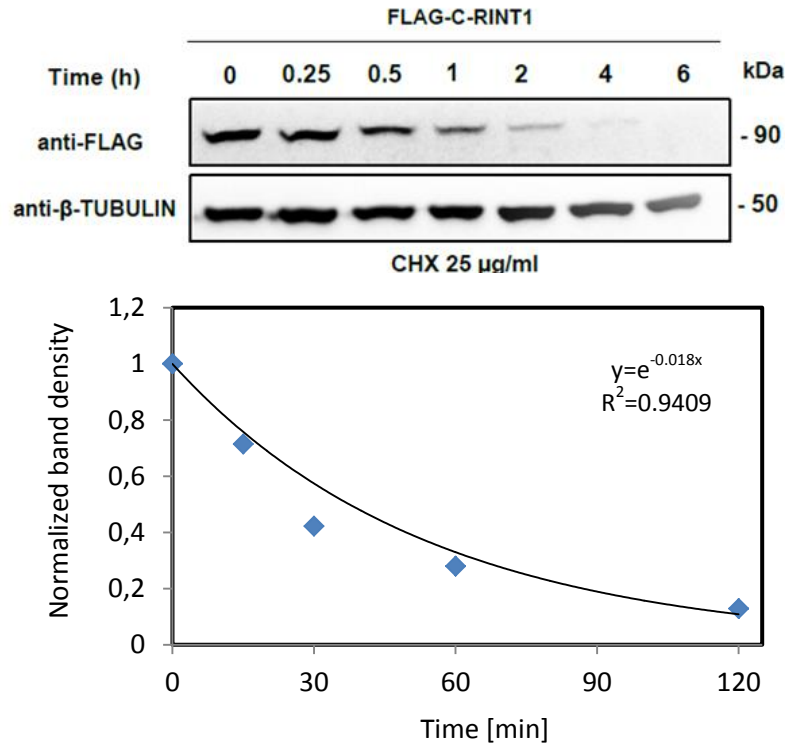

Figure 20. RINT1 has a short half-life. HEK293T cells were transfected with plasmid FLAG-N-RINT1 **(A)** or FLAG-C-RINT1 **(B)**. At 24 h post-transfection, the cells were incubated with 25µg/ml CHX for different times (15 min to 6 h) and harvested for WB. ß-tubulin was used as a loading control (upper panels). Half-life was calculated based on WB bands intensities measured by the ImageJ software and evaluated following the gel analysis method outlined in the ImageJ documentation (lower panels).

Since no significant effect of the FLAG-tag positioning on degradation pattern of RINT1 was observed (Fig. 11-12), the N-terminally FLAG-tagged protein version was applied for all subsequent experiments.

3.1.2. RINT1 is degraded *via* proteasomal pathway

Apart from investigating CHX influence on RINT1 cellular levels, protein stability was tested by the treatment of HEK293T cells transiently expressing FLAG-Rint1 plasmid with proteasome inhibitor, MG132. Interestingly, after 8h of the treatment, MG132 not only prevented RINT1 from degradation leading to significant protein accumulation, but a shifted-up band appeared, indicating putative post-translational modification (PTM) of the protein (Fig. 21, arrow indicates a “shifted-up band”).

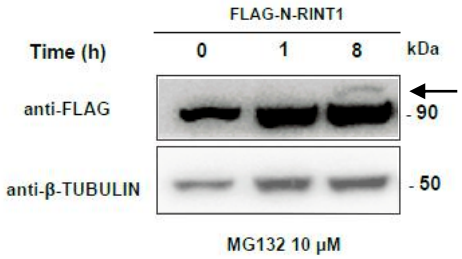

Figure 21. RINT1 is stabilized upon MG132 treatment. HEK293T cells expressing RINT1 were treated with 10 µM of proteasomal inhibitor MG132 for 0 h, 1 h and 8 h. Cells were harvested and analyzed by WB. ß-tubulin was used as a loading control. MG132 strongly stabilized RINT1 levels and 8 h of the treatment resulted in a shifted-up band.

To delineate biological pathways involved in the regulation of RINT1 stability, RINT1-transfected COS-7 cells were treated with or without addition of CHX with following agents: (i) leupeptin, an inhibitor of cysteine and trypsin-like proteases, (ii) ammonium chloride (NH_4Cl) or (iii) chloroquine, inhibitors of lysosomal protein degradation and autophagy, (iv) rapamycin, an autophagy inducer, and (v) MG132, an inhibitor of proteasomal activity. Thus, three putative degradation pathways were tested: (1) lysosomal degradation pathway, (2) autophagy and (3) proteasomal degradation pathway. None of the (i-iv) treatments significantly affected RINT1 stability. All the chemicals were inefficient to block RINT1 degradation with an exception of MG132, which

clearly stabilized protein levels (Fig. 22). These results showed that RINT1 is degraded *via* a proteasomal pathway.

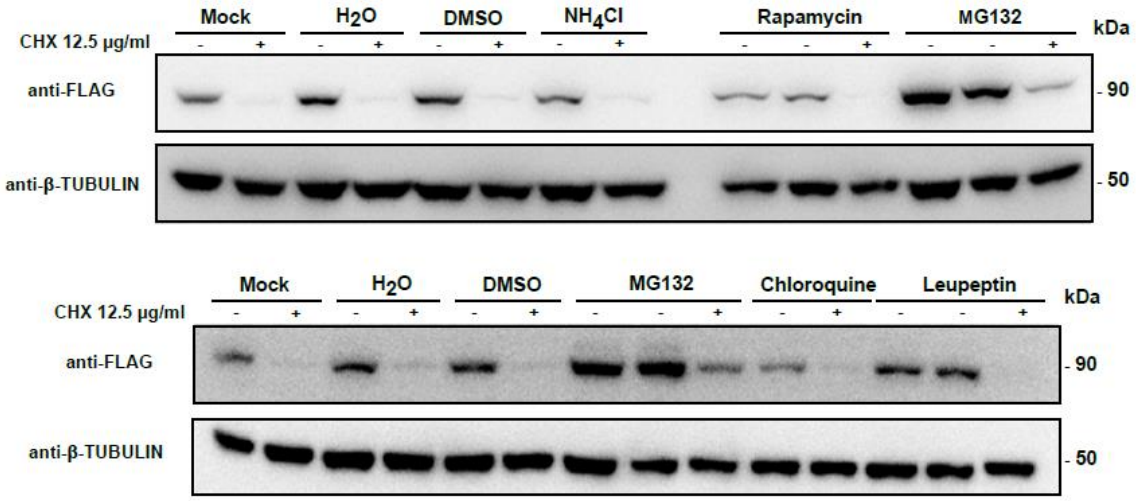

Figure 22. RINT1 is degraded *via* proteasomal degradation pathway. COS-7 cells were electroporated with FLAG-Rint1 plasmid. At 24h post-electroporation, indicated chemicals were added: 12.5 µg/ml CHX, 5 mM NH_4Cl, 0.2 µM rapamycin, 10 µM MG132, 25 µM chloroquine or 20 µM leupeptin. After 8h of the treatment, cells were collected for WB analysis. ß-tubulin was used as a loading control.

3.2. RINT1 ubiquitination

Proteins degraded by the proteasome are usually modified by polyubiquitination (polyubiquitin, polyUb), a post-translational modification (PTMs) mediated by the activity of an E3 ligase. RINT1 was found to be degraded *via* proteasomal pathway, and the inhibition of proteasome activity resulted in the generation of an additional RINT1 form of higher molecular weight (“shifted-up band”) indicating a PTM.

3.2.1. RINT1 is polyubiquitinated

To verify covalent attachment of polyUb chains to the RINT1 molecule, a co-immunoprecipitation (co-IP)-mediated approach was applied. HEK293T cells were co-transfected with plasmids harboring cDNA of human FLAG-tagged RINT1 and HA-tagged ubiquitin. 24 h after transfection, cells were treated with or without MG132 for 8 h, lysed and subjected to IP with either anti-FLAG or anti-HA antibodies. Immunoprecipitates were analyzed by WB (Fig. 23).

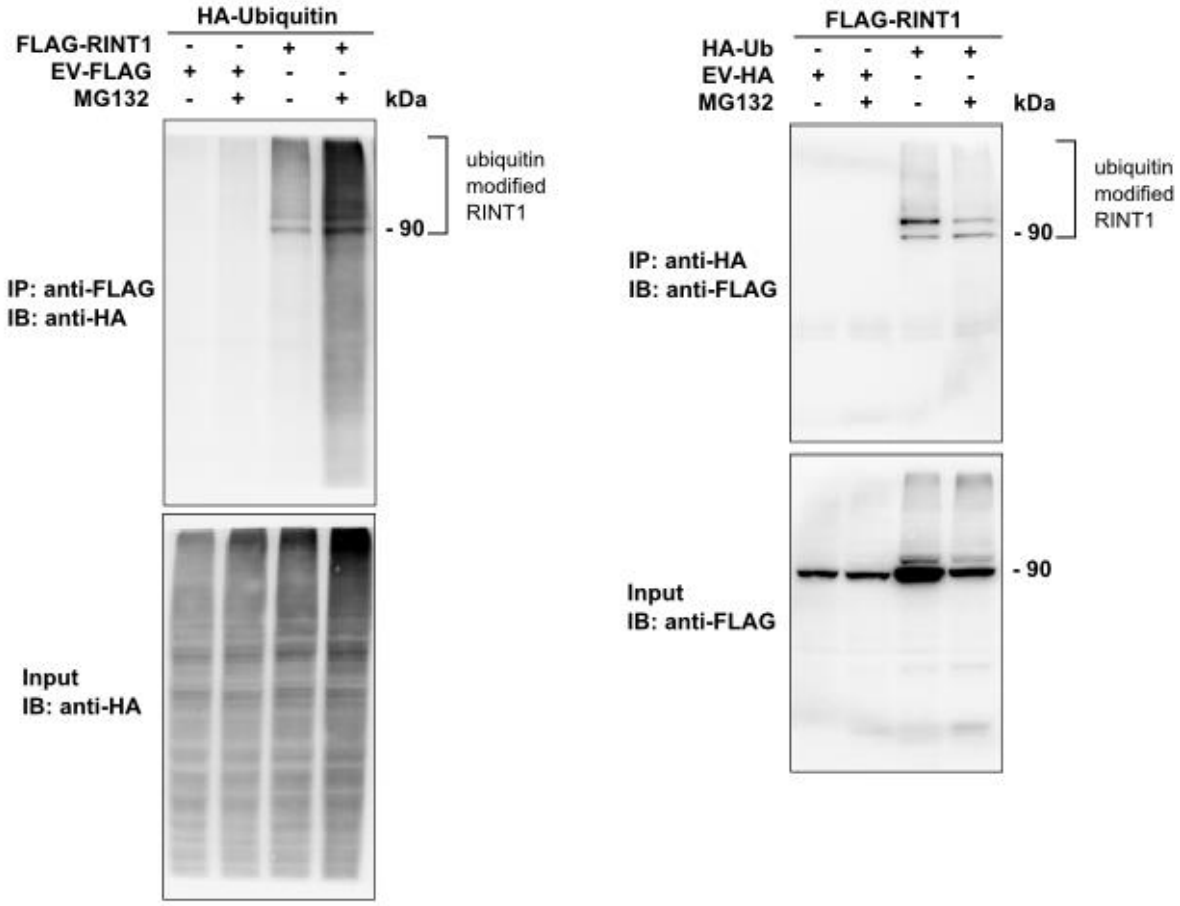

Figure 23. RINT1 is polyubiquitinated. HEK293T cells were co-transfected with indicated plasmids, treated or not with 10 µM MG132 for 8 h and lysed. Co-immunoprecipitates were subjected to WB analysis.

In samples, in which RINT1 and ubiquitin were co-expressed, high molecular complexes were detected representing polyubiquitinated fraction of RINT1. The results clearly demonstrated, that RINT1 protein is modified by ubiquitination.

3.2.2. K48-linked polyubiquitin chains target RINT1 for proteasomal degradation

Protein ubiquitination has different functions depending on which lysine (K) residue of ubiquitin is used as a polyUb chain linker. K48-mediated polyubiquitination is the most established as a mediator of proteasomal protein degradation. In K48-mediated polyubiquitin chain ubiquitin monomers are linked one to another *via* their lysine residue on the position 48. To define whether RINT1 ubiquitination is associated with protein degradation, FLAG-RINT1 was co-expressed in HEK293T cells together with plasmid encoding HA-tagged ubiquitin mutant, which lacked six out of seven lysines of ubiquitin aa sequence. All the lysines except lysine 48 were mutated to arginine (HA-Ub-K48). Thus, the detected ubiquitin chain could only be formed *via* the remained, non-mutated lysine. Co-IP-mediated analysis clearly confirmed that RINT1 was modified by K48-linked polyUb chains marking it for proteasomal degradation (Fig. 24).

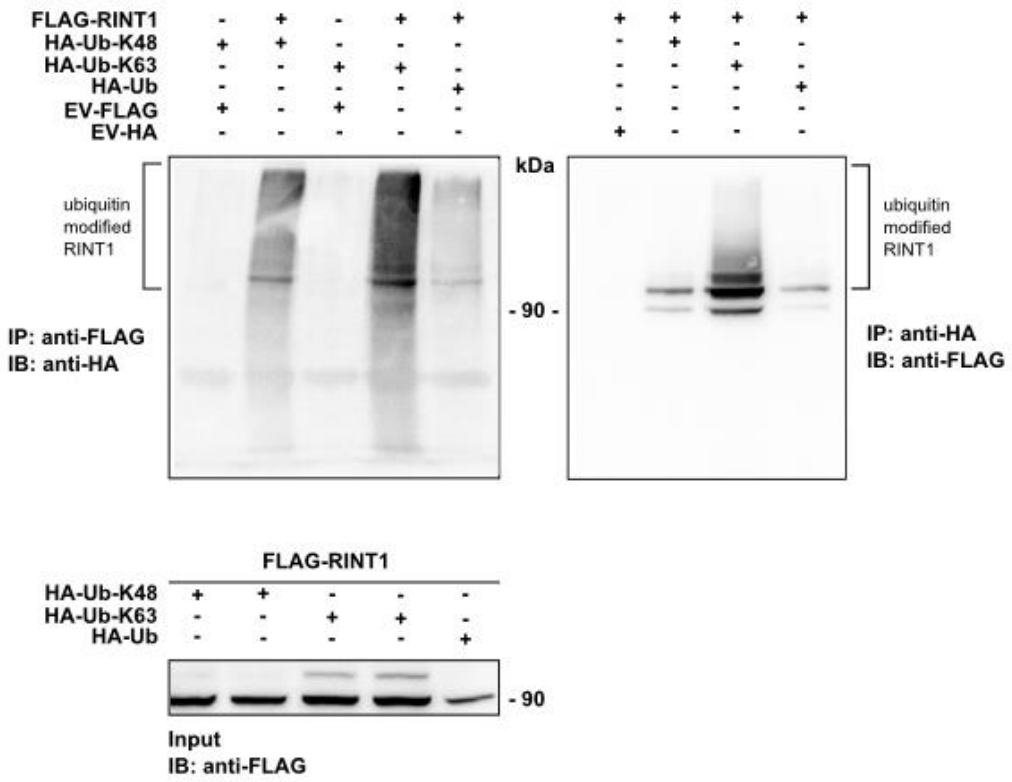

Figure 24. RINT1 is polyubiquitinated *via* K48- and K63-linked ubiquitin chains. HEK293T cells were co-transfected with indicated plasmids. Co-immunoprecipitates were subjected to WB analysis.

3.2.3. RINT1 is also polyubiquitinated by K29- and K63-linked chains

The finding that RINT1 is markedly ubiquitinated with or without addition of MG132 (Fig. 15), suggested the existence of additional ubiquitination modes of RINT1, besides the one mediated by K48 linkage. Thus, next experiments were designed to verify whether RINT1 ubiquitination had only degradative functions, or other, related to signaling and/or regulation of protein functions. To answer this question, the series of co-IP experiments was performed. HEK293T cells were co-transfected with FLAG-RINT1 plasmid and HA-tagged ubiquitin mutants: HA-Ub-K29, encoding ubiquitin with only one lysine residue on the position 29 (Fig. 25), or HA-Ub-K63 mutant, harboring ubiquitin with only K63 lysine residue (Fig. 24). All other lysines were mutated to arginine. In an analogous manner to previously described experiment, if RINT1-ubiquitin interaction was detected, it could only originate from the polyUb chains formed *via* K29- or K63-linkage. Cells were lysed, subjected to IP with either FLAG- or HA-antibody and analyzed by WB. The study revealed that RINT1 was also polyubiquitinated by K29- and K63-mediated polyUb chains, which are often addressed to have regulatory functions.

IP results:

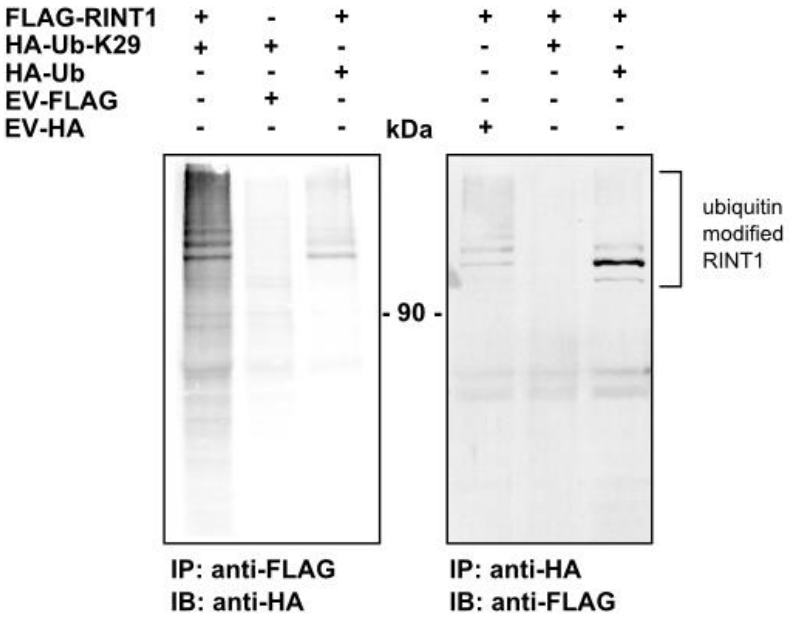

Input control:

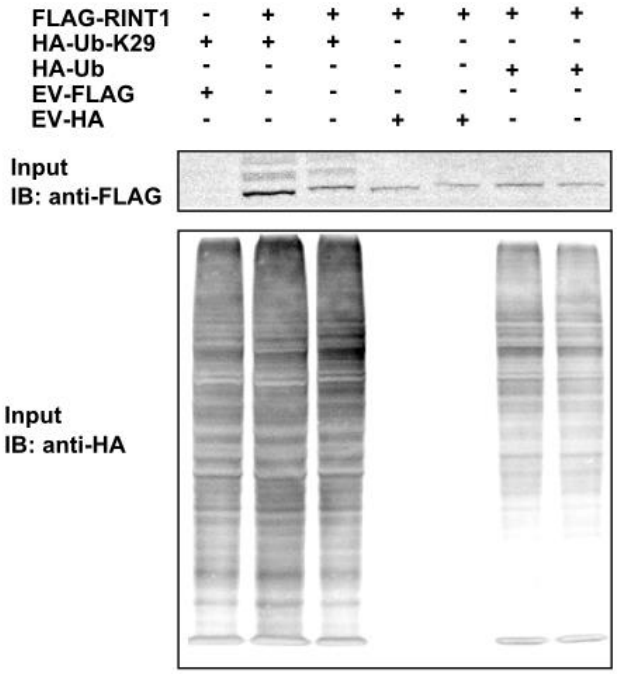

Figure. 25. RINT1 is polyubiquitinated *via* K29-linked ubiquitin chains. HEK293T cells were co-transfected with indicated plasmids as described for Fig. 16. Co-immunoprecipitates were subjected to WB analysis.

3.2.4. RINT1 is modified by mono- or linear ubiquitin chains

Modification of a target protein function could also be achieved by attaching unbranched polyUb chain, which is a particular way of inter-ubiquitin linkage, called “head-to-tail” (or linear, or M1-linked) chain, leading to linear polyubiquitination. To investigate whether RINT1 could be subjected to this special way of ubiquitination, a co-IP experiment was performed, using lysine-less Ub mutant (Ub-K0), and FLAG-RINT1. Notably, in addition to forming linear polyUb chains, Ub-K0 might also attach to the target protein as a monomer, at one or multiple sites (monoubiquitination). Interestingly, RINT1 interacted covalently with Ub-K0 (Fig. 26), indicating linear ubiquitination of RINT1 and/or monoubiquitination.

IP results:

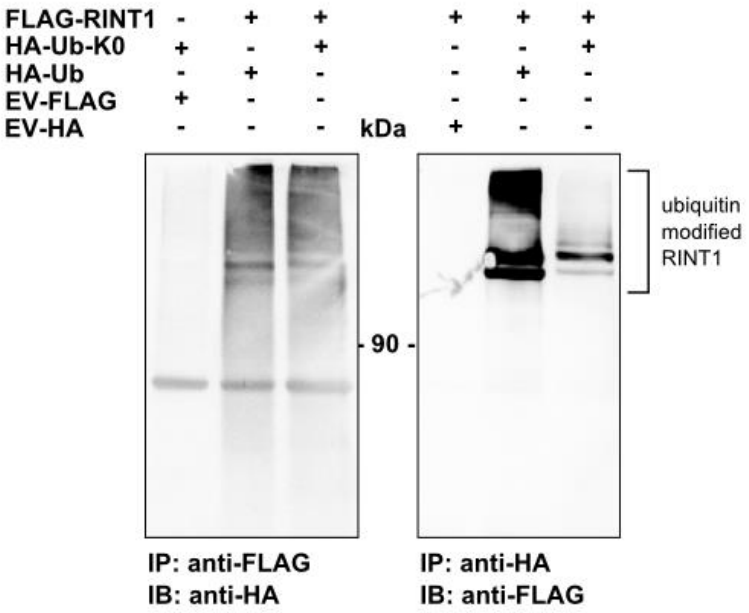

Input control:

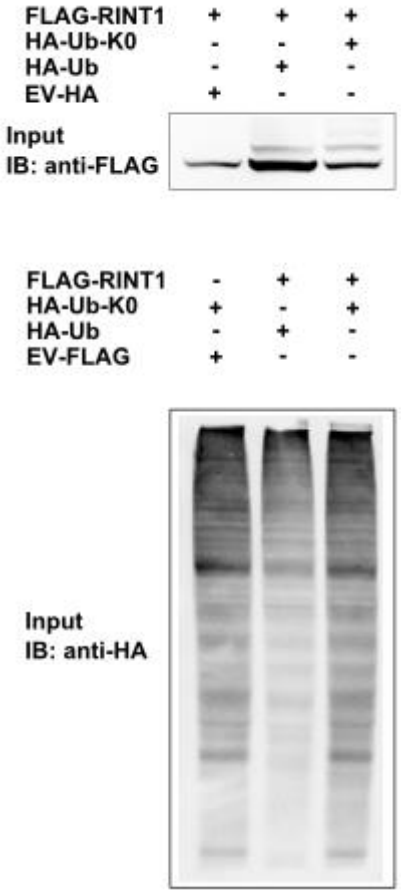

Figure. 26. RINT1 is polyubiquitinated *via* lysineless ubiquitin mutant. HEK293T cells were co-transfected with indicated plasmids (as previously described for Fig. 16). Co-immunoprecipitates were subjected to WB analysis.

In conclusion, RINT1 was demonstrated to be polyubiquitinated not only by K48-polyUb chains, which target the protein for degradation, but also by K29-, K63-poluUb, and linear ubiquitin chains, or even monoubiquitination, at one or multiple sites, for regulatory and/or signaling purposes. To assay a relative abundance of the identified Ub linkages at the RINT1 protein, a co-transfection/co-IP experiment with all HA-Ub constructs previously applied (Fig. 23-26) and analyzed by detection with common antibodies was performed.

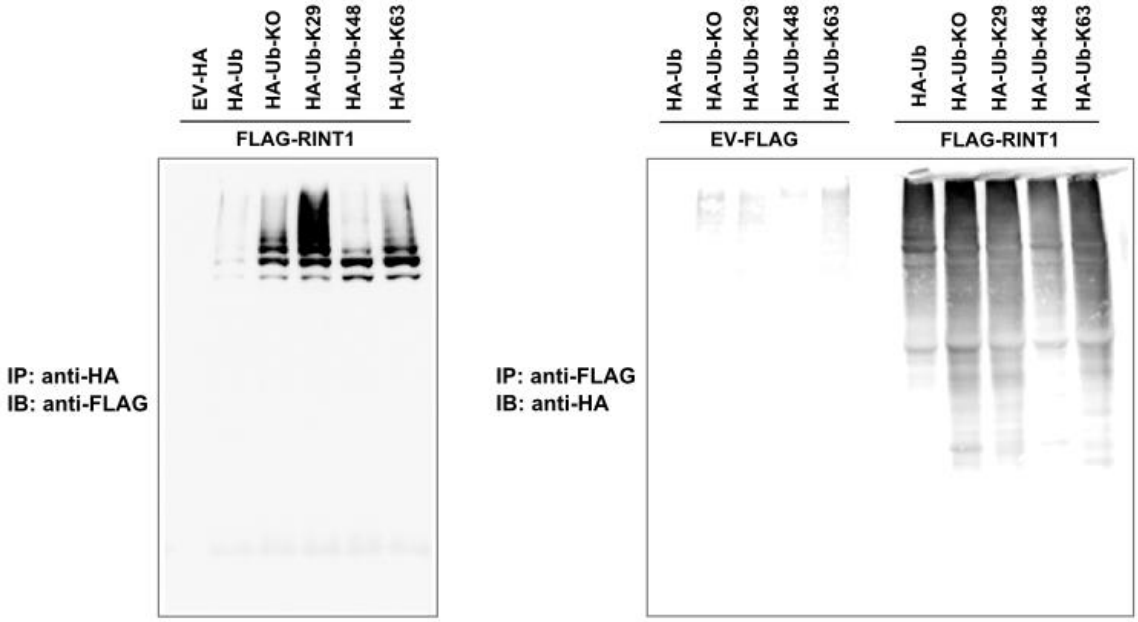

Figure 27. RINT1 is polyubiquitinated by K29-, K48-, K63- and K0 ubiquitin chains. HEK293T cells were co-transfected with indicated plasmids. Co-immunoprecipitates were subjected to WB analysis.

The results shown in Figures 27 and 28 summarize all verified modes of ubiquitination of RINT1. Interestingly, as shown in Fig. 28, co-transfection of HEK293T cells with FLAG-RINT1 and plasmids encoding HA-tagged non-mutated ubiquitin, or ubiquitin lysine mutants, resulted in relatively different RINT1-specific signal, depending on the ubiquitin mutant introduced to the cells. The strongest signal and clearly detectable ladder was observed in the case of co-transfection with HA-Ub-K29 and HA-Ub-K0 plasmids, suggesting a relative prevalence of these RINT1 modifications.

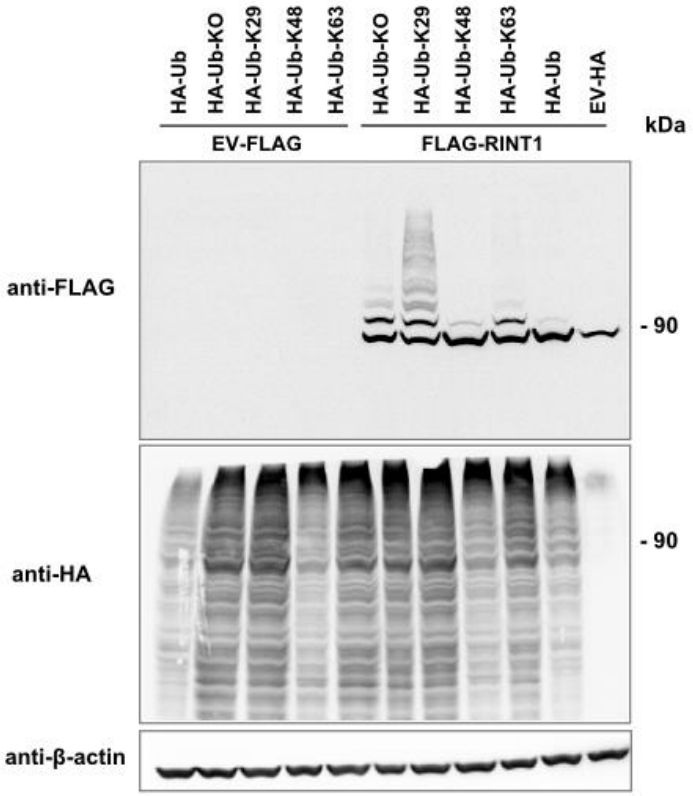

Figure 28. RINT1-specific signal intensity depends on the ubiquitin mutant interacting with RINT1. HEK293T cells were co-transfected with indicated plasmids. Lysates were subjected to WB analysis. ß-actin was used as a loading control.

3.2.5. Screening for RINT1 interactors reveals protein candidates involved in ubiquitination

In order to unravel the mechanism of RINT1 ubiquitination as well as a putative role of this process and possibly the function of the RINT1 itself, two screens, a yeast two-hybrid (Y2H) assay and mass spectrometry analysis, were performed. The specific objective of these screens was to identify proteins interacting with RINT1, especially E3 ubiquitin ligase(s), and mediating post-translational modifications.

3.2.5.1. Results of yeast two-hybrid screen

Yeast two-hybrid screen was executed by Dr. Stefan Pusch, DKFZ, Heidelberg, Germany. It resulted in detection of several interesting candidates for RINT1-binding partners. The candidates were proteins related to introduction of ubiquitination or other post-translation protein modifications. Following proteins, which fulfilled this requirement, were detected:

- SUMO2 (small ubiquitin-related modifier 2),
- PSME1 (proteasome activator complex subunit 1),
- PKIA (cAMP-dependent protein kinase inhibitor alpha),
- SENP8 (sentrin-specific protease 8 or NEDD8-specific protease 1), and
- STK10 (serine/threonine protein kinase 10).

Proteins listed above, indicated that RINT1 might be subjected to other PTMs, besides ubiquitination. In particular, detection of SUMO2 suggested a possibility of SUMOylation of RINT1, as SUMO protein is known to be involved in this process. Thus, SUMO2 was selected as promising candidate for further analysis and verification of the results of yeast two-hybrid assay. Of note, no E3 ubiquitin ligase was found by the screen procedure.

3.2.5.2. Mass spectrometry analysis

Next, mass spectrometry-mediated analysis was applied as another approach to detect binding partners of RINT1. In particular, the analysis was aimed at identification of proteins involved in PTM mediation and/or cellular pathways previously described as common with RINT1. HEK293T cells overexpressing GFP-tagged RINT1 were lysed and subjected to IP with GFP-binding alpaca antibody (having reduced background signal due to the lack of the light Ig light chains). In order to provide specificity for test, independent GFP-EV control analysis was included. Putative binding-partners were considered only when they were identified in the GFP-RINT1 pull down experiment and not in the GFP-EV one. Two independent screens were performed in cooperation with two core facility laboratories. SDS-PAGE gels containing immunoprecipitates were submitted for mass spectrometric analysis to the DKFZ Genomics and Proteomics Core Facility, and the ZMBH Core Facility for Mass Spectrometry (both Heidelberg, Germany). Similarly to the analysis

of the results of the yeast two-hybrid assay, proteins of interest were identified on the basis of possible engagement in mediation of PTMs as well as participation in cellular processes previously identified in the context of RINT1 function. In addition, they were verified for specificity of interaction using GFP-RINT1-transfected samples *versus* EV-GFP-transfected control. The list of identified binding partners as well as examples of false-positive results (*e.g.* CAND1_HUMAN) are shown in the table (Tab. VII). Partner proteins should be considered as a RINT1-specific interactors only if found in GFP-RINT1, and not in GFP-EV sample. The examples of false-positive results (*e.g.* CAND1_HUMAN) are shown in the table.

Table VII. ZMBH Core Facility for Mass Spectrometry results. List of selected RINT1-binding partners.

Protein identified	GFP-RINT1	GFP-EV	Accession number	Sequence coverage [%] (probability over 95%)						Total nr of unique peptides (probability over 95%)					
				X-13-150-03	X-13-150-04	X-13-150-05	X-13-150-06	X-13-150-07	X-13-150-08	X-13-150-03	X-13-150-04	X-13-150-05	X-13-150-06	X-13-150-07	X-13-150-08
Cullin-associated NEDD8-dissociated protein 1 [CAND1_HUMAN]	YES	YES	Q86VP6												
DNA repair protein RAD50 [RAD50_HUMAN]	YES	NO	Q92878			0.76						1			
DNA-dependent protein kinase catalytic subunit [PRKDC_HUMAN]	YES	NO	P78527		6	0.48		0,.8			22	2		2	
E3 ubiquitin/ISG15 ligase TRIM25 [TRI25_HUMAN]	YES	YES	Q14258												
E3 ubiquitin-protein ligase BRE1A [BRE1A_HUMAN]	YES	NO	Q5VTR2			5.3						3			
E3 ubiquitin-protein ligase BRE1B [BRE1B_HUMAN]	YES	NO	O75150			7.7						7			
E3 ubiquitin-protein ligase HUWE1 [HUWE1_HUMAN]	YES	NO	Q7Z6Z7	1.5						4					
Poly [ADP-ribose] polymerase 1 [PARP1_HUMAN]	YES	YES	P09874												
Pyruvate kinase isozymes M1/M2 [KPYM_HUMAN]	YES	YES	P14618												
RAD50-interacting protein 1 [RINT1_HUMAN]	YES	NO	Q6NUQ1			23	26	5.7	6.2			14	18	3	3
Small ubiquitin-related modifier 2 [SUMO2_HUMAN]	YES	NO	P61956			13						1			
Ubiquitin-like modifier-activating enzyme 6 [UBA6_HUMAN]	YES	NO	A0AVT1			3						3			
Xaa-Pro aminopeptidase 1 [XPP1_HUMAN]	YES	NO	Q9NQW7					1.8						1	

Conditions of mass spectrometry analysis

Database:
Database Name: the SwissProt_2013_07 database
Taxonomy: *Homo sapiens*
Number of Proteins: 20341

Search Engine:
Mascot, Version: 2.4.1
Fragment Tolerance: 0,50 Da (Monoisotopic)
Parent Tolerance: 100 PPM (Monoisotopic)
Digestion Enzyme: Trypsin
Max Missed Cleavages: 1
Probability Model:
X-13-150-03: Peptide Prophet with Delta Mass Correction [+2 and below,+3,+4,+5,+6 and above]
X-13-150-04: Peptide Prophet with Delta Mass Correction [+2 and below,+3,+4,+5,+6 and above]
X-13-150-05: Peptide Prophet with Delta Mass Correction [+2 and below,+3,+4,+5,+6 and above]
X-13-150-06: Peptide Prophet with Delta Mass Correction [+1,+2,+3,+4,+5,+6 and above]
X-13-150-07: Peptide Prophet with Delta Mass Correction [+2 and below,+3,+4,+5,+6,+7 and above]
X-13-150-08: Peptide Prophet with Delta Mass Correction [+1,+2,+3,+4,+5,+6 and above]

Scaffold Version:
Scaffold_4.0.7
Peptide Thresholds: 90% minimum
Protein Thresholds: 90% minimum and 1 peptide minimum
Peptide FDR: 1,9% (Prophet)
Protein FDP: 1,9% (Prophet)

Database search: Charge state deconvolution and deisotoping were not performed. All MS/MS samples were analyzed using Mascot (Matrix Science, London, UK; version 2.4.1). Mascot was set up to search the SwissProt_2013_07 database (selected for *Homo sapiens*, 20341 entries) assuming the digestion enzyme to be trypsin. Mascot was searched with a fragment ion mass tolerance of 0,50 Da and a parent ion tolerance of 100 ppm. Carbamidomethyl of cysteine was specified in Mascot as a fixed modification. Deamidated of asparagine and glutamine, oxidation of methionine, phosphorylation of serine, threonine and tyrosine and GlyGly of lysine were specified in Mascot as variable modifications.

Criteria for protein identification: Scaffold (version Scaffold_4.0.7, Proteome Software Inc., Portland, OR) was used to validate MS/MS based peptide and protein identifications. Peptide identifications were accepted if they could be established at greater than 90,0% probability by the Peptide Prophet algorithm (Ramakrishnan, Vogel et al. 2009) with Scaffold delta-mass correction. Protein identifications were accepted if they could be established at greater than 90,0% probability and contained at least 1 identified peptide. Protein probabilities were assigned by the Protein Prophet algorithm (Nesvizhskii, Keller et al. 2003). Proteins that contained similar peptides and could not be differentiated based on MS/MS analysis alone were grouped to satisfy the principles of parsimony.

In both experiments, HUWE1 E3 ubiquitin ligase was identified as a binding partner of RINT1. In addition, the analysis performed by the ZMBH core facility identified three other E3 ubiquitin ligases: RNF20 and RNF40, known to form a functional heterodimeric complex RNF20/40, and TRIM25 E3 ligase. Since TRIM25 was also identified in EV control-transfected sample, this protein was not regarded as a specific interactor of RINT1. Interestingly, SUMO2 was also found to be a binding partner of RINT1 by one of the screens, which confirmed the result of the yeast two-hybrid assay. In consequence, the proteins: HUWE1, RNF20, RNF40 and SUMO2, were subjected to further tests in order to verify their binding to RINT1 and the role in RINT1 post-translational modifications. Of note, the analysis identified Xaa-Pro aminopeptidase 1 (XPP1) as RINT1 binding partner confirming its specificity, since this proteins was previously reported to be RINT1 interaction-partner (source database: IntAct, (Stelzl, Worm et al. 2005)).

3.2.6. HUWE1 and RNF20/40 interact with RINT1

Since mass spectrometry analysis strongly suggested, that HUWE1 and RNF20/40 are E3 ubiquitin ligases able to interact with RINT1, subsequent IP experiments were performed to confirm the relevance of these interactions.

HEK293T cells were co-transfected to express GFP-tagged RINT1 and HA-tagged HUWE1 or RNF40 proteins. EV (tag)-co-transfected cells were included into analysis to verify specificity of binding. The cellular lysates were subsequently subjected to GFP-mediated

IP. Then, the WB membranes were probed with anti-HA antibody. In the immunoprecipitates of RINT1, an interaction band(s) were observed (Fig. 29), indicating HUWE1-and RNF40-specific signals. No signal was detected for cells harboring GFP-EV control. Thus, interaction between RINT1 and HUWE1 and between RINT1 and RNF40, was confirmed.

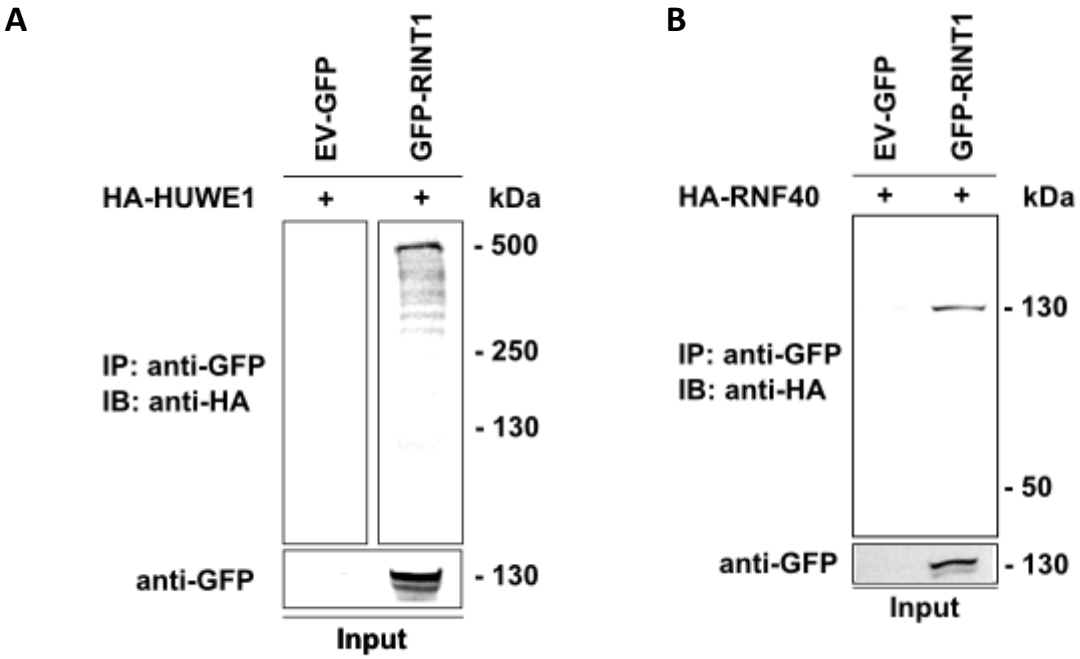

Figure 29. HUWE1 and RNF40 E3 ubiquitin ligases interact with RINT1. A. HEK293T cells were co-transfected with GFP-RINT1 and HA-tagged HUWE1. HUWE1 was identified in RINT1 immunoprecipitate. **B.** HEK293T cells were co-transfected with GFP-RINT1 and HA-tagged RNF40. RNF40 was identified in RINT1 pull-down.

To verify whether the observed interaction between RINT1 and HUWE1 is not tag-dependent, and given a substrate promiscuity of HUWE1, a FLAG-RINT1 expression construct was used for additional IP experiment. The analysis was performed as described for GFP-tagged RINT1. Anti-FLAG antibody-mediated detection showed a clear HUWE1-specific signal, and positively verified binding of HUWE1 to RINT1 (Fig. 30). RINT1 could not be detected in HUWE1 cell lysate pull-down (data not shown). This result could be explained by a low amount of total cellular HUWE1 protein interacting with RINT1, thus staying below detection limits even after pull-down.

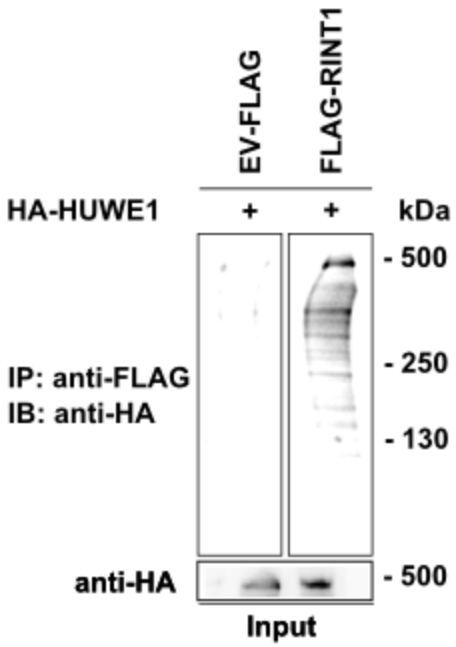

Figure 30. HUWE1 E3 ubiquitin ligase interact with RINT1. HEK293T cells were co-transfected with FLAG-RINT1 and HA-tagged HUWE1. HUWE1 was identified in RINT1 immunoprecipitate.

3.2.6.1. HUWE1 and RNF20/40 are RINT1 E3 ligases

The co-IP analyses confirmed mass spectrometry results and binding RINT1 to HUWE1 and RNF40 E3 ligases. To corroborate the function of HUWE1 and RNF20/40 complex in RINT1 degradation, the experiments involving shRNA-mediated depletion of ligases were performed. HEK293T cells were co-transfected with FLAG-RINT and the plasmids harboring shRNA against *HUWE1*-, *RNF40*- or *RNF20*-specific mRNA (respectively), to down-regulate E3 ligases expression. The plasmid encoding shRNA-scramble was included into study as an EV-control. 24 h after transfection, cells were lysed and subjected to WB analysis. To confirm the reduction of the cellular levels of E3 ligase upon overexpression of shRNA plasmid, membranes were probed with anti-HUWE1, anti-RNF40, or anti-RNF20 antibodies, depending on the experiment and the specific shRNA plasmid used. Subsequently, WB membranes were probed with anti-FLAG antibody, to determine the impact of E3 ligase depletion on putative stabilization of RINT1. Anti-calnexin or anti-ß-actin antibodies were used as loading controls. The experimental assumption was made that the knock-down of E3 ligase responsible for RINT1 polyubiquitination leading to protein degradation, could prevent the protein from proteasomal processing, thus resulting in stabilization of its cellular levels. Indeed, shRNA-mediated depletion of all

tested E3 ligases led to strong stabilization of RINT1, being a consequence of the inhibition of protein degradation (Fig. 31). The observed changes in protein levels were additionally quantified by densitometric analysis. In addition, in the case of HUWE1, knock-down was also confirmed at the mRNA level using reverse-transcription qRT-PCR (data not shown).

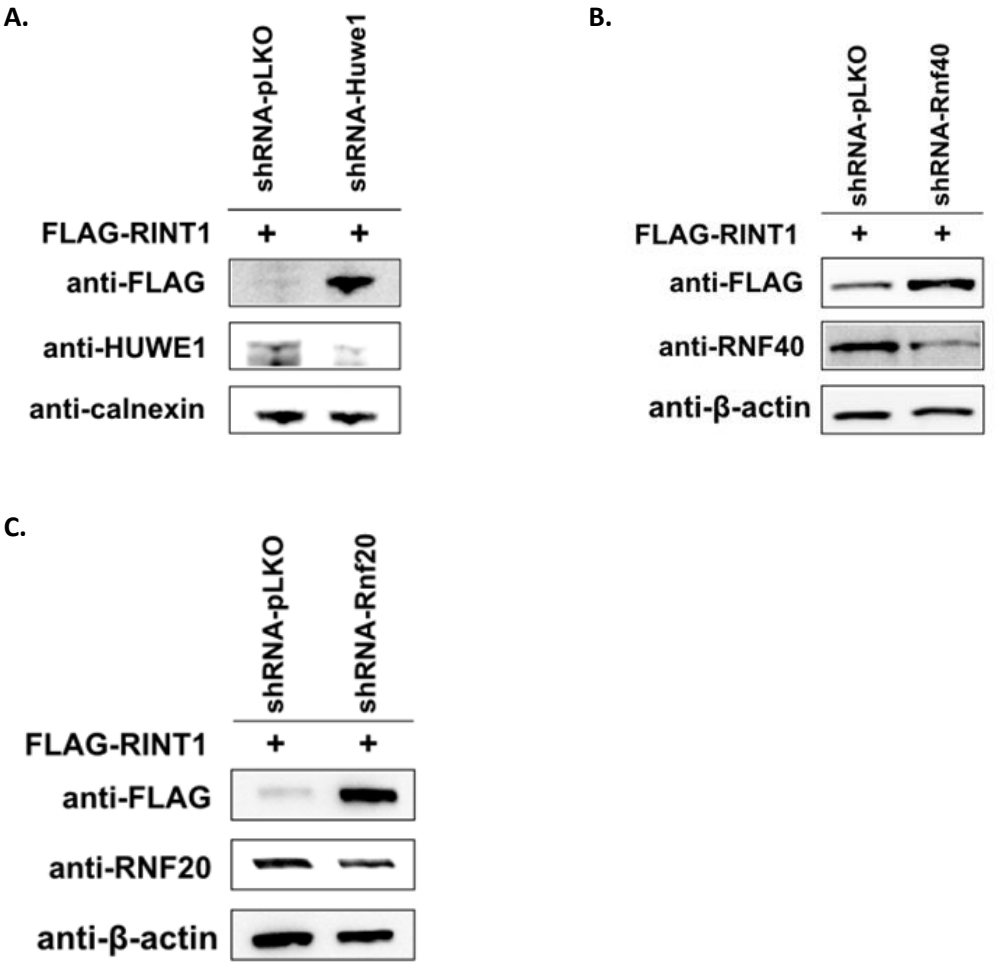

Figure 31. HUWE1 and RNF20/40 E3 ligases regulate RINT1 stability. A. shRNA-mediated depletion of HUWE1 promotes stabilization of RINT1. **B.** shRNA-mediated depletion of RNF40 promotes stabilization of RINT1. **C.** shRNA-mediated depletion of RNF20 promotes stabilization of RINT1.

Interestingly, this effect was the most pronounced in the case of the RNF20 knock-down, since the minor reduction in the ubiquitin ligase protein level resulted in a high increase of RINT1-specific signal (Fig. 31C).

These experiments demonstrated the functional importance of revealed interactions between HUWE1, RNF20, RNF40 and RINT1, and showed that these ligases regulate RINT1 stability by targeting it towards proteasomal degradation pathway.

3.2.7. Mapping ubiquitination sites of RINT1

3.2.7.1. *In silico* analysis predicted several putative ubiquitination sites along RINT1 sequence

In order to identify target sites within RINT1, which could be subjected to ubiquitination, the *in silico* prediction using the on-line available software was performed (www.ubpred.org and www.bdmpub.biocuckoo.org). The analysis revealed multiple, lysine residues, which could presumably be modified by ubiquitination, and assigned confidence (probability) of their occurrence (Fig. 32). Specifically, six lysine residues (K24, K29, K41, K108, K293, K578) were assigned high or medium confidence, while four lysine residues (K62, K114, K525, K771) were of low for possible regarding ubiquitination.

Figure 32. RINT1 has multiple putative ubiquitination target sites. RINT1 lysine residues predicted to be a possible subject of ubiquitination**.** Colors mark the confidence of prediction: red = high confidence, blue = medium confidence, green = low confidence.

3.2.7.2. Site-directed mutagenesis of major *in silico* predicted ubiquitination site does not affect polyubiquitination of RINT1

Since lysine 24 (K24) was *in silico* predicted to be one of two major RINT1 residues probable to undergo ubiquitination (highest confidence score assigned together with residue K288), a site-directed mutagenesis approach was performed. RINT1 mutant protein where lysine on the position 24 was mutated to arginine was generated and designated “RINT1-K24R” (K to R mutation, FLAG-*RINT1*-c.71A>G). Positioning of the K24

residue near the beginning of the protein sequence (N terminus) and in the vicinity of several putative ubiquitination sites of lower probability, suggested its particular role. HEK293T cells were transfected to co-express FLAG-tagged RINT1 or RINT1-K24R proteins together with HA-tagged ubiquitin, and co-IP experiment was performed. Unfortunately, upon FLAG-mediated IPs against RINT1 or RINT1-K24R proteins, no difference in signal intensity for ubiquitin (HA-mediated ubiquitin detection) could be detected. No difference was also seen for FLAG-mediated RINT1 detection in case of HA-mediated IP against ubiquitin. This result strongly suggested a lack of major functional role of K24 site in the ubiquitination of RINT1 protein (Fig 33).

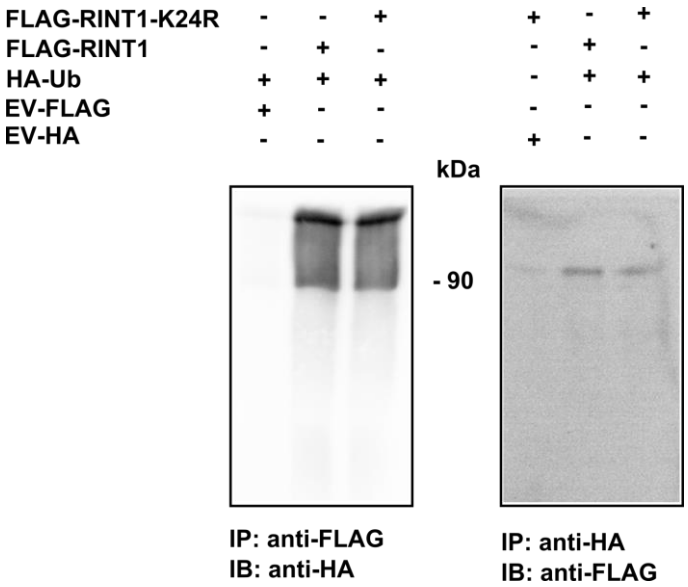

Figure 33. RINT1 K24 is not of a major importance for RINT1 ubiquitination. HEK293T cells were co-transfected with indicated plasmids. Co-immunoprecipitates were subjected to WB analysis.

Although this experiment did not entirely exclude a role for K24 residue in targeting RINT1 for degradation, the similarly high intensity of ubiquitination-specific signals for WT and K24R-mutated version of RINT1 indicated an existence of multiple active ubiquitination sites along RINT1 sequence.

3.2.7.3. Truncated versions of RINT1 are stabilized upon proteasome inhibition

In order to determine which region of RINT1 protein sequence is of a major importance for K48-mediated ubiquitination and subsequent protein degradation, several RINT1-

truncated mutants were analyzed. The mutant constructs were as follows: (i) RINT1-N, N-terminal part of the protein, 1-264 amino acids out of 792, (ii) RINT1-M, middle part of the protein, 200-585 amino acids, (iii) RINT1-C, C-terminal part of RINT1, 565-792 amino acids, (iv) RINT1-Δ1, lacking first 62 amino acids of RINT1, (v) RINT1-Δ2, 115-792 amino acids, and (vi) RINT1-Δ3, 294-792 amino acids (Fig. 34). Three generated RINT1 "Δ" truncated mutants lacked the three major groups of putative ubiquitination adjacent sites, as defined *via in silico* prediction).

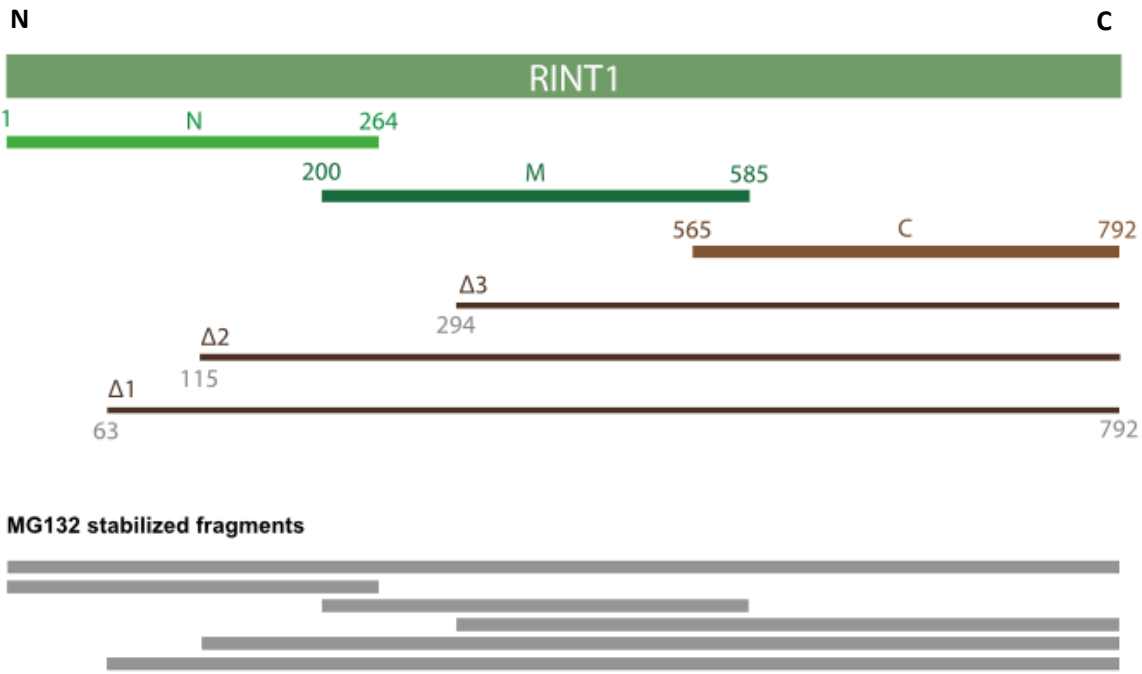

Figure 34. RINT1 truncated mutants are stabilized upon MG132 treatment. Scheme represent RINT1-truncated fragments (RINT1-N, RINT1-M, RINT1-C, RINT1-Δ1, RINT1-Δ2, RINT-Δ3) and shows MG132-stabilized parts of the protein.

The constructs, encoding FLAG-tagged RINT1 truncated mutants, were introduced to HEK293T cells. 24 h after transfection MG132 or CHX were added to the cell culture, in order to inhibit proteasomal degradation or block protein translation, respectively. WB analysis showed that (1) all the expressed mutant proteins were stabilized upon MG132 treatment, and (2) the level of mutant proteins decreased upon CHX treatment (Fig. 35).

In addition, as previously reported for the wild-type protein, the protein levels of RINT1-Δ1, RINT1-Δ2 and RINT1-Δ3 mutants were not only stabilized by MG132, but the

additional, shifted-up band was detected (Fig. 35, arrows), directly indicating their post-translational modification.

All of tested proteins were successfully expressed in the cells except one, FLAG-RINT1-C mutant, which signal could not be reliably detected despite several attempts. MG132 treatment did not lead to the appearance of RINT1-C mutant-specific band, thus to the protein stabilization. Therefore, inability to detect this mutant seems not be related to rapid proteasome-mediated degradation, but rather to other mechanism leading to protein instability (other proteases, protein misfolding).

Altogether, these findings indicated that RINT1 truncated mutants are degraded *via* proteasomal degradation pathway. Thus, the sequence of the expressed protein fragments include lysines residues tagged by ubiquitin for the degradation. Therefore, it indicates the existence of multiple ubiquitination sites within RINT1 protein, all leading to K48-mediated proteasomal decay. Moreover, in truncated mutants different ubiquitination sites might be active, thus having alternative function, *i.e.* substituting for each other. This observation suggests also an involvement of more than one E3 ubiquitin ligase, which is consistent with the previous results, and/or, of an E3 ligase of low substrate specificity for the recognition of protein sequences for K48-linkage anchoring.

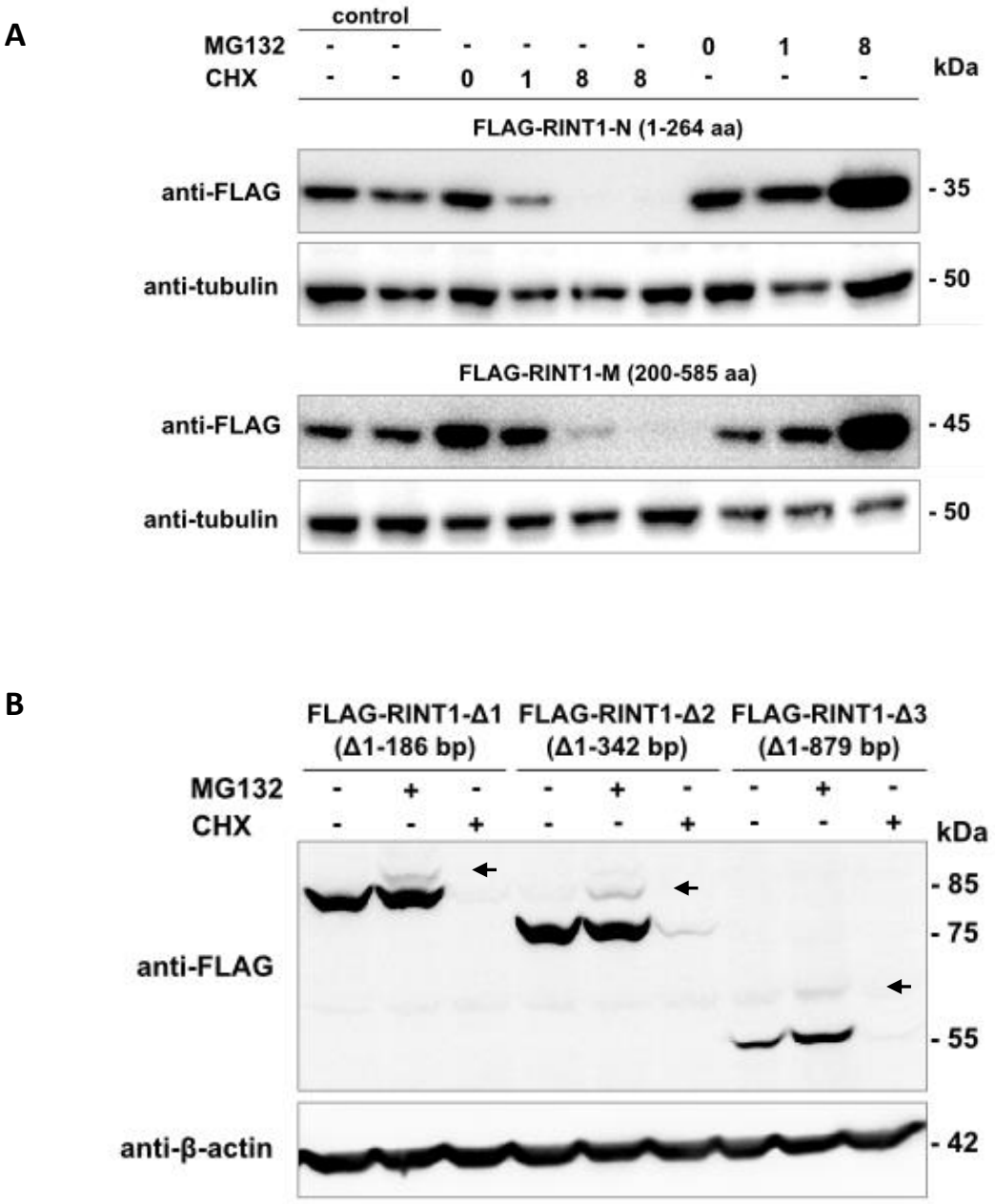

Figure 35. RINT1 truncated mutants are degraded *via* proteasomal pathway. HEK293T cells were transfected with indicated RINT1-mutants and treated or not with 10 μM MG132 or 25 μg/ml CHX. **A.** RINT1-N and RINT1-M mutants are stabilized upon MG132 treatment and depleted upon CHX treatment. **B.** RINT1-Δ1, RINT1-Δ2, and RINT1-Δ3 mutants are stabilized upon MG132 treatment and depleted upon CHX treatment. Additional "shifted-up" bands for higher molecular form of RINT1 are indicated with arrows.

3.3. RINT1 and SUMOylation

The screens, originally intended to discover RINT1-binding partners related to the ubiquitination, revealed several other interesting proteins, potentially involved in different RINT1 post-translational modifications. SUMO2 protein was one of them, found independently as a RINT1 interaction partner in yeast two-hybrid assay, as well as in the mass spectrometry screen.

3.3.1. Prediction of putative SUMOylation sites of RINT1

As a first step in unraveling presumed RINT1 SUMOylation, *in silico* prediction of putative SUMO-target sites within RINT1 was performed. Software used (www.phosida.com, sumosp.biocuckoo.org/online.php) indicated two lysines, K449 and K525, as potentially capable of being modified by SUMO protein(s).

Based on the position of the two sites identified, two mutant versions of RINT1 were generated by site-directed mutagenesis: RINT1-K449R (point mutation c.A1346G) and RINT1-K525R (point mutation c.1574G). HEK293T cells were transfected to transiently express FLAG-RINT1 WT, FLAG-RINT1-K449R or FLAG-RINT10K525R mutants, with HA-SUMO1, HA-SUMO2 or EV-HA control. Subsequently, WB analysis of cellular lysates was performed. In the samples expressing FLAG-RINT1-K449R mutant together with HA-tagged SUMO1 protein, the RINT1 FLAG-specific band appeared shifted up as compared with RINT1 WT co-transfected with EV-HA control (Fig. 36A). This effect was not observed in the sample co-expressing FLAG-RINT1-K525R mutant together with HA-SUMO1 (Fig. 36B). This result suggested that lysine residue on the position 449 is not involved in the SUMOylation of RINT1, while K525 appears to be an active SUMO1-target site. In the case of experiments with co-expression of the HA-tagged SUMO2 protein, WBs were not conclusive.

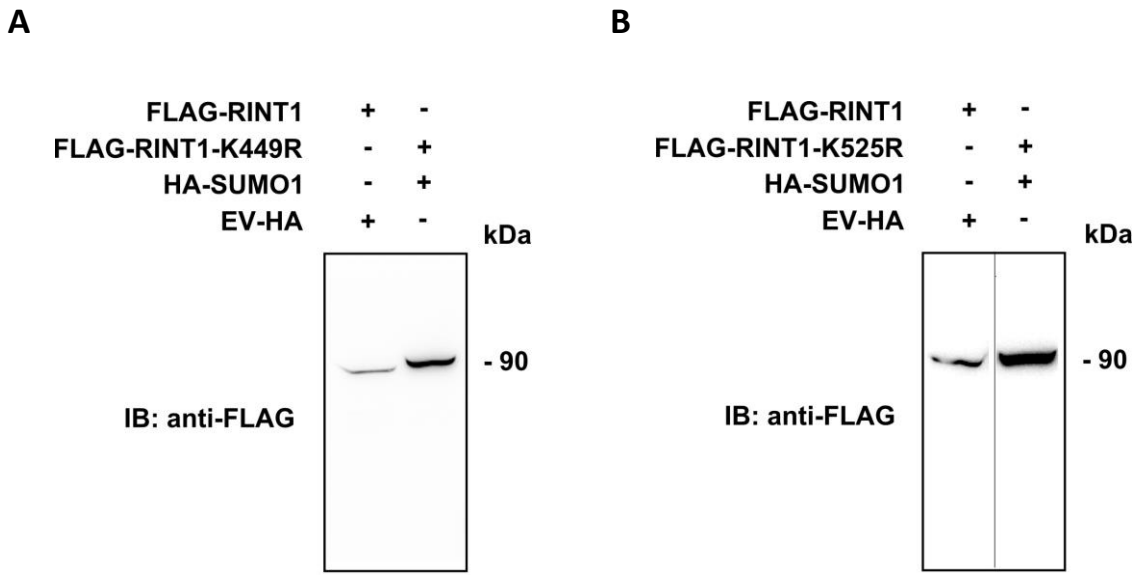

Figure 36. Putative SUMOylation of RINT1. HEK293T cells were co-transfected with indicated plasmids. **A.** RINT1-specific band in the sample co-transfected with FLAG-RINT1-K449R and HA-SUMO1 was shifted-up to a higher molecular weight as compared to the control sample transfected with FLAG-RINT1 WT and EV-HA. K525 of RINT1 is potential SUMO-target residue. **B.** This effect was not observed in the case of lysates of the cells co-transfected with FLAG-RINT1-K525R, indicating that K525 of RINT1 is a potential SUMO-target residue.

3.3.2. Putative interaction of RINT1 with SUMO1 and SUMO2 proteins

To further verify, if RINT1 is a subject of SUMOylation several experimental approaches were applied. Results of these preliminary experiments indicated covalent modification of RINT1 by SUMO1 and/or SUMO2 proteins, however further optimization steps and independent repetitions are needed to definitely confirm this finding.

HEK293T cells were transfected to co-express FLAG-RINT1 protein (or FLAG-EV control plasmid) together with HA-tagged SUMO1 or SUMO2 proteins. The samples were subsequently subjected to FLAG- or HA-mediated IP. The WB membranes were probed with anti-HA and anti-FLAG antibodies, respectively. In the samples expressing FLAG-RINT1 and HA-SUMO1, a very weak signal for FLAG-specific band was detected (HA-mediated IP), suggesting the putative interaction between FLAG-RINT1 and HA-SUMO1 proteins. This band was not observed in the samples expressing FLAG-RINT1 and HA-SUMO2 protein. Notably, the levels of over-expressed HA-SUMO2 protein were low as compared with HA-SUMO1 over-expression (data not shown).

To increase specificity of the detection, a GFP-directed IP approach, using anti-GFP alpaca antibody (low background noise due to high specificity and a lack of light chains), was applied. EGFP-RINT1 or EGFP-EV control plasmids were overexpressed in HEK293T cells. Next, IP with an anti-GFP-antibody, WB and probing for endogenous SUMO1/2 proteins with specific anti-SUMO1 and anti-SUMO2 antibodies was performed. As a result, SUMO2-specific signal was detected, in contrary to the lysates of EGFP-EV control-transfected cells. Interestingly, no SUMO1-specific band was detected (data not shown).

4. Discussion

4.1. Unstable proteins and their significance for cellular homeostasis

Protein turnover, including intracellular degradation and changes in the protein dilution rate, controls many vital cellular processes, such as signal transduction pathways, cell cycle progression, transcription, differentiation, or apoptosis (Hershko and Ciechanover 1998; Ciechanover, Orian et al. 2000; Glickman and Ciechanover 2002; Ciechanover 2005). At the level of the individual protein, the half-life is extremely important, as it is fundamental for the metabolism and the communication between the cell and its external environment. Moreover, at the level of organism, protein turnover rate plays an important role in disease (Schwartz and Ciechanover 1999; Nakayama and Nakayama 2006). For example, disturbance in protein half-life may cause cancer (*e.g.* neuroendocrine tumors as a consequence of increased turnover of succinate dehydrogenase) or neurodegeneration (*e.g.* during mice embryonic development due to extension of a half-life Hes7 transcription factor by 8 min) (Hirata, Bessho et al. 2004; Yang, Matro et al. 2012).

Proteins vary widely in term of the lability. The proteins with the shortest lifespan exist only minutes (*e.g. E. coli* heat shock response protein sigma 32 has a half-life of 4 min, eukaryotic p53 tumor suppressor has a life of ~5-20 min, and c-myc proto-oncogene has a half-life of ~30 min), whereas others are highly stable and their half-life is measured in months or even years, in case of the proteins of certain postmitotic tissues (*e.g.* eye lens crystalline with a half-life of ~70 years or elastin with a half-life of ~80 years) (Ramsay, Evan et al. 1984; Grossman, Straus et al. 1987; Giaccia and Kastan 1998; Verzijl, DeGroot et al. 2000; D'Angelo, Raices et al. 2009; Savas, Toyama et al. 2012). The significance of short-lived proteins cannot be underestimated, as they are among the most substantial to the cell survival and have mainly regulatory functions. For example, rapid removal of cyclins and cyclin-dependent kinases (CDKs) as well as cell cycle regulators, such as p21, p53 or p73, provides means for cell cycle control and allows for quick response to the changes in the environment and adaptation to new conditions, therefore for maintenance of the cellular homeostasis. Short-lived proteins also contribute to the regulation of

biological clock and circadian rhythm (*e.g.* TOC1) (Glickman and Ciechanover 2002; Lecker, Goldberg et al. 2006; van der Lee, Lang et al. 2014).

With only ~40 min of experimentally determined lifespan, RINT1 certainly belongs to the category of the proteins with a short half-life. It is probably this feature, which allows RINT1 to fulfill regulatory functions. This assumption is reflected by an involvement of RINT1 in multiple, apparently unrelated, cellular processes, such as cell cycle progression (Xiao, Liu et al. 2001), ER-Golgi trafficking (Hirose, Arasaki et al. 2004; Arasaki, Taniguchi et al. 2006; Lin, Liu et al. 2007; Sun, Shestakova et al. 2007; Arasaki, Takagi et al. 2013), telomere length maintenance (Kong, Meloni et al. 2006), or the potential oncogenic and tumor suppressor functions (Lin, Liu et al. 2007; Quayle, Chheda et al. 2012; Fan, Wang et al. 2014; Park, Tao et al. 2014). Thus, modulation of the RINT1 half-life might be of a great importance for the cell survival and overall cellular homeostasis.

4.2. Post-translational modifications and their modulatory effects on protein functions

By definition, post-translational modifications (PTMs) occur after the translation of a given protein from respective mRNA has been completed. PTMs could involve different chemical alterations, like covalent addition of functional groups to proteins (*e.g.* phosphorylation, acetylation, glycosylation, methylation) or small regulatory proteins (*e.g.* ubiquitination, SUMOylation, neddylation, ISGylation) or the proteolytic cleavage of certain regulatory protein subunits (*e.g.* activation of proteolytic function of caspases upon cleavage). By all these different means, PTMs highly increase functional diversity of proteins beyond this encoded by the genome, and are an actual driver of plasticity of the proteome in response to changing cellular needs.

4.2.1. Putative roles of RINT1 ubiquitination in the context of known cellular functions of RINT1

Ubiquitination is well known for its potent role in the degradation of proteins, as well as for its miscellaneous regulatory functions. Moreover, different modes of (poly)ubiquitin chain formation modulate the impact of this PTM on proteins and enhance functional

meaning of the ubiquitination itself. Therefore, it is of particular interest to discuss the current findings in the light of the already established cellular roles of RINT1.

4.2.1.1. Degradative functions of RINT1 ubiquitination

The experimental work clearly showed that RINT1 cellular levels are tightly regulated by ubiquitination. RINT1 is not only polyubiquitinated at different sites, but also by different inter-ubiquitin chain linkage types: K29-, K48-, K63- and K0 (as linear polyubiquitination and/or monoubiquitination). Depending on a particular lysine residue involved in the chain formation, ubiquitination of RINT1 may have different roles and different impact on protein functions. In that respect, K48-linked polyubiquitination, as a PTM which is best established for targeting proteins for 26S proteasomal degradation, could be of a major importance for the regulation of the protein half-life, since RINT1 depletion was completely blocked by MG132 treatment (Figs. 21 and 22). In addition, pharmacological modulation of lysosomal and autophagic protein degradation pathways had no significant effects on RINT1 stability (Fig. 22).

In contrast to K48-mediated modification, functions of K29-, K63- and K0 ubiquitination are much more elusive. Since a role in the regulation of protein degradation by K63-, and to a lesser extent K0-/linear or K29-mediated ubiquitin linkages, appears to be mostly limited to autophagic or lysosomal processes, detection of these specific modifications on RINT1 protein, may indicate their other, non-degradative but rather modulatory roles (Kim, Hailey et al. 2008; Zotti, Uva et al. 2011; Shaid, Brandts et al. 2013; Zhang, Xu et al. 2013). Nevertheless, some experimental evidence point also towards the K29-, monoubiquitination and linear polyubiquitination as possible promoters of the proteasomal protein degradation (Kirisako, Kamei et al. 2006; Boutet, Disatnik et al. 2007; Kravtsova-Ivantsiv, Cohen et al. 2009; Prakash, Inobe et al. 2009; Carvallo, Munoz et al. 2010; Yin, Gui et al. 2010; Zhao and Ulrich 2010; Dammer, Na et al. 2011). Since this observation relates to eukaryotic cells as well as bacteria and considering the fact that the proteasome has the ability of recognizing very diverse ubiquitin(-chains)-derived signals (except K63-polyubiquitination), it is also possible that the RINT1 is directed to the 26S proteasome turnover not only by K48-, but also by other ubiquitin-linkage type(s) (Xu, Duong et al. 2009).

4.2.1.2. Non-degradative functions of RINT1 ubiquitination

Ubiquitination serves not only for degradation of targeted proteins. It is also involved in the regulation of many other vital cellular processes and pathways. The canonically non-degradative modes of ubiquitination, such as attachment of monoubiquitin as well as linear-(K0-), K29- and K63-mediated polyubiquitinations were found to be present at RINT1. These modifications are known to play a role in processes such as: DNA damage response and error-free post-replication repair, cell cycle progression, protein sorting, endocytosis, or in general, in signal transduction (Passmore and Barford 2004; Pickart and Eddins 2004; Huang and D'Andrea 2006; Mukhopadhyay and Riezman 2007; Clague and Urbe 2010; Ramadan and Meerang 2011; Mocciaro and Rape 2012).

Therefore, considering the many different cellular roles of the above mentioned ubiquitination modes (K29-, K63-, linear- and monoubiquitination), it is tempting to speculate that participation of RINT1 in a DNA damage-induced G2/M cell cycle arrest, as well as in the ER-Golgi trafficking, could be modulated by non-degradative poly- and/or multiple monoubiquitination. The involvement of RINT1 in such spatially and temporally separated processes (Xiao, Liu et al. 2001; Hirose, Arasaki et al. 2004; Sun, Shestakova et al. 2007; Aoki, Ichimura et al. 2009; Schmitt 2010), suggests the necessity of altering its cellular location and interaction with different protein binding partners, which could be achieved by such versatile post-translational modification as ubiquitination.

One of the examples of modulatory effect of polyubiquitination on the protein function is its ability to change protein conformation. The attachment of ubiquitin molecules modifies structure of the target protein and precisely regulates formation of different protein complexes, thus affects protein activity in a specific time and compartment within the cell. The control of protein-protein interactions may be executed by modifications identified for RINT1, in particular K63-, but also K29-linked polyubiquitin chains (Passmore and Barford 2004; Wang, Gao et al. 2012; Shembade and Harhaj 2015). The structural protein modification may result not only from the coupling of multiple ubiquitins, but also from the single molecule of Ub appended to the substrate (monoubiquitination), which subsequently attaches to a ubiquitin-binding domain (UBD) of the same protein (Schnell and Hicke 2003). The detection of the covalent interaction-pattern between Ub-K0 mutant and RINT1 protein in the co-immunoprecipitation experiments (Fig. 26) suggests

linear polyubiquitination, but also multiple monoubiquitination of RINT1. It is thus very likely that the supposed monoubiquitination of RINT1 serves as a modifier of a protein structure, leading to augmentation of RINT1 binding-partners spectrum.

Still, modulation of protein conformation might not be the sole function of RINT1 monoubiquitination. This kind of post-translational modification is, in general, characteristic for proteins involved in the membrane protein trafficking (Rotin, Staub et al. 2000; Katzmann, Odorizzi et al. 2002), a cellular process in which RINT1 was found to play an important role (Hirose, Arasaki et al. 2004; Arasaki, Taniguchi et al. 2006; Arasaki, Takagi et al. 2013).

Monoubiquitination is known to be an essential and at the same time sufficient endocytic signal for the proteins located on the surface of the cell (Shih, Sloper-Mould et al. 2000; Haglund, Sigismund et al. 2003), as well as for the sorting of transmembrane proteins. However, its modulatory role in case of the involvement of RINT1 in the membrane trafficking might be more indirect. Some of the proteins incorporated to the cell and sorted in an ubiquitin-dependent process are not modified by Ub, but need to interplay with an intermediary protein-factor, which regulates their transport and is itself subjected to monoubiquitination. For example epsins, proteins involved in endocytosis and participating in the formation of clathrin-coated vesicles, contain ubiquitin-interacting motifs (UIMs), which bind monoUb prior to the internalization of receptors at the plasma membrane. Another example is Vps27p protein from *Saccharomyces cerevisiae.* Like epsins, it interacts with monoUb through its UIM and this interaction is essential for endosomal cargo sorting (Myat, Henry et al. 2002; Shih, Katzmann et al. 2002; Schnell and Hicke 2003). It is thus possible, that the presumed multiple monoubiquitination of RINT1 is a necessary signal allowing RINT1 to act as such an intermediary protein factor for the efficient and accurate inter-membrane transport of other proteins and, in consequence, changes their intracellular localization.

Another putative role of monoubiquitination of RINT1 is related to its function in the process of the DNA repair (Xiao, Liu et al. 2001). In order to properly correct genetic material, accurate recruitment of proteins constituting DNA repair machinery to the spot where DNA damage occurred, is essential. The signal for translocation might be provided by monoubiquitination. Such mechanism was described for the Fanconi anemia protein

(FANCD2), which is targeted to the nuclear foci and co-localizes with BRCA1 upon monoubiquitination in the S phase of the cell cycle (Garcia-Higuera, Taniguchi et al. 2001; Gregory, Taniguchi et al. 2003; Nakanishi, Yang et al. 2005). It is quite likely, that the co-localization of RINT1 with RAD50, and their acting in the process of the radiation-induced G2/M cell cycle checkpoint, is driven by (mono)ubiquitination of the protein(s). To provide more information on this topic, it would be interesting to investigate RINT1 monoubiquitination in the context of various DNA-damage triggers and in different stages of the cell cycle. It should be stressed, that hypothetically monoubiquitination of RINT1 might steer both binding to different interaction-partners, and, at the same time, its intracellular location during the specific stage of the cell cycle.

Linear attachment of ubiquitin molecules by polyUb K0-linkage is yet another, and importantly, rarely occurring non-degradative mode of ubiquitination, which was found to be mediated by the Linear Ubiquitin Chain Assembly Complex (LUBAC). Interestingly, current experimental work identified K0-mediated Ub linkages at the RINT1 protein, which could be indicative of linear polyubiquitination. Moreover, LUBAC is recognized as a major player in signaling pathways crucial for innate and adaptive immunity (Rieser, Cordier et al. 2013), such as TNFR1-induced signaling during inflammatory response. Although there is yet no evidence of RINT1 participation in the immunity-related signaling pathways, bearing in mind functions of linear ubiquitination and the fact, that this modification potentially affects RINT1, it is suggestive to investigate a putative role of RINT1 in the immune system. To this end, high levels of RINT1 transcripts detected in T and B cells of mice are of potential interest (according to BioGPS database search, www.biogps.org).

4.2.2. Characteristics and functions of HUWE1 and RNF20/40 in relation to known functions of RINT1

The alignment of amino acid sequences of stabilized RINT1 fragments strongly suggested the existence of more than one ubiquitin-binding site within RINT1 protein, as well as presumably, more than one E3 ligase targeting RINT1 for the proteasomal degradation. Indeed, mass spectrometry analysis of RINT1 immunoprecipitates identified two E3 ligases, HUWE1 and RNF20/40 complex, as RINT1 binding partners. Subsequently, series

of co-immunoprecipitation experiments confirmed these interactions (Fig. 29-30). The current study has shown that both enzymes regulate RINT1 stability (Fig. 31), which is in line with the previous reports describing them as crucial modulators of protein levels. On the one hand, HUWE1 polyubiquitinates and targets for the proteasomal degradation such important proteins as: major anti-apoptotic regulator Mcl1 (Zhong, Gao et al. 2005), tumor suppressor BRCA1 (Wang, Lu et al. 2014), proto-oncogenes N-Myc and c-Myc (Zhao, Heng et al. 2008) or developmental master regulator MyoD (Noy, Suad et al. 2012). On the other hand, the RNF20/40 complex acts as a proteasomal-degradation promoter of Syntaxin 1, a major component of exocytosis membrane fusion machinery (Chin, Vavalle et al. 2002), a transcription factor AP-2α (Ren, Sheng et al. 2013), and of p42 isoform of tumor supressor Ebp1 (Liu, Oh et al. 2009).

However, both ligases are known to have not only degradative, but also regulatory impact on their targets. This is possible through their capability to form ubiquitin chains other than mediated by K48-inter-ubiquitin linkages. For example, HUWE1 was found to catalyze formation of the K63-ubiquitin poly-chains at the c-Myc protein (Adhikary, Marinoni et al. 2005). Moreover, both HUWE1 and RNF20/40 are able to monoubiquitinate their substrates: HUWE1 modifies DNA polymerase ß (Parsons, Tait et al. 2009), while RNF20/40 complex is responsible for monoubiquitination of histone H2B (Zhu, Zheng et al. 2005). The above-mentioned different modes of the ubiquitination catalyzed by HUWE1 and RNF20/40, suggest that K63- and/or putative multiple monoubiquitination of RINT1 might be triggered by HUWE1 and RNF20/40 E3 ubiquitin ligases in addition to their primarily role as modulators of stability, and thus cellular levels of RINT1 protein.

While it is relatively common, that a given protein interacts with, and is modified by more than one E3 ubiquitin ligase, it remains very often challenging to determine the cellular function of the introduced ubiquitin chains. Strikingly, both newly identified RINT1 interactors, HUWE1 and RNF20/40 complex, intersect with RINT1 regarding their participation in common cellular processes. For instance, both HUWE1 and RNF20/40 ligases modify substrates crucial for the cell cycle arrest, DNA repair, genome stability and tumorigenesis.

4.2.2.1. Role of HUWE1 in the context of cellular functions of RINT1

The first literature report regarding RINT1 addressed its role as a protein interacting with RAD50, thus involved in the G2/M cell cycle checkpoint activation, upon the irradiation-induced DNA damage (Xiao, Liu et al. 2001). It is not yet known which mechanisms regulate RINT1 activation or function in this process. Presumably, certain post-translational modifications, such as the ubiquitination, might play a modulatory or triggering role. HUWE1 is known to control the DNA repair pathway by monoubiquitinating and, in turn, regulating steady-state levels of the DNA polymerase ß, one of the crucial enzymes for the base excision repair (BER) pathway (Parsons, Tait et al. 2009). However, in the context of an established RINT1 function in ensuring proper genomic integrity (Xiao, Liu et al. 2001; Lin, Liu et al. 2007; Park, Tao et al. 2014), the role of HUWE1 might be more indirect. For instance, both modifications identified for RINT1, putative monoubiquitination at multiple sites, as well as K63-polyubiquitination, might potentially control the recruitment of RINT1 to RAD50, and favor this interaction over others. Importantly, as mentioned before, both modes of ubiquitination are known to be catalyzed by HUWE1 E3 ubiquitin ligase (Zhao, Heng et al. 2008; de Groot, Ganji et al. 2014; Jang, Shi et al. 2014). It is worth noting, that HUWE1 also regulates cellular functions of other proteins involved in the cell cycle checkpoint triggering and DNA repair signaling, such as p53, Cdc6, BRCA1 or TopBP1 (Hall, Kow et al. 2007; Herold, Hock et al. 2008; Peter, Bultinck et al. 2014; Wang, Lu et al. 2014). Hereby, the regulation is achieved by modulating protein levels *via* targeting for proteasomal degradation.

Correspondingly, one of the best described functions of HUWE1 is its involvement in the regulation of the extracellular signal-regulated kinase 1/2 (ERK1/2) pathway, by controlling levels of Shoc2 scaffold complex and the Raf-1 protein (Jang, Shi et al. 2014). It is another example of significant, regulatory role of HUWE1 ligase, resulting from assuring appropriate cellular levels of the proteins which are the key-players in the specific signaling pathways. Similarly, by targeting RINT1 for the 26S proteasomal degradation, HUWE1 contributes to the regulation of all the downstream processes demanding RINT1 functional activity.

HUWE1 was also found to act as a modulator of the dishevelled protein Dvl, hereby being involved in the Wnt/ß-catenin canonical signaling pathway. Interestingly, in this case

regulatory role of the E3 ubiquitin ligase is linked to the formation of K63-polyubiquitin chains and the negative feedback loop (de Groot, Ganji et al. 2014). Modification of Dvl by HUWE1 inhibits its multimerization, which is indispensable for the protein acting in the cell proliferation, segmentation and in the neuroblast specification. The K63-mediated polyubiquitination of Dvl illustrates how HUWE1 may influence protein function by modifying its spatial structure, thus capability of complex formation. Further research would answer the question, whether this mechanism of HUWE1 action is applicable to the RINT1 protein.

Another link between known functions of RINT1 and HUWE1 is their tumor supressor activity. It was shown, that RINT1-depleted cells exhibit abnormalities during the cell division (Arasaki, Taniguchi et al. 2006), and the inactivation and subsequent heterozygous loss of *Rint1* gene led to tumor formation in animal model (Lin, Liu et al. 2007). Moreover, recent exome sequencing studies of breast cancer patients supported role of RINT1 as a tumor suppressor protein (Park, Tao et al. 2014). However, it is not recognized yet what kind of mechanisms underlie and provide this function for the RINT1 protein. It is very likely, that one of the several currently reported modes of RINT1 ubiquitination: K29-, K63-, and/or mono-/linear-ubiquitination, are driving its oncosuppresor activity. However, it is of course also possible, that HUWE1 provides this function of RINT1 simply by tagging it for the proteasomal degradation (K48-linked Ub chains) and acting as a regulator of RINT1 cellular levels. Such a mechanism was already described for another HUWE1 target, transcription factor and potent tumor suppressor Ebp1 (Liu, Oh et al. 2009).

Last but not least, both HUWE1 and RINT1 are strongly involved in maintaining correct cell proliferation and differentiation programs, thus cellular homeostasis. As a E3 ubiquitin ligase polyubiquitinating and leading to the degradation of p53 molecule and many other substrates like Myc, ARF, PP5, or Mcl-1 proteins, HUWE1 is one of the key regulators of apoptosis. The control of cellular levels for listed proteins, imply HUWE1 function in neural differentiation, proliferation, as well as in the development and growth of Myc-driven solid tumors (Adhikary, Marinoni et al. 2005; Chen, Kon et al. 2005; Zhong, Gao et al. 2005; Kurokawa, Kim et al. 2013). It is therefore possible, that the *in vivo* tumor formation observed for primary murine astrocytes overexpressing RINT1 (Quayle, Chheda

et al. 2012) is caused by overriding the control mechanism provided by HUWE1 E3 ubiquitin ligase with excessive amounts of overexpressed RINT1 protein, which under normal conditions would lead to effective removal of ubiquitinated RINT1.

4.2.2.2. Role of RNF20/40 *vs.* RINT1 functions

RNF20/40 E3 ubiquitin ligase is well known for its functions regarding the gene regulation and transcriptional activation as well as for its potent role in the DNA damage response and the cell cycle progression.

By selective regulation of gene expression, RNF20/40 was found to act as a putative tumor suppressor (Kim, Hake et al. 2005; Shema, Tirosh et al. 2008). This function is mostly associated with the histone monoubiquitination by RNF20, and resulting changes in the gene expression pattern (Kim, Hake et al. 2005; Zhu, Zheng et al. 2005; Kim, Guermah et al. 2009). Nevertheless, RNF20/40 complex acts also as a factor inhibiting tumor suppressive activity by polyubiquitinating and tagging for the proteasomal degradation isoform 2 of PA2G4 protein in cancer cells (Liu, Oh et al. 2009). Interestingly, *RINT1* was described as a both tumor suppressor (Lin, Liu et al. 2007; Park, Tao et al. 2014) and oncogene (Quayle, Chheda et al. 2012; Fan, Wang et al. 2014). Thus, it is tempting to hypothesize, that RNF20/40 might be the key regulator of the RINT1 activity in the tumor formation: either by its monoubiquitination, or by regulating cellular levels of the RINT1 protein.

Another process, in which RNF20/40 ubiquitin ligase plays a significant role, is the regulation of the DNA repair by homologous recombination (HR). RNF20 is localized at the sites of double-stranded breaks (DSBs) and required for the DSB-induced monoubiquitination of histone H2B. Interestingly, the repair pathway involving RNF20 is not depend on H2AX, but associated with NBS1. Moreover, RNF20 activity seems to be a prerequisite for the accumulation of DNA repair proteins like BRCA1 and RAD51 at the sites of damage (Nakamura, Kato et al. 2011). Summarizing, RNF20/40 E3 ubiquitin ligase was found to have potent roles in the HR repair and in cell cycle checkpoint response to the irradiation-induced DNA damage. This is particularly interesting in the context of known roles of RINT1 in the DNA repair and in G2/M cell cycle checkpoint upon irradiation, as well as RINT1 interaction with RAD50 protein (Xiao, Liu et al. 2001).

Moreover, RAD50 plays a central role in the DSB repair and is a part of the MRN complex, which apart from RAD50 consists also of MRE11 and NBS1 proteins. Interestingly, MRE11 and NBS1 are recruited to the DSBs by RNF20. This strongly suggests that RINT1, being a RAD50 interactor and itself ubiquitinated by RNF20/40 complex, can undergo the same mode of regulation for its recruitment to the MRN complex upon DNA damage-induced checkpoint control at the G2/M stage of the cell cycle. Therefore, the interaction between RINT1 and RAD50, as well as function of RINT1 in the DNA repair pathway might be driven by the activity of RNF20/40 ligase.

4.2.3. A role of SUMOylation as possible modulator of known functions of RINT1

SUMO protein was identified as the binding-partners of the RINT1 protein using both, the yeast two-hybrid assay and mass spectrometry screens. The interaction between RINT1 and SUMO molecules was also suggested by preliminary co-immunoprecipitation experiments. These results indicate existence of yet another, besides ubiquitination, post-translational modification of RINT1. The exact role of SUMOylation of RINT1 is to be discovered. However, knowing the crucial role of SUMO proteins in divergent cellular pathways, some assumptions of the impact of SUMOylation on RINT1 function could be made.

Many described SUMO targets are transcription factors or proteins with general ability to influence gene expression (Wilson and Heaton 2008) and/or located in the nucleus. Therefore, SUMOylation is classically viewed as a major regulator of nuclear function. This overlaps with the observation, that apart from well-described cytosolic and membrane localizations of RINT1, the protein was additionally confirmed to be localized within the nucleus (Dr. P. Grigaravičius, unpublished data of our laboratory) corresponding with RINT1 function in regulation of DNA damage-induced cell cycle checkpoint as well as in telomere length maintenance (Xiao, Liu et al. 2001; Kong, Meloni et al. 2006). Nevertheless, more recent studies refer to SUMOylation as a possible modifier of the extra-nuclear proteins as well and regulator of very diverse cellular processes (Wasik and Filipek 2014). Similarly to the interaction between RINT1 and ubiquitin, functional importance of interaction between RINT1 and SUMO proteins could be crucial for

maintenance of cellular homeostasis. This may be predicted on the basis of common participation of RINT1 and SUMO1/2 in cellular processes as important as cell cycle progression, cell cycle checkpoint regulation, DNA damage repair and membrane trafficking (Sarangi and Zhao 2015). For RINT1, binding of SUMO to one or more lysine(s) might potentially modulate protein activity, subcellular localization or even stability (Geiss-Friedlander and Melchior 2007; Yang and Paschen 2009).

In general, SUMOylation has a great impact on the DNA repair, for example it was shown, that SUMO proteins accumulate at DNA DSBs (Galanty, Belotserkovskaya et al. 2009; Morris, Boutell et al. 2009; Shima, Suzuki et al. 2013). In the course of DNA damage response (DDR), the role of SUMO manifests itself by the multilevel modulation of its target proteins. To this end, SUMOylation could be of potential, functional importance regarding involvement of RINT1 in DDR pathway as a binding partner of RAD50.

SUMOylation plays also a crucial role in carcinogenesis, *e.g.* of prostate cancer or breast cancer, by regulating functions of key tumor suppressors and oncogenes such as p53 (indirectly, *via* E3 ubiquitin ligase MDM2) or PTEN (Kim and Baek 2006; Geiss-Friedlander and Melchior 2007; Alshareeda, Negm et al. 2014; Chen and Lu 2015). Through its impact on genome stability, gene expression and protein-protein interactions, SUMOylation is also important for etiology of other human diseases, such as neuronal dysfunctions (*e.g.* Alzheimer's, Parkinson's and Huntington's diseases) (Zhao 2007; Sarge and Park-Sarge 2009; Yang and Chiang 2013; Henley, Craig et al. 2014). It is worth mentioning, that studies reporting the crosstalk between ubiquitination and SUMOylation exist (Papouli, Chen et al. 2005; Hunter and Sun 2008; Zhao, Brickner et al. 2014). In addition, possibility of targeting the same protein at one time by both ubiquitin and SUMO proteins was also reported (Lu, Liu et al. 2015). Moreover, it is also possible, that the same lysine residue within the same protein might be a target for both modifiers, and as a consequence, they might compete for the same site within the protein. Such mechanisms allow for modulating cellular functions (Chen and Lu 2015). It is thus reasonable to speculate that RINT1, as a tumor suppressor and an oncogene, might be subjected to this double modification and complex regulatory mechanism. However, further studies are required to support this hypothesis.

4.3. Conclusions and perspectives

Experimental evidence presented in this work describes biochemical characteristics of the RINT1 protein, a novel oncogene and a tumor suppressor. Since RINT1 is a multifunctional protein involved in very diverse and crucial cellular pathways, and is indispensable for maintaining the cellular homeostasis, the information about its half-life and the mode of degradation may have broad implications and be the basis to disclose mechanisms governing modulation of its activity. Identification of ubiquitination and putative SUMOylation as two post-translational modifications affecting the RINT1 protein, as well as the novel finding that two E3 ubiquitin ligases modify RINT1, would potentially allow to design therapeutic strategy for the treatment of RINT1-related diseases, such as glioblastoma, breast cancer and Lynch syndrome cancers (Quayle, Chheda et al. 2012; Park, Tao et al. 2014). Nevertheless, it remains to be shown whether and how the reported RINT1 functions, like G2/M cell cycle checkpoint regulation, membrane trafficking and putative tumor suppression, could be modulated by HUWE1 and RNF20/40 complex, novel binding partners reported in the present study.

5. List of figures and tables

Figures

Tables

6. List of publications

Scientific articles based on the research work performed during a period of doctoral studies (chronologically):

1. P Grigaravicius, **E Kaminska**, CA Hübner, PJ McKinnon, A von Deimling, P-O Frappart, "*Rint1* inactivation triggers genomic instability, ER stress and autophagy inhibition in the brain", *Cell Death and Differentiation*, 2015 Sep 18; [Epub ahead of print]

2. **EK Kamińska**, P Grigaravicius, S Pusch, A von Deimling, P-O Frappart, "The E3 ligases HUWE1 and RNF20/RNF40, regulate RINT1 Stability", *Archives of Biochemistry and Biophysics*, *prepared to be re-submitted after the first round of revisions*

7. Acknowledgments

It is my pleasure to thank the people who I have had the great fortune to work with and whose contribution I wish to acknowledge.

First and foremost, I would like to thank Prof. Dr. Andreas von Deimling and my supervisor Dr. Pierre-Olivier Frappart, for giving me the opportunity to work on interesting topic and pursue my PhD in the research group. I truly appreciate a guidance, advice and constant help of Dr. Frappart. He ensured that my PhD was both challenging and rewarding.

I greatly appreciate the support and resources received through the collaborative work with Prof. Dr. Frauke Melchior, Dr. Stefan Pusch, Dr. Thomas Hofmann and Dr. Jörg Balss.

I am especially grateful to Dr. Paulius Grigaravicius for his enthusiasm and significant contribution. He has been a great teacher and colleague.

I would also like to thank my labmate, Martina Remus, for her friendly help and wonderful working atmosphere.

Especially, I would like to acknowledge my husband Marcin, for his constant encouragement, great support and constructive help during reading and editing of my thesis.

Last but not least, I would like to thank my Parents and entire Family for their belief in me.

8. Appendix

8.1. The impact of RINT1 on the cell cycle and cell death in mouse embryonic fibroblasts (MEFs)

It has been previously reported, that RINT1 could be involved in the regulation of cell cycle G2/M checkpoint (Xiao, Liu et al. 2001). Thus, to assay the effects of RINT1-deficiency on cellular fate, two different mouse embryonic fibroblasts (MEFs) cell lines, POF35-5 and POF39-4, harboring inducible *Rint1* genetic knockout under control of 4-hydroxytamoxifen (4-OHT)-driven Cre recombinase were used. In addition, for each of the cell line, an EV control cell line, which did not express Cre recombinase (without possibility to knockout the *Rint1* gene) was applied. In all experiments, cells were treated with 4-OHT for 0, 2 and 4 days. PCR analysis was performed to confirm the efficiency of *Rint1* knock-out.

8.1.1. Rint1-deficiency potentially leads to the cell cycle arrest of MEF cells

To test the effects of 4-OHT-induced *Rint1* knock-out on the cell cycle, two MEFs cell lines were used and the cell cycle profile was assayed using propidium iodide (PI) staining and the classical fluorescence-activated cell sorting (FACS)-mediated analysis. The results showed a possible block of the cell cycle in the G2/M phase of the cell cycle (in the case of POF39-4 cell line), when compared with the respective EV control line. The conclusions were drawn on the basis of event frequency (%) using FACS gating, however, further analysis by *e.g.* BrdU/PI staining or WB are needed to confirm this observation.

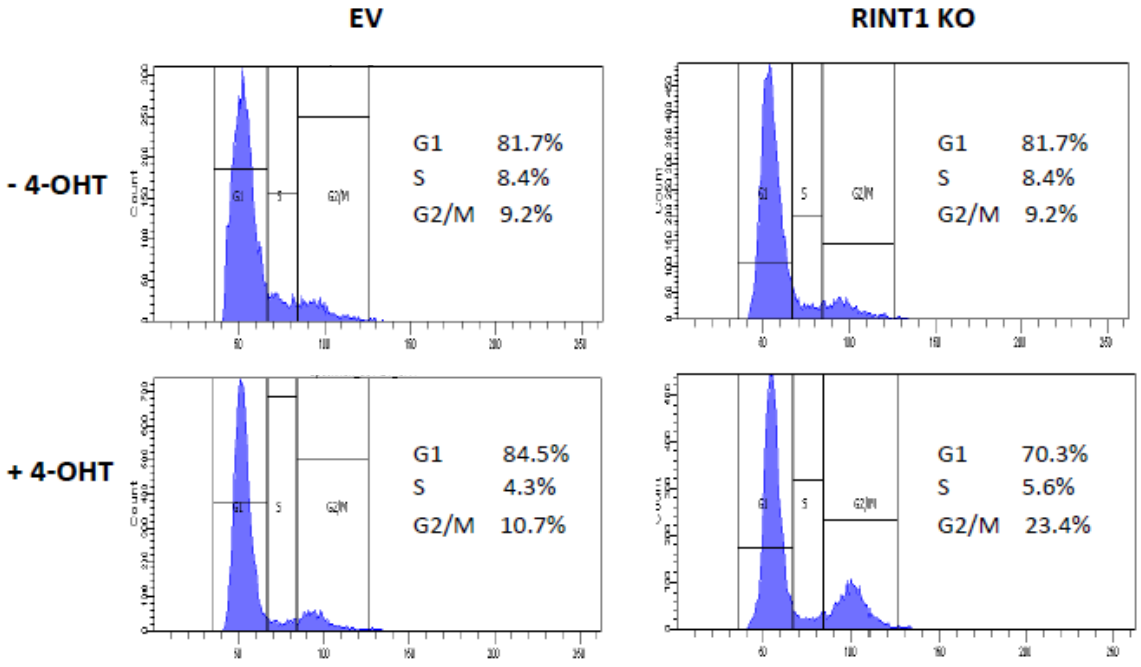

Figure A-1. Cell cycle analysis suggests block in G1/M phase upon *Rint1* knock-out. Control cells (POF39-4 EV) or RINT1 KO cells (POF39-4 CER) were treated with 4-OHT for 4 days. Results of representative experiment are presented.

8.1.2. Rint1-deficiency leads to cell death of MEF cells

To measure possibility of cell death induction upon *Rint1* knock-out, a FACS-based measurement of membrane integrity loss monitored by PI uptake was applied (as described in the "Materials and methods" section). The experiments clearly showed, that *Rint1* deficiency (upon 2 or 4 days of CRE-induced recombination) leads to an increased cell death in both cell lines investigated, as compared with the respective 4-OHT-treated EV control cell lines (regardless of a mild toxic effect ascribed to 4-OHT alone observed for EV control cell lines). Cell death observed at day 4th upon the 4-OHT treatment was more pronounced than after 2 days of the treatment. To compare the observed effects between different cell lines, a "specific cell death" (%) index was calculated, described in "Materials and Methods" section (cell death was normalized to the one observed for non-4-OHT-treated controls). In conclusion, Rint1 protein was found to be essential for the survival of MEFs cells, since its knockout results in cell death.

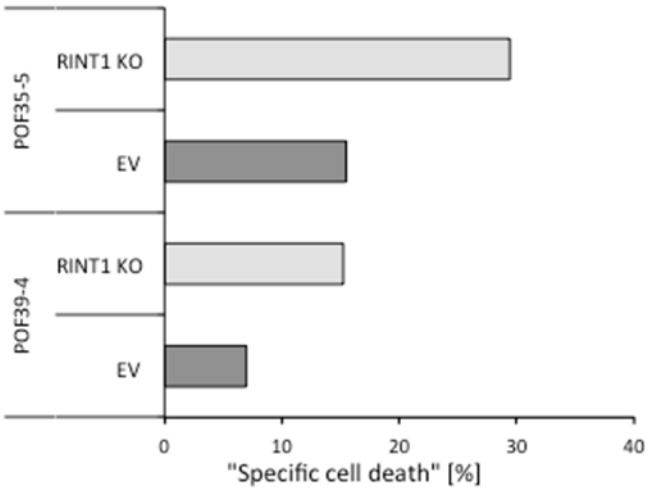

Figure A-2. Cell death induced by *RINT1* knock-out. Cells were treated with 4-OHT for 4 days. Average values of duplicated measurements are presented.

8.1.3. Analysis of cell apoptosis-induced nuclear fragmentation

Intra-nucleosomal fragmentation of the genomic DNA and subsequent formation of characteristic nuclear fragments (so-called “subG1” population on the cell cycle diagram), constitute major features of the apoptotic cell death. Thus, to further characterize cell death process observed upon the *Rint1* knock-out, analysis of nuclear fragmentation was performed.

8.1.3.1. Microscopic analysis of DAPI staining

4-OHT treatment of MEFs cell lines was performed in order to knock-out *Rint1* (for 4 days). Subsequently, cells were stained with DNA-intercalating dye DAPI and examined by fluorescence microscopy. Microscopic analysis demonstrated that no morphological changes characteristic for apoptotic fragmentation of the nuclei were detected in POF35-5 or POF39-4 4-OHT-treated cells (data not shown).

8.1.3.2. FACS-mediated analysis of nuclear fragmentation

The classical method of apoptotic nuclear fragmentation described by Nicoletti *et. al*., (Nicoletti, Migliorati et al. 1991) uses FACS to detect an apoptosis-specific subG1 population of nuclear fragments (see "Materials and Methods" section). Although marginal increase in (%) of subG1 population was observed (2-5%) upon the 4-OHT treatment alone (2 and 4 days), it was not Rint1 related, since the same effect was observed for EV control cell lines.

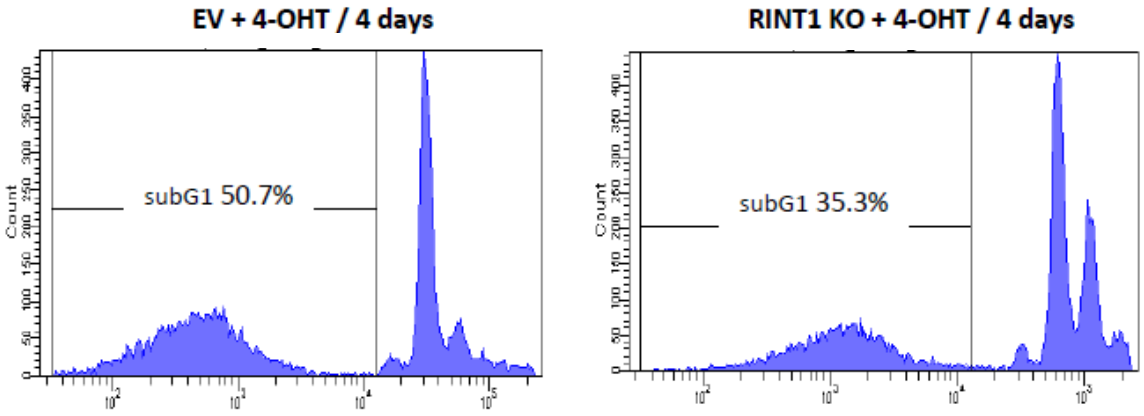

Figure A-3. *Rint1* knock-out-induced cell death is not characterized by apoptotic nuclear fragmentation. Control cells (POF39-4 EV) or Rint1 KO cells (POF39-4 CER) were treated with 4-OHT for 4 days. Results of representative experiment are presented.

8.1.3.3. TUNEL test

Apoptosis-induced intranucleosomal fragmentation of chromatin can be detected by terminal deoxynucleotidyl transferase dUTP nick end labeling (TUNEL) test (see "Materials and Methods" section for details). Both CRE MEF cell lines (POF35-5 and POF39-4), as well as EV control lines were treated for 0, 2 and 4 days with 4-OHT, to knock-out *Rint1*. Next, cells were stained using commercially available TUNEL kit, and fluorescence microscopic analysis was performed. The results did not show any significant apoptosis-related DNA damage in none of the investigated samples.

8.1.3.4. WB analysis of activation of apoptotic and DNA damage response signaling pathways upon *Rint1* knock-out

8.1.3.4.1. Apoptosis-related cleavage of poly (ADP-ribose) polymerase-1 (PARP) protein

Generation of a cleaved form of PARP1 by activated Caspase-3 protein belongs to the late signaling events in an apoptotic process. Cells, in which *Rint1* knock-out was induced upon the 4-OHT treatment (POF35-5 and POF39-4 cell lines; CRE and EV controls) were lysed and subjected to WB analysis. Membranes were probed with anti-PARP1 antibody. No cleaved form of PARP1, indicative for the apoptotic type of cell death was observed upon RINT1 depletion (Fig. A-4). However, clear caspase-induced PARP1 cleavage was observed in POF39-4 cell line upon control treatment with etoposide (10 µM, 8 h), a classical apoptotic inducer. Similarly, no cleavage of caspase 3 could be detected in the cells dying upon *Rint1* knock-out, additionally indicating a lack of activation of the apoptotic pathway, *i.e.* proteolytic activation of caspase 3 constitutes a necessary step in apoptosis.

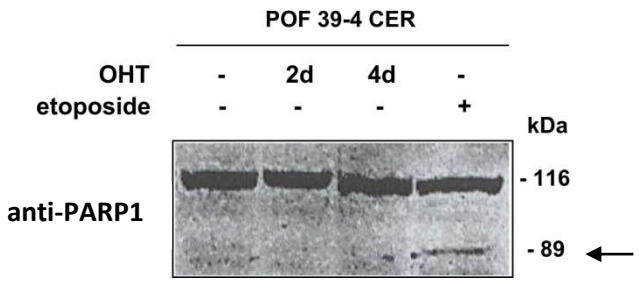

Figure A-4. *Rint1* knock-out-induced cell death does not lead to PARP1 cleavage. Black arrow marks cleaved form of PARP1 in positive control sample treated with etoposide.

8.1.3.5. DNA damage-induced expression of GADD153

RINT1 is an interaction partner of Rad50, a protein involved in DNA double-strand break repair. Thus, activation of the DNA damage response upon *Rint1* knock-out was investigated. GADD153 (CHOP10) is known as a growth arrest- and DNA damage-inducible gene. However, GADD153 was also postulated to play a role in the ER stress-mediated

apoptosis pathway (Fornace, Nebert et al. 1989; Luethy, Fargnoli et al. 1990; McCullough, Martindale et al. 2001; Oyadomari and Mori 2004).

POF39-4 MEFs CRE and EV cell lines were treated with 4-OHT for 0, 2 and 4 days. Subsequently, WB analysis was performed. Membranes were probed with anti-GADD153 antibody. As a result, in POF39-4-CRE cells, treated with 4-OHT, a time-dependent accumulation of *GADD153* protein was observed, which suggests an activation of DNA damage response upon *Rint1* knock-out (data not shown).

In conclusion, the observed cell death mode in MEFs cell lines upon the *Rint1* knock-down does not resemble apoptosis, since no typical apoptotic features, such as apoptotic nuclear fragmentation, intranucleosomal cleavage of chromatin, caspase-3 proteasomal cleavage (activation) or cleavage of PARP1 were observed. It does not however relate to DNA damage-induced response and cell cycle arrest. Further experiments are necessary to delineate cell death modality and signaling pathways triggered by a Rint1 deficiency in MEFs (*e. g.* mitotic catastrophe, ER stress-induced cell death or other cell death forms).

8.2. Analysis of sequence conservation among RINT1 homologs

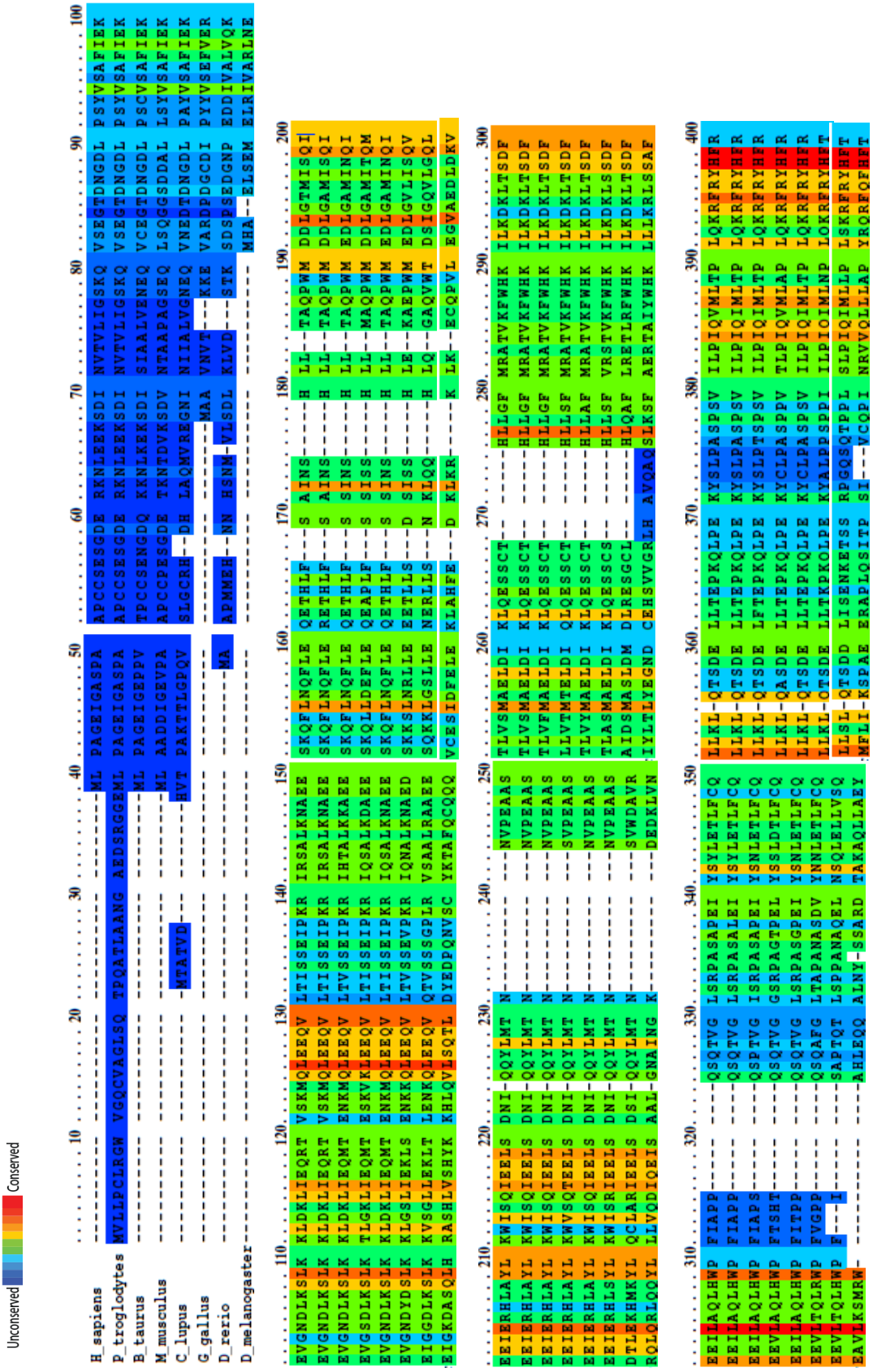

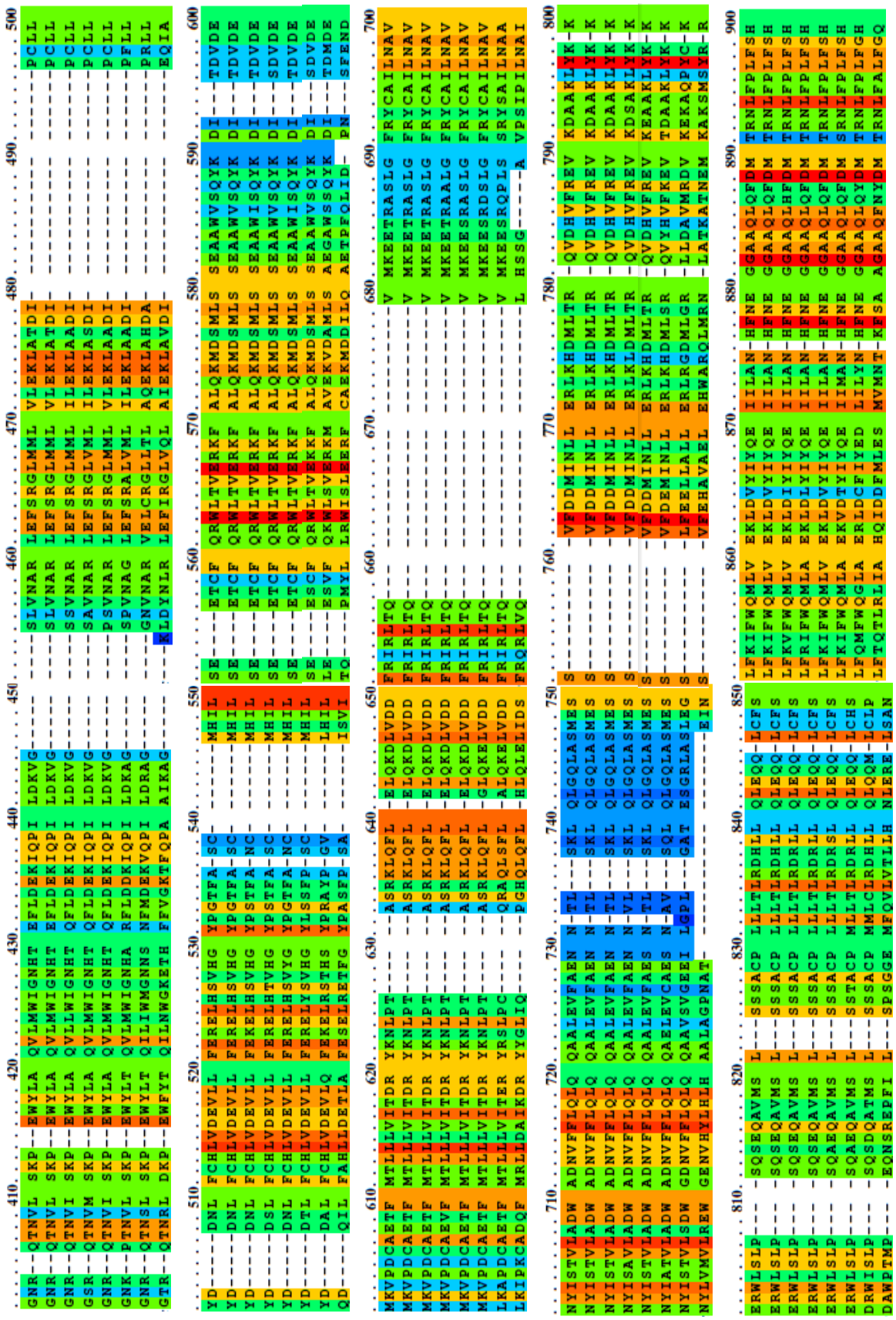

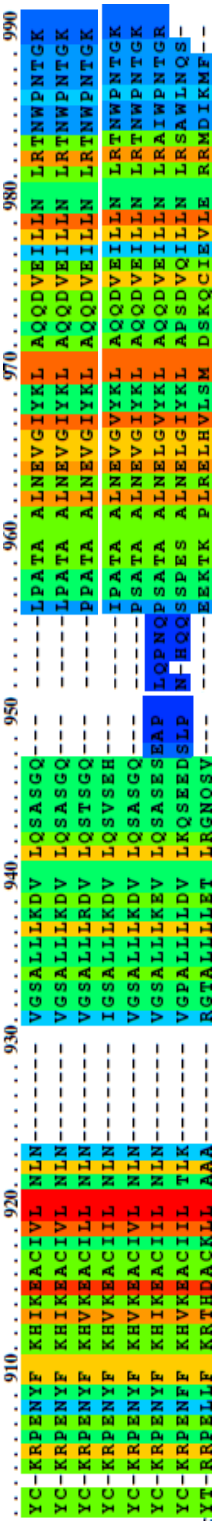

Figure A-5. Analysis of sequence conservation of RINT1 homologs. Scheme represents colour-coded results for amino acid conservation. The alignment was performed for indicated organisms, using PRALINE on-line software (http://www.ibi.vu.nl/programs/pralinewww).

9. References

Adhikary, S., F. Marinoni, et al. (2005). "The ubiquitin ligase HectH9 regulates transcriptional activation by Myc and is essential for tumor cell proliferation." Cell **123**(3): 409-21.

Alshareeda, A. T., O. H. Negm, et al. (2014). "SUMOylation proteins in breast cancer." Breast Cancer Res Treat **144**(3): 519-30.

Anisimova, M. and O. Gascuel (2006). "Approximate likelihood-ratio test for branches: A fast, accurate, and powerful alternative." Syst Biol **55**(4): 539-52.

Aoki, T., S. Ichimura, et al. (2009). "Identification of the neuroblastoma-amplified gene product as a component of the syntaxin 18 complex implicated in Golgi-to-endoplasmic reticulum retrograde transport." Mol Biol Cell **20**(11): 2639-49.

Appelqvist, H., P. Waster, et al. (2013). "The lysosome: from waste bag to potential therapeutic target." J Mol Cell Biol **5**(4): 214-26.

Arasaki, K., D. Takagi, et al. (2013). "A new role for RINT-1 in SNARE complex assembly at the trans-Golgi network in coordination with the COG complex." Mol Biol Cell **24**(18): 2907-17.

Arasaki, K., M. Taniguchi, et al. (2006). "RINT-1 regulates the localization and entry of ZW10 to the syntaxin 18 complex." Mol Biol Cell **17**(6): 2780-8.

Ben-Saadon, R., D. Zaaroor, et al. (2006). "The polycomb protein Ring1B generates self atypical mixed ubiquitin chains required for its in vitro histone H2A ligase activity." Mol Cell **24**(5): 701-11.

Bergink, S. and S. Jentsch (2009). "Principles of ubiquitin and SUMO modifications in DNA repair." Nature **458**(7237): 461-7.

Berndsen, C. E. and C. Wolberger (2014). "New insights into ubiquitin E3 ligase mechanism." Nat Struct Mol Biol **21**(4): 301-7.

Besnault-Mascard, L., C. Leprince, et al. (2005). "Caspase-8 sumoylation is associated with nuclear localization." Oncogene **24**(20): 3268-73.

Bian, Y., C. Song, et al. (2014). "An enzyme assisted RP-RPLC approach for in-depth analysis of human liver phosphoproteome." J Proteomics **96**: 253-62.

Bienko, M., C. M. Green, et al. (2005). "Ubiquitin-binding domains in Y-family polymerases regulate translesion synthesis." Science **310**(5755): 1821-4.

Bonifacino, J. S. and B. S. Glick (2004). "The mechanisms of vesicle budding and fusion." Cell **116**(2): 153-66.

Boutet, S. C., M. H. Disatnik, et al. (2007). "Regulation of Pax3 by proteasomal degradation of monoubiquitinated protein in skeletal muscle progenitors." Cell **130**(2): 349-62.

Boya, P., F. Reggiori, et al. (2013). "Emerging regulation and functions of autophagy." Nat Cell Biol **15**(7): 713-20.

Branzei, D. and M. Foiani (2008). "Regulation of DNA repair throughout the cell cycle." Nat Rev Mol Cell Biol **9**(4): 297-308.

Bucciantini, M., E. Giannoni, et al. (2002). "Inherent toxicity of aggregates implies a common mechanism for protein misfolding diseases." Nature **416**(6880): 507-11.

Burkhard, P., J. Stetefeld, et al. (2001). "Coiled coils: a highly versatile protein folding motif." Trends Cell Biol **11**(2): 82-8.

Cadwell, K. and L. Coscoy (2005). "Ubiquitination on nonlysine residues by a viral E3 ubiquitin ligase." Science **309**(5731): 127-30.

Cai, Q. and E. S. Robertson (2010). "Ubiquitin/SUMO modification regulates VHL protein stability and nucleocytoplasmic localization." PLoS One **5**(9).

Carvallo, L., R. Munoz, et al. (2010). "Non-canonical Wnt signaling induces ubiquitination and degradation of Syndecan4." J Biol Chem **285**(38): 29546-55.

Castresana, J. (2000). "Selection of conserved blocks from multiple alignments for their use in phylogenetic analysis." Mol Biol Evol **17**(4): 540-52.

Chastagner, P., A. Israel, et al. (2006). "Itch/AIP4 mediates Deltex degradation through the formation of K29-linked polyubiquitin chains." EMBO Rep **7**(11): 1147-53.

Chau, V., J. W. Tobias, et al. (1989). "A multiubiquitin chain is confined to specific lysine in a targeted short-lived protein." Science **243**(4898): 1576-83.

Chen, D., N. Kon, et al. (2005). "ARF-BP1/Mule is a critical mediator of the ARF tumor suppressor." Cell **121**(7): 1071-83.

Chen, L. and K. Madura (2014). "Degradation of specific nuclear proteins occurs in the cytoplasm in Saccharomyces cerevisiae." Genetics **197**(1): 193-7.

Chen, Z. and W. Lu (2015). "Roles of ubiquitination and SUMOylation on prostate cancer: mechanisms and clinical implications." Int J Mol Sci **16**(3): 4560-80.

Chevenet, F., C. Brun, et al. (2006). "TreeDyn: towards dynamic graphics and annotations for analyses of trees." BMC Bioinformatics **7**: 439.

Chin, L. S., J. P. Vavalle, et al. (2002). "Staring, a novel E3 ubiquitin-protein ligase that targets syntaxin 1 for degradation." J Biol Chem **277**(38): 35071-9.

Chiu, Y. H., M. Zhao, et al. (2009). "Ubiquitin in NF-kappaB signaling." Chem Rev **109**(4): 1549-60.

Ciccia, A. and S. J. Elledge (2010). "The DNA damage response: making it safe to play with knives." Mol Cell **40**(2): 179-204.

Ciechanover, A. (2005). "Intracellular protein degradation: from a vague idea, through the lysosome and the ubiquitin-proteasome system, and onto human diseases and drug targeting (Nobel lecture)." Angew Chem Int Ed Engl **44**(37): 5944-67.

Ciechanover, A. (2005). "Proteolysis: from the lysosome to ubiquitin and the proteasome." Nat Rev Mol Cell Biol **6**(1): 79-87.

Ciechanover, A. and Y. T. Kwon (2015). "Degradation of misfolded proteins in neurodegenerative diseases: therapeutic targets and strategies." Exp Mol Med **47**: e147.

Ciechanover, A., A. Orian, et al. (2000). "Ubiquitin-mediated proteolysis: biological regulation via destruction." Bioessays **22**(5): 442-51.

Civril, F., A. Wehenkel, et al. (2010). "Structural analysis of the RZZ complex reveals common ancestry with multisubunit vesicle tethering machinery." Structure **18**(5): 616-26.

Clague, M. J. and S. Urbe (2010). "Ubiquitin: same molecule, different degradation pathways." Cell **143**(5): 682-5.

D'Angelo, M. A., M. Raices, et al. (2009). "Age-dependent deterioration of nuclear pore complexes causes a loss of nuclear integrity in postmitotic cells." Cell **136**(2): 284-95.

Dammer, E. B., C. H. Na, et al. (2011). "Polyubiquitin linkage profiles in three models of proteolytic stress suggest the etiology of Alzheimer disease." J Biol Chem **286**(12): 10457-65.

de Groot, R. E., R. S. Ganji, et al. (2014). "Huwe1-mediated ubiquitylation of dishevelled defines a negative feedback loop in the Wnt signaling pathway." Sci Signal **7**(317): ra26.

de la Chapelle, A. (2005). "The incidence of Lynch syndrome." Fam Cancer **4**(3): 233-7.

Deckbar, D., P. A. Jeggo, et al. (2011). "Understanding the limitations of radiation-induced cell cycle checkpoints." Crit Rev Biochem Mol Biol **46**(4): 271-83.

Dereeper, A., V. Guignon, et al. (2008). "Phylogeny.fr: robust phylogenetic analysis for the non-specialist." Nucleic Acids Res **36**(Web Server issue): W465-9.

Deshaies, R. J. and C. A. Joazeiro (2009). "RING domain E3 ubiquitin ligases." Annu Rev Biochem **78**: 399-434.

Dikic, I., S. Wakatsuki, et al. (2009). "Ubiquitin-binding domains - from structures to functions." Nat Rev Mol Cell Biol **10**(10): 659-71.

Edgar, R. C. (2004). "MUSCLE: multiple sequence alignment with high accuracy and high throughput." Nucleic Acids Res **32**(5): 1792-7.

Ehret, A., M. O. Westendorp, et al. (1996). "Resistance of chimpanzee T cells to human immunodeficiency virus type 1 Tat-enhanced oxidative stress and apoptosis." J Virol **70**(9): 6502-7.

Emmerich, C. H., A. C. Schmukle, et al. (2011). "The emerging role of linear ubiquitination in cell signaling." Sci Signal **4**(204): re5.

Enserink, J. M. (2015). "Sumo and the cellular stress response." Cell Div **10**: 4.

Fan, X., Y. Y. Wang, et al. (2014). "Expression of RINT1 predicts seizure occurrence and outcomes in patients with low-grade gliomas." J Cancer Res Clin Oncol.

Ficari, F., A. Cama, et al. (2000). "APC gene mutations and colorectal adenomatosis in familial adenomatous polyposis." Br J Cancer **82**(2): 348-53.

Floyd, Z. E., J. S. Trausch-Azar, et al. (2001). "The nuclear ubiquitin-proteasome system degrades MyoD." J Biol Chem **276**(25): 22468-75.

Fornace, A. J., Jr., D. W. Nebert, et al. (1989). "Mammalian genes coordinately regulated by growth arrest signals and DNA-damaging agents." Mol Cell Biol **9**(10): 4196-203.

Galanty, Y., R. Belotserkovskaya, et al. (2009). "Mammalian SUMO E3-ligases PIAS1 and PIAS4 promote responses to DNA double-strand breaks." Nature **462**(7275): 935-9.

Garcia-Higuera, I., T. Taniguchi, et al. (2001). "Interaction of the Fanconi anemia proteins and BRCA1 in a common pathway." Mol Cell **7**(2): 249-62.

Gareau, J. R. and C. D. Lima (2010). "The SUMO pathway: emerging mechanisms that shape specificity, conjugation and recognition." Nat Rev Mol Cell Biol **11**(12): 861-71.

Gasteiger, E., A. Gattiker, et al. (2003). "ExPASy: The proteomics server for in-depth protein knowledge and analysis." Nucleic Acids Res **31**(13): 3784-8.

Geiss-Friedlander, R. and F. Melchior (2007). "Concepts in sumoylation: a decade on." Nat Rev Mol Cell Biol **8**(12): 947-56.

Giaccia, A. J. and M. B. Kastan (1998). "The complexity of p53 modulation: emerging patterns from divergent signals." Genes Dev **12**(19): 2973-83.

Giacinti, C. and A. Giordano (2006). "RB and cell cycle progression." Oncogene **25**(38): 5220-7.

Girdwood, D. W., M. H. Tatham, et al. (2004). "SUMO and transcriptional regulation." Semin Cell Dev Biol **15**(2): 201-10.

Glickman, M. H. and A. Ciechanover (2002). "The ubiquitin-proteasome proteolytic pathway: destruction for the sake of construction." Physiol Rev **82**(2): 373-428.

Goldberg, A. L. (2003). "Protein degradation and protection against misfolded or damaged proteins." Nature **426**(6968): 895-9.

Goodsell, D. S. (1991). "Inside a living cell." Trends Biochem Sci **16**(6): 203-6.

Gregory, R. C., T. Taniguchi, et al. (2003). "Regulation of the Fanconi anemia pathway by monoubiquitination." Semin Cancer Biol **13**(1): 77-82.

Grossman, A. D., D. B. Straus, et al. (1987). "Sigma 32 synthesis can regulate the synthesis of heat shock proteins in Escherichia coli." Genes Dev **1**(2): 179-84.

Guindon, S., J. F. Dufayard, et al. (2010). "New algorithms and methods to estimate maximum-likelihood phylogenies: assessing the performance of PhyML 3.0." Syst Biol **59**(3): 307-21.

Guo, Y., D. W. Sirkis, et al. (2014). "Protein sorting at the trans-Golgi network." Annu Rev Cell Dev Biol **30**: 169-206.

Haas, T. L., C. H. Emmerich, et al. (2009). "Recruitment of the linear ubiquitin chain assembly complex stabilizes the TNF-R1 signaling complex and is required for TNF-mediated gene induction." Mol Cell **36**(5): 831-44.

Haglund, K., P. P. Di Fiore, et al. (2003). "Distinct monoubiquitin signals in receptor endocytosis." Trends Biochem Sci **28**(11): 598-603.

Haglund, K., S. Sigismund, et al. (2003). "Multiple monoubiquitination of RTKs is sufficient for their endocytosis and degradation." Nat Cell Biol **5**(5): 461-6.

Hall, J. R., E. Kow, et al. (2007). "Cdc6 stability is regulated by the Huwe1 ubiquitin ligase after DNA damage." Mol Biol Cell **18**(9): 3340-50.

Hay, R. T. (2005). "SUMO: a history of modification." Mol Cell **18**(1): 1-12.

Haynes, C. M., E. A. Titus, et al. (2004). "Degradation of misfolded proteins prevents ER-derived oxidative stress and cell death." Mol Cell **15**(5): 767-76.

He, S., D. Ni, et al. (2013). "PtdIns(3)P-bound UVRAG coordinates Golgi-ER retrograde and Atg9 transport by differential interactions with the ER tether and the beclin 1 complex." Nat Cell Biol **15**(10): 1206-19.

Hein, A. L., M. M. Ouellette, et al. (2014). "Radiation-induced signaling pathways that promote cancer cell survival (review)." Int J Oncol **45**(5): 1813-9.

Henley, J. M., T. J. Craig, et al. (2014). "Neuronal SUMOylation: mechanisms, physiology, and roles in neuronal dysfunction." Physiol Rev **94**(4): 1249-85.

Herold, S., A. Hock, et al. (2008). "Miz1 and HectH9 regulate the stability of the checkpoint protein, TopBP1." EMBO J **27**(21): 2851-61.

Hershko, A. and A. Ciechanover (1998). "The ubiquitin system." Annu Rev Biochem **67**: 425-79.

Hicke, L. (2001). "Protein regulation by monoubiquitin." Nat Rev Mol Cell Biol **2**(3): 195-201.

Hirata, H., Y. Bessho, et al. (2004). "Instability of Hes7 protein is crucial for the somite segmentation clock." Nat Genet **36**(7): 750-4.

Hirose, H., K. Arasaki, et al. (2004). "Implication of ZW10 in membrane trafficking between the endoplasmic reticulum and Golgi." EMBO J **23**(6): 1267-78.

Hochstrasser, M. (1995). "Ubiquitin, proteasomes, and the regulation of intracellular protein degradation." Curr Opin Cell Biol **7**(2): 215-23.

Hochstrasser, M. (2006). "Lingering mysteries of ubiquitin-chain assembly." Cell **124**(1): 27-34.

Hoeijmakers, J. H. (2009). "DNA damage, aging, and cancer." N Engl J Med **361**(15): 1475-85.

Hoeller, D., C. M. Hecker, et al. (2007). "E3-independent monoubiquitination of ubiquitin-binding proteins." Mol Cell **26**(6): 891-8.

Hong, Y., X. Xing, et al. (2011). "SUMOylation of DEC1 protein regulates its transcriptional activity and enhances its stability." PLoS One **6**(8): e23046.

Hsieh, P. and K. Yamane (2008). "DNA mismatch repair: molecular mechanism, cancer, and ageing." Mech Ageing Dev **129**(7-8): 391-407.

Huang, T. T. and A. D. D'Andrea (2006). "Regulation of DNA repair by ubiquitylation." Nat Rev Mol Cell Biol **7**(5): 323-34.

Huang, T. T., S. M. Wuerzberger-Davis, et al. (2003). "Sequential modification of NEMO/IKKgamma by SUMO-1 and ubiquitin mediates NF-kappaB activation by genotoxic stress." Cell **115**(5): 565-76.

Hunter, T. (2007). "The age of crosstalk: phosphorylation, ubiquitination, and beyond." Mol Cell **28**(5): 730-8.

Hunter, T. and H. Sun (2008). "Crosstalk between the SUMO and ubiquitin pathways." Ernst Schering Found Symp Proc(1): 1-16.

Ikeda, F., Y. L. Deribe, et al. (2011). "SHARPIN forms a linear ubiquitin ligase complex regulating NF-kappaB activity and apoptosis." Nature **471**(7340): 637-41.

Ikeda, F. and I. Dikic (2008). "Atypical ubiquitin chains: new molecular signals. 'Protein Modifications: Beyond the Usual Suspects' review series." EMBO Rep **9**(6): 536-42.

Iyer, R. R., A. Pluciennik, et al. (2006). "DNA mismatch repair: functions and mechanisms." Chem Rev **106**(2): 302-23.

Jang, E. and D. C. Chung "Hereditary colon cancer: lynch syndrome." Gut Liver **4**(2): 151-60.

Jang, E. R., P. Shi, et al. (2014). "HUWE1 is a molecular link controlling RAF-1 activity supported by the Shoc2 scaffold." Mol Cell Biol **34**(19): 3579-93.

Jensen, R. B. and L. Shapiro (2000). "Proteins on the move: dynamic protein localization in prokaryotes." Trends Cell Biol **10**(11): 483-8.

Jin, L., A. Williamson, et al. (2008). "Mechanism of ubiquitin-chain formation by the human anaphase-promoting complex." Cell **133**(4): 653-65.

Johnson, E. S. (2004). "Protein modification by SUMO." Annu Rev Biochem **73**: 355-82.

Jung, J. J., S. M. Inamdar, et al. (2012). "Regulation of intracellular membrane trafficking and cell dynamics by syntaxin-6." Biosci Rep **32**(4): 383-91.

Katzmann, D. J., G. Odorizzi, et al. (2002). "Receptor downregulation and multivesicular-body sorting." Nat Rev Mol Cell Biol **3**(12): 893-905.

Kaytor, M. D. and S. T. Warren (1999). "Aberrant protein deposition and neurological disease." J Biol Chem **274**(53): 37507-10.

Kim, J., M. Guermah, et al. (2009). "RAD6-Mediated transcription-coupled H2B ubiquitylation directly stimulates H3K4 methylation in human cells." Cell **137**(3): 459-71.

Kim, J., S. B. Hake, et al. (2005). "The human homolog of yeast BRE1 functions as a transcriptional coactivator through direct activator interactions." Mol Cell **20**(5): 759-70.

Kim, K. I. and S. H. Baek (2006). "SUMOylation code in cancer development and metastasis." Mol Cells **22**(3): 247-53.

Kim, P. K., D. W. Hailey, et al. (2008). "Ubiquitin signals autophagic degradation of cytosolic proteins and peroxisomes." Proc Natl Acad Sci U S A **105**(52): 20567-74.

Kimura, Y. and K. Tanaka (2010). "Regulatory mechanisms involved in the control of ubiquitin homeostasis." J Biochem **147**(6): 793-8.

Kirchhausen, T. (2000). "Three ways to make a vesicle." Nat Rev Mol Cell Biol **1**(3): 187-98.

Kirisako, T., K. Kamei, et al. (2006). "A ubiquitin ligase complex assembles linear polyubiquitin chains." EMBO J **25**(20): 4877-87.

Klein, D. K., S. Hoffmann, et al. (2015). "Cyclin F suppresses B-Myb activity to promote cell cycle checkpoint control." Nat Commun **6**: 5800.

Klionsky, D. J. (2007). "Autophagy: from phenomenology to molecular understanding in less than a decade." Nat Rev Mol Cell Biol **8**(11): 931-7.

Kohlmann, W. and S. B. Gruber (1993). "Lynch Syndrome."

Komander, D. and M. Rape (2012). "The ubiquitin code." Annu Rev Biochem **81**: 203-29.

Kong, L. J., A. R. Meloni, et al. (2006). "The Rb-related p130 protein controls telomere lengthening through an interaction with a Rad50-interacting protein, RINT-1." Mol Cell **22**(1): 63-71.

Kornitzer, D. and A. Ciechanover (2000). "Modes of regulation of ubiquitin-mediated protein degradation." J Cell Physiol **182**(1): 1-11.

Kravtsova-Ivantsiv, Y., S. Cohen, et al. (2009). "Modification by single ubiquitin moieties rather than polyubiquitination is sufficient for proteasomal processing of the p105 NF-kappaB precursor." Mol Cell **33**(4): 496-504.

Kretz-Remy, C. and R. M. Tanguay (1999). "SUMO/sentrin: protein modifiers regulating important cellular functions." Biochem Cell Biol **77**(4): 299-309.

Krogh, A., B. Larsson, et al. (2001). "Predicting transmembrane protein topology with a hidden Markov model: application to complete genomes." J Mol Biol **305**(3): 567-80.

Kulathu, Y. and D. Komander (2012). "Atypical ubiquitylation - the unexplored world of polyubiquitin beyond Lys48 and Lys63 linkages." Nat Rev Mol Cell Biol **13**(8): 508-23.

Kunkel, T. A. and D. A. Erie (2005). "DNA mismatch repair." Annu Rev Biochem **74**: 681-710.

Kurokawa, M., J. Kim, et al. (2013). "A network of substrates of the E3 ubiquitin ligases MDM2 and HUWE1 control apoptosis independently of p53." Sci Signal **6**(274): ra32.

Langerak, P. and P. Russell (2011). "Regulatory networks integrating cell cycle control with DNA damage checkpoints and double-strand break repair." Philos Trans R Soc Lond B Biol Sci **366**(1584): 3562-71.

Lauwers, E., C. Jacob, et al. (2009). "K63-linked ubiquitin chains as a specific signal for protein sorting into the multivesicular body pathway." J Cell Biol **185**(3): 493-502.

Lecker, S. H., A. L. Goldberg, et al. (2006). "Protein degradation by the ubiquitin-proteasome pathway in normal and disease states." J Am Soc Nephrol **17**(7): 1807-19.

Lee, E. Y. and W. J. Muller (2010). "Oncogenes and tumor suppressor genes." Cold Spring Harb Perspect Biol **2**(10): a003236.

Levine, B., N. Mizushima, et al. (2011). "Autophagy in immunity and inflammation." Nature **469**(7330): 323-35.

Li, G. M. (1999). "The role of mismatch repair in DNA damage-induced apoptosis." Oncol Res **11**(9): 393-400.

Li, G. M. (2008). "Mechanisms and functions of DNA mismatch repair." Cell Res **18**(1): 85-98.

Li, L., T. Shimada, et al. (2006). "MAIGO2 is involved in exit of seed storage proteins from the endoplasmic reticulum in Arabidopsis thaliana." Plant Cell **18**(12): 3535-47.

Li, T., E. Evdokimov, et al. (2004). "Sumoylation of heterogeneous nuclear ribonucleoproteins, zinc finger proteins, and nuclear pore complex proteins: a proteomic analysis." Proc Natl Acad Sci U S A **101**(23): 8551-6.

Liang, L., L. Deng, et al. (2005). "Modulation of DNA end joining by nuclear proteins." J Biol Chem **280**(36): 31442-9.

Liang, M., F. Melchior, et al. (2004). "Regulation of Smad4 sumoylation and transforming growth factor-beta signaling by protein inhibitor of activated STAT1." J Biol Chem **279**(22): 22857-65.

Lin, X., C. C. Liu, et al. (2007). "RINT-1 serves as a tumor suppressor and maintains Golgi dynamics and centrosome integrity for cell survival." Mol Cell Biol **27**(13): 4905-16.

Liu, H., S. Urbe, et al. (2012). "Selective protein degradation in cell signalling." Semin Cell Dev Biol **23**(5): 509-14.

Liu, Z., S. M. Oh, et al. (2009). "Human BRE1 is an E3 ubiquitin ligase for Ebp1 tumor suppressor." Mol Biol Cell **20**(3): 757-68.

Liu, Z., R. Oughtred, et al. (2005). "Characterization of E3Histone, a novel testis ubiquitin protein ligase which ubiquitinates histones." Mol Cell Biol **25**(7): 2819-31.

Lobrich, M. and P. A. Jeggo (2007). "The impact of a negligent G2/M checkpoint on genomic instability and cancer induction." Nat Rev Cancer **7**(11): 861-9.

Longerich, S., Y. Kwon, et al. (2014). "Regulation of FANCD2 and FANCI monoubiquitination by their interaction and by DNA." Nucleic Acids Res **42**(9): 5657-70.

Lu, W., S. Liu, et al. (2015). "SKP2 inactivation suppresses prostate tumorigenesis by mediating JARID1B ubiquitination." Oncotarget **6**(2): 771-88.

Luethy, J. D., J. Fargnoli, et al. (1990). "Isolation and characterization of the hamster gadd153 gene. Activation of promoter activity by agents that damage DNA." J Biol Chem **265**(27): 16521-6.

Luo, M., J. Zhou, et al. (2015). "Polycomb protein SCML2 associates with USP7 and counteracts histone H2A ubiquitination in the XY chromatin during male meiosis." PLoS Genet **11**(1): e1004954.

Mahajan, R., C. Delphin, et al. (1997). "A small ubiquitin-related polypeptide involved in targeting RanGAP1 to nuclear pore complex protein RanBP2." Cell **88**(1): 97-107.

Matsuoka, S., B. A. Ballif, et al. (2007). "ATM and ATR substrate analysis reveals extensive protein networks responsive to DNA damage." Science **316**(5828): 1160-6.

McCullough, K. D., J. L. Martindale, et al. (2001). "Gadd153 sensitizes cells to endoplasmic reticulum stress by down-regulating Bcl2 and perturbing the cellular redox state." Mol Cell Biol **21**(4): 1249-59.

McDowell, G. S. and A. Philpott (2013). "Non-canonical ubiquitylation: mechanisms and consequences." Int J Biochem Cell Biol **45**(8): 1833-42.

Meng, J. and J. Wang (2015). "Role of SNARE proteins in tumourigenesis and their potential as targets for novel anti-cancer therapeutics." Biochim Biophys Acta **1856**(1): 1-12.

Metzger, M. B., V. A. Hristova, et al. (2012). "HECT and RING finger families of E3 ubiquitin ligases at a glance." J Cell Sci **125**(Pt 3): 531-7.

Micel, L. N., J. J. Tentler, et al. (2013). "Role of ubiquitin ligases and the proteasome in oncogenesis: novel targets for anticancer therapies." J Clin Oncol **31**(9): 1231-8.

Mocciaro, A. and M. Rape (2012). "Emerging regulatory mechanisms in ubiquitin-dependent cell cycle control." J Cell Sci **125**(Pt 2): 255-63.

Modrich, P. and R. Lahue (1996). "Mismatch repair in replication fidelity, genetic recombination, and cancer biology." Annu Rev Biochem **65**: 101-33.

Morris, J. R., C. Boutell, et al. (2009). "The SUMO modification pathway is involved in the BRCA1 response to genotoxic stress." Nature **462**(7275): 886-90.

Mukhopadhyay, D. and H. Riezman (2007). "Proteasome-independent functions of ubiquitin in endocytosis and signaling." Science **315**(5809): 201-5.

Muller-Rischart, A. K., A. Pilsl, et al. (2013). "The E3 ligase parkin maintains mitochondrial integrity by increasing linear ubiquitination of NEMO." Mol Cell **49**(5): 908-21.

Myat, A., P. Henry, et al. (2002). "Drosophila Nedd4, a ubiquitin ligase, is recruited by Commissureless to control cell surface levels of the roundabout receptor." Neuron **35**(3): 447-59.

Nakajima, K., H. Hirose, et al. (2004). "Involvement of BNIP1 in apoptosis and endoplasmic reticulum membrane fusion." EMBO J **23**(16): 3216-26.

Nakamura, K., A. Kato, et al. (2011). "Regulation of homologous recombination by RNF20-dependent H2B ubiquitination." Mol Cell **41**(5): 515-28.

Nakanishi, K., Y. G. Yang, et al. (2005). "Human Fanconi anemia monoubiquitination pathway promotes homologous DNA repair." Proc Natl Acad Sci U S A **102**(4): 1110-5.

Nakayama, K. I. and K. Nakayama (2006). "Ubiquitin ligases: cell-cycle control and cancer." Nat Rev Cancer **6**(5): 369-81.

Nesvizhskii, A. I., A. Keller, et al. (2003). "A statistical model for identifying proteins by tandem mass spectrometry." Anal Chem **75**(17): 4646-58.

Nickel, W., B. Brugger, et al. (2002). "Vesicular transport: the core machinery of COPI recruitment and budding." J Cell Sci **115**(Pt 16): 3235-40.

Nicoletti, I., G. Migliorati, et al. (1991). "A rapid and simple method for measuring thymocyte apoptosis by propidium iodide staining and flow cytometry." J Immunol Methods **139**(2): 271-9.

Noda, T., K. Suzuki, et al. (2002). "Yeast autophagosomes: de novo formation of a membrane structure." Trends Cell Biol **12**(5): 231-5.

Noy, T., O. Suad, et al. (2012). "HUWE1 ubiquitinates MyoD and targets it for proteasomal degradation." Biochem Biophys Res Commun **418**(2): 408-13.

Olivier, M., M. Hollstein, et al. (2010). "TP53 mutations in human cancers: origins, consequences, and clinical use." Cold Spring Harb Perspect Biol **2**(1): a001008.

Oyadomari, S. and M. Mori (2004). "Roles of CHOP/GADD153 in endoplasmic reticulum stress." Cell Death Differ **11**(4): 381-9.

Papouli, E., S. Chen, et al. (2005). "Crosstalk between SUMO and ubiquitin on PCNA is mediated by recruitment of the helicase Srs2p." Mol Cell **19**(1): 123-33.

Park-Sarge, O. K. and K. D. Sarge (2009). "Detection of sumoylated proteins." Methods Mol Biol **464**: 255-65.

Park, D. J., K. Tao, et al. (2014). "Rare mutations in RINT1 predispose carriers to breast and Lynch syndrome-spectrum cancers." Cancer Discov **4**(7): 804-15.

Parsons, J. L., P. S. Tait, et al. (2009). "Ubiquitin ligase ARF-BP1/Mule modulates base excision repair." EMBO J **28**(20): 3207-15.

Passmore, L. A. and D. Barford (2004). "Getting into position: the catalytic mechanisms of protein ubiquitylation." Biochem J **379**(Pt 3): 513-25.

Pavri, R., B. Zhu, et al. (2006). "Histone H2B monoubiquitination functions cooperatively with FACT to regulate elongation by RNA polymerase II." Cell **125**(4): 703-17.

Peltomaki, P. (2005). "Lynch syndrome genes." Fam Cancer **4**(3): 227-32.

Peng, J., D. Schwartz, et al. (2003). "A proteomics approach to understanding protein ubiquitination." Nat Biotechnol **21**(8): 921-6.

Perutz, M. F. (1989). "Mechanisms of cooperativity and allosteric regulation in proteins." Q Rev Biophys **22**(2): 139-237.

Peter, S., J. Bultinck, et al. (2014). "Tumor cell-specific inhibition of MYC function using small molecule inhibitors of the HUWE1 ubiquitin ligase." EMBO Mol Med **6**(12): 1525-41.

Pickart, C. M. (2001). "Mechanisms underlying ubiquitination." Annu Rev Biochem **70**: 503-33.

Pickart, C. M. and M. J. Eddins (2004). "Ubiquitin: structures, functions, mechanisms." Biochim Biophys Acta **1695**(1-3): 55-72.

Pirngruber, J., A. Shchebet, et al. (2009). "CDK9 directs H2B monoubiquitination and controls replication-dependent histone mRNA 3'-end processing." EMBO Rep **10**(8): 894-900.

Prakash, S., T. Inobe, et al. (2009). "Substrate selection by the proteasome during degradation of protein complexes." Nat Chem Biol **5**(1): 29-36.

Pyo, J. O., J. Nah, et al. (2012). "Molecules and their functions in autophagy." Exp Mol Med **44**(2): 73-80.

Quayle, S. N., M. G. Chheda, et al. (2012). "Integrative functional genomics identifies RINT1 as a novel GBM oncogene." Neuro Oncol **14**(11): 1325-31.

Ramadan, K. and M. Meerang (2011). "Degradation-linked ubiquitin signal and proteasome are integral components of DNA double strand break repair: New perspectives for anti-cancer therapy." FEBS Lett **585**(18): 2868-75.

Ramakrishnan, S. R., C. Vogel, et al. (2009). "Mining gene functional networks to improve mass-spectrometry-based protein identification." Bioinformatics **25**(22): 2955-61.

Ramsay, G., G. I. Evan, et al. (1984). "The protein encoded by the human proto-oncogene c-myc." Proc Natl Acad Sci U S A **81**(24): 7742-6.

Ren, P., Z. Sheng, et al. (2013). "RNF20 promotes the polyubiquitination and proteasome-dependent degradation of AP-2alpha protein." Acta Biochim Biophys Sin (Shanghai) **46**(2): 136-40.

Rieser, E., S. M. Cordier, et al. (2013). "Linear ubiquitination: a newly discovered regulator of cell signalling." Trends Biochem Sci **38**(2): 94-102.

Rotin, D. and S. Kumar (2009). "Physiological functions of the HECT family of ubiquitin ligases." Nat Rev Mol Cell Biol **10**(6): 398-409.

Rotin, D., O. Staub, et al. (2000). "Ubiquitination and endocytosis of plasma membrane proteins: role of Nedd4/Rsp5p family of ubiquitin-protein ligases." J Membr Biol **176**(1): 1-17.

Royds, J. A. and B. Iacopetta (2006). "p53 and disease: when the guardian angel fails." Cell Death Differ **13**(6): 1017-26.

Sadowski, M., R. Suryadinata, et al. (2012). "Protein monoubiquitination and polyubiquitination generate structural diversity to control distinct biological processes." IUBMB Life **64**(2): 136-42.

Saito, K. and T. Katada (2015). "Mechanisms for exporting large-sized cargoes from the endoplasmic reticulum." Cell Mol Life Sci.

Sarangi, P. and X. Zhao (2015). "SUMO-mediated regulation of DNA damage repair and responses." Trends Biochem Sci **40**(4): 233-42.

Sarcevic, B., A. Mawson, et al. (2002). "Regulation of the ubiquitin-conjugating enzyme hHR6A by CDK-mediated phosphorylation." EMBO J **21**(8): 2009-18.

Sarge, K. D. and O. K. Park-Sarge (2009). "Sumoylation and human disease pathogenesis." Trends Biochem Sci **34**(4): 200-5.

Savas, J. N., B. H. Toyama, et al. (2012). "Extremely long-lived nuclear pore proteins in the rat brain." Science **335**(6071): 942.

Schekman, R. and L. Orci (1996). "Coat proteins and vesicle budding." Science **271**(5255): 1526-33.

Schimmel, J., K. Eifler, et al. (2014). "Uncovering SUMOylation dynamics during cell-cycle progression reveals FoxM1 as a key mitotic SUMO target protein." Mol Cell **53**(6): 1053-66.

Schmitt, H. D. (2010). "Dsl1p/Zw10: common mechanisms behind tethering vesicles and microtubules." Trends Cell Biol **20**(5): 257-68.

Schnell, J. D. and L. Hicke (2003). "Non-traditional functions of ubiquitin and ubiquitin-binding proteins." J Biol Chem **278**(38): 35857-60.

Schulze, H., T. Kolter, et al. (2009). "Principles of lysosomal membrane degradation: Cellular topology and biochemistry of lysosomal lipid degradation." Biochim Biophys Acta **1793**(4): 674-83.

Schwartz, A. L. and A. Ciechanover (1999). "The ubiquitin-proteasome pathway and pathogenesis of human diseases." Annu Rev Med **50**: 57-74.

Shaid, S., C. H. Brandts, et al. (2013). "Ubiquitination and selective autophagy." Cell Death Differ **20**(1): 21-30.

Shaltiel, I. A., L. Krenning, et al. (2015). "The same, only different - DNA damage checkpoints and their reversal throughout the cell cycle." J Cell Sci **128**(4): 607-20.

Sharma, K., R. C. D'Souza, et al. (2014). "Ultradeep human phosphoproteome reveals a distinct regulatory nature of Tyr and Ser/Thr-based signaling." Cell Rep **8**(5): 1583-94.

Shema, E., I. Tirosh, et al. (2008). "The histone H2B-specific ubiquitin ligase RNF20/hBRE1 acts as a putative tumor suppressor through selective regulation of gene expression." Genes Dev **22**(19): 2664-76.

Shembade, N. and E. W. Harhaj (2015). "Elucidating dynamic protein-protein interactions and ubiquitination in NF-kappaB signaling pathways." Methods Mol Biol **1280**: 283-95.

Shi, W., Z. Ma, et al. (2008). "Disassembly of MDC1 foci is controlled by ubiquitin-proteasome-dependent degradation." J Biol Chem **283**(46): 31608-16.

Shih, S. C., D. J. Katzmann, et al. (2002). "Epsins and Vps27p/Hrs contain ubiquitin-binding domains that function in receptor endocytosis." Nat Cell Biol **4**(5): 389-93.

Shih, S. C., K. E. Sloper-Mould, et al. (2000). "Monoubiquitin carries a novel internalization signal that is appended to activated receptors." EMBO J **19**(2): 187-98.

Shima, H., H. Suzuki, et al. (2013). "Activation of the SUMO modification system is required for the accumulation of RAD51 at sites of DNA damage." J Cell Sci **126**(Pt 22): 5284-92.

Song, Y. and S. T. Brady (2015). "Post-translational modifications of tubulin: pathways to functional diversity of microtubules." Trends Cell Biol **25**(3): 125-36.

Spang, A. (2015). "The Road not Taken: Less Traveled Roads from the TGN to the Plasma Membrane." Membranes (Basel) **5**(1): 84-98.

Srivastava, D. and O. Chakrabarti (2014). "Mahogunin-mediated alpha-tubulin ubiquitination via noncanonical K6 linkage regulates microtubule stability and mitotic spindle orientation." Cell Death Dis **5**: e1064.

Stamenova, S. D., M. E. French, et al. (2007). "Ubiquitin binds to and regulates a subset of SH3 domains." Mol Cell **25**(2): 273-84.

Stelzl, U., U. Worm, et al. (2005). "A human protein-protein interaction network: a resource for annotating the proteome." Cell **122**(6): 957-68.

Stojic, L., R. Brun, et al. (2004). "Mismatch repair and DNA damage signalling." DNA Repair (Amst) **3**(8-9): 1091-101.

Stow, J. L. (2013). "Nobel Prize discovery paves the way for immunological traffic." Nat Rev Immunol **13**(12): 839-41.

Sun, Y., A. Shestakova, et al. (2007). "Rab6 regulates both ZW10/RINT-1 and conserved oligomeric Golgi complex-dependent Golgi trafficking and homeostasis." Mol Biol Cell **18**(10): 4129-42.

Sweet, D. J. and H. R. Pelham (1993). "The TIP1 gene of Saccharomyces cerevisiae encodes an 80 kDa cytoplasmic protein that interacts with the cytoplasmic domain of Sec20p." EMBO J **12**(7): 2831-40.

Tagaya, M., K. Arasaki, et al. (2014). "Moonlighting functions of the NRZ (mammalian Dsl1) complex." Front Cell Dev Biol **2**: 25.

Taylor, W. R. and G. R. Stark (2001). "Regulation of the G2/M transition by p53." Oncogene **20**(15): 1803-15.

Thrower, J. S., L. Hoffman, et al. (2000). "Recognition of the polyubiquitin proteolytic signal." EMBO J **19**(1): 94-102.

Tiwari, A. K., H. K. Roy, et al. (2015). "Lynch Syndrome in the 21st Century: Clinical Perspectives." QJM.

Todaro, G. J. and H. Green (1963). "Quantitative studies of the growth of mouse embryo cells in culture and their development into established lines." J Cell Biol **17**: 299-313.

Tokunaga, F. and K. Iwai (2012). "LUBAC, a novel ubiquitin ligase for linear ubiquitination, is crucial for inflammation and immune responses." Microbes Infect **14**(7-8): 563-72.

Tokunaga, F., S. Sakata, et al. (2009). "Involvement of linear polyubiquitylation of NEMO in NF-kappaB activation." Nat Cell Biol **11**(2): 123-32.

Toyama, B. H. and M. W. Hetzer (2013). "Protein homeostasis: live long, won't prosper." Nat Rev Mol Cell Biol **14**(1): 55-61.

Tripathi, A., Y. Ren, et al. (2009). "Structural characterization of Tip20p and Dsl1p, subunits of the Dsl1p vesicle tethering complex." Nat Struct Mol Biol **16**(2): 114-23.

van der Lee, R., B. Lang, et al. (2014). "Intrinsically disordered segments affect protein half-life in the cell and during evolution." Cell Rep **8**(6): 1832-44.

Verzijl, N., J. DeGroot, et al. (2000). "Effect of collagen turnover on the accumulation of advanced glycation end products." J Biol Chem **275**(50): 39027-31.

von Mikecz, A., M. Chen, et al. (2008). "The nuclear ubiquitin-proteasome system: visualization of proteasomes, protein aggregates, and proteolysis in the cell nucleus." Methods Mol Biol **463**: 191-202.

Wagner, S. A., P. Beli, et al. (2011). "Proteomic analyses reveal divergent ubiquitylation site patterns in murine tissues." Mol Cell Proteomics **11**(12): 1578-85.

Walczak, H., K. Iwai, et al. (2012). "Generation and physiological roles of linear ubiquitin chains." BMC Biol **10**: 23.

Wang, G., Y. Gao, et al. (2012). "K63-linked ubiquitination in kinase activation and cancer." Front Oncol **2**: 5.

Wang, Q., P. Young, et al. (2005). "Structure of S5a bound to monoubiquitin provides a model for polyubiquitin recognition." J Mol Biol **348**(3): 727-39.

Wang, X., R. A. Herr, et al. (2007). "Ubiquitination of serine, threonine, or lysine residues on the cytoplasmic tail can induce ERAD of MHC-I by viral E3 ligase mK3." J Cell Biol **177**(4): 613-24.

Wang, X., G. Lu, et al. (2014). "HUWE1 interacts with BRCA1 and promotes its degradation in the ubiquitin-proteasome pathway." Biochem Biophys Res Commun **444**(4): 549-54.

Wasik, U. and A. Filipek (2014). "Non-nuclear function of sumoylated proteins." Biochim Biophys Acta **1843**(12): 2878-2885.

Weiler, M., J. Blaes, et al. (2014). "mTOR target NDRG1 confers MGMT-dependent resistance to alkylating chemotherapy." Proc Natl Acad Sci U S A **111**(1): 409-14.

Williams, C., M. van den Berg, et al. (2007). "A conserved cysteine is essential for Pex4p-dependent ubiquitination of the peroxisomal import receptor Pex5p." J Biol Chem **282**(31): 22534-43.

Wilson, V. G. and P. R. Heaton (2008). "Ubiquitin proteolytic system: focus on SUMO." Expert Rev Proteomics **5**(1): 121-35.

Wu, H. and R. P. Leng (2011). "UBE4B, a ubiquitin chain assembly factor, is required for MDM2-mediated p53 polyubiquitination and degradation." Cell Cycle **10**(12): 1912-5.

Xiao, J., C. C. Liu, et al. (2001). "RINT-1, a novel Rad50-interacting protein, participates in radiation-induced G(2)/M checkpoint control." J Biol Chem **276**(9): 6105-11.

Xu, P., D. M. Duong, et al. (2009). "Quantitative proteomics reveals the function of unconventional ubiquitin chains in proteasomal degradation." Cell **137**(1): 133-45.

Yang, C., J. C. Matro, et al. (2012). "Missense mutations in the human SDHB gene increase protein degradation without altering intrinsic enzymatic function." FASEB J **26**(11): 4506-16.

Yang, W. and W. Paschen (2009). "Gene expression and cell growth are modified by silencing SUMO2 and SUMO3 expression." Biochem Biophys Res Commun **382**(1): 215-8.

Yang, W. L., X. Zhang, et al. (2010). "Emerging role of Lys-63 ubiquitination in protein kinase and phosphatase activation and cancer development." Oncogene **29**(32): 4493-503.

Yang, X. J. and C. M. Chiang (2013). "Sumoylation in gene regulation, human disease, and therapeutic action." F1000Prime Rep **5**: 45.

Ye, Y. and M. Rape (2009). "Building ubiquitin chains: E2 enzymes at work." Nat Rev Mol Cell Biol **10**(11): 755-64.

Yin, H., Y. Gui, et al. (2010). "Dependence of phospholipase D1 multi-monoubiquitination on its enzymatic activity and palmitoylation." J Biol Chem **285**(18): 13580-8.

Zhang, L., M. Xu, et al. (2013). "Both K63 and K48 ubiquitin linkages signal lysosomal degradation of the LDL receptor." J Lipid Res **54**(5): 1410-20.

Zhao, J. (2007). "Sumoylation regulates diverse biological processes." Cell Mol Life Sci **64**(23): 3017-33.

Zhao, S. and H. D. Ulrich (2010). "Distinct consequences of posttranslational modification by linear versus K63-linked polyubiquitin chains." Proc Natl Acad Sci U S A **107**(17): 7704-9.

Zhao, X., J. I. Heng, et al. (2008). "The HECT-domain ubiquitin ligase Huwe1 controls neural differentiation and proliferation by destabilizing the N-Myc oncoprotein." Nat Cell Biol **10**(6): 643-53.

Zhao, Y., J. R. Brickner, et al. (2014). "Crosstalk between ubiquitin and other post-translational modifications on chromatin during double-strand break repair." Trends Cell Biol **24**(7): 426-34.

Zhong, Q., W. Gao, et al. (2005). "Mule/ARF-BP1, a BH3-only E3 ubiquitin ligase, catalyzes the polyubiquitination of Mcl-1 and regulates apoptosis." Cell **121**(7): 1085-95.

Zhu, B., Y. Zheng, et al. (2005). "Monoubiquitination of human histone H2B: the factors involved and their roles in HOX gene regulation." Mol Cell **20**(4): 601-11.

Zotti, T., A. Uva, et al. (2011). "TRAF7 protein promotes Lys-29-linked polyubiquitination of IkappaB kinase (IKKgamma)/NF-kappaB essential modulator (NEMO) and p65/RelA protein and represses NF-kappaB activation." J Biol Chem **286**(26): 22924-33.